POLITECNICO DI TORINO

Master Degree Course in Biomedical Engineering

Master Degree Thesis

Development of clinical grade Pulse Wave Velocity estimation equipment using MEMS microphones

Supervisors:

Prof. Danilo Demarchi

Ing. Davide Lena

Ing. Irene Buraioli

Candidate:

Beatrice Lattanzi

December 2018

Ringrazio il Professor Danilo De Marchi, per avermi dato l'opportunità di collaborare con lui, con l'Ing. Davide Lena e l'ing Irene Buraioli; grazie alla loro dedizione, conoscenza e professionalità, l'esperienza nei laboratori è stata stimolante, utile e formativa. Grazie per la pazienza e per tutti i preziosi consigli.

Ma, il grazie più grande va alla mia famiglia. Passare questi due anni lontana da voi è stata la cosa più difficile che abbia mai fatto. La consapevolezza della fiducia che, da sempre, avete risposto in me, mi ha dato la forza di superare ogni cosa. Grazie *Mamma e Papà,* non sarei qui senza di voi.

E grazie a mio fratello *Saverio*, per esserci stato, seppur a suo modo, e per essere il rompiscatole che è.

Non potrei mai sentirmi a casa in un posto senza di lui.

Il grazie "speciale" va invece a *Riccardo*, semplicemente per essere il mio oggi e il mio domani.

Grazie infine, a tutte quelle belle persone che Torino mi ha donato, per le serate, per le sclerate e per tutti i nuovi termini coniati che hanno ispirato. Se mi chiederanno di Torino io dirò di voi. Grazie anche alla mia *amore e odio*, perchè non sarebbe stato lo stesso senza di lei, lo so per certezza. Grazie alle mie *sbarbatelle*, siete state un tocco di spensieratezza e allegria che porterò sempre nel cuore. Grazie a *Federica e Claudia*, amiche di una vita, è stato come se foste venute a Torino insieme a me. Grazie a *Simonc e Alessia*, vecchie CDM ma solo per modo di dire; riuscirò a chiamarvi sempre e solo così.

Ma alla fine grazie anche a me stessa, per non aver mollato e per esserci riuscita.

Summary

Table of Figures

Chapter 1

Introduction

Cardiovascular diseases represent the primary cause of death in western society, as *Figure* 1.1 shows. For this reason, in recent years, medical field and industry companies, such as STMicroelectronics, became very interested to developed devices for the assessment of cardiovascular risk. One of the pursued targets, is to customize an ambulatory available technology to measure the state of heart's health in a continuous, no invasive and reliable way.

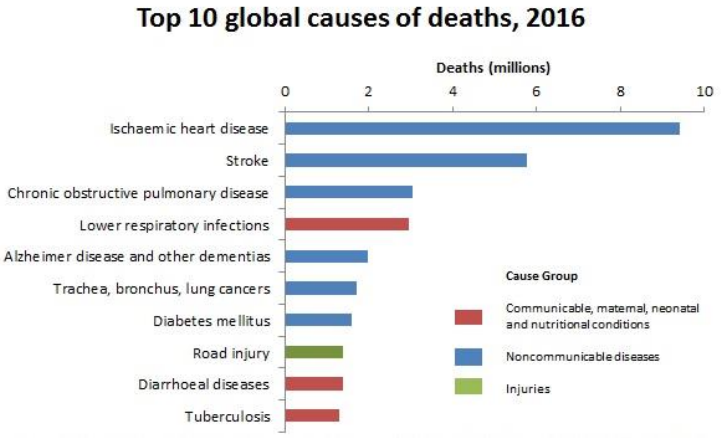

Figure 1.1 Histogram with the top ten global causes of deaths in 2016 [1].

In particular, the expectation of medical community is the possibility to have available a low cost and easy to use device. On medical devices market there is a clear transition toward low development and production costs. The statistics show that the medical equipment industry is in its highest growth in history especially in the developed countries, i.e. Western Europe and the USA. So, as the growing demand of healthcare technology is obvious, the corresponding market requires high quality and high performance products. Today, Healthcare technology is composed by a wide range of equipment with increasingly complex technologies, but the costs must be lowered. In fact, as Krishnan and Atal [2] said,

"*The costs of current high end medical devices could be lowered by 40% without damaging the functionality of the products*"

The explained considerations highlight the usefulness of this thesis work. As of today it is not available on the market a low-cost and easy to use device for assessment of cardiovascular risk, so the aim of this work is to developed a reliable systems for Pulse Wave Velocity (PWV) parameter extraction.

This hemodynamic parameter, that allows to evaluate the pulse wave propagation velocity along the arterial tree, because of its relative ease in acquisition and its perceived reliability, PWV has emerged as the gold standard method to asses arterial stiffness. In fact, usually some of the patients affected by cardiovascular diseases do not have early symptoms, but changes in arterial stiffening can be already detected in the firsts stages of the event development. For this reason, PWV estimation has been considered as step of clinical routine assessment of patients.

Over the years, several techniques have been implemented to extract PWV in a non-invasive way, but all have one or more potential drawbacks. Some equipment, like magnetic resonance(MRI) and ultrasonic sensors, are very often used in a hospital environment although they are rarely employed by the population. The just mentioned techniques, are very expensive and complex to use, and for this reason, new simplified procedures have been adopted to detect the PWV. Pressure sensors, such as the tonometer, are considered the gold standard method; however, this technique is regarded as difficult to use because the operator's skills may influence the measurement. For this reason, pressure sensors are mainly employed by a limited number of skilled operators in clinical environment.

The aim of this thesis work is to investigate a low-cost, handy and easy to use system for PWV parameter extraction, possibly not impacted by operator skills. For this purpose, phonocardiogram signal has been chosen to be analysed and compared with others signals and with the today golden standard. In particular, PCG, Electrocardiogram (ECG), Arterial Pulse pressure (used as reference) and Accelerometer signals have been extracted. The developed prototype allows simultaneously collection of each signals for both distal and proximal sites, by using a proper designed conditioning circuits. Then, signals are acquired and converted by using a STMicroelectronics evaluation board and data are transferred to a laptop by means of a USB interface. Finally, the acquired waveforms are analysed and evaluated in Matlab numerical computing environment for features and parameters extraction purpose. It is possible to see the final configuration system in *Figure* 1.2.

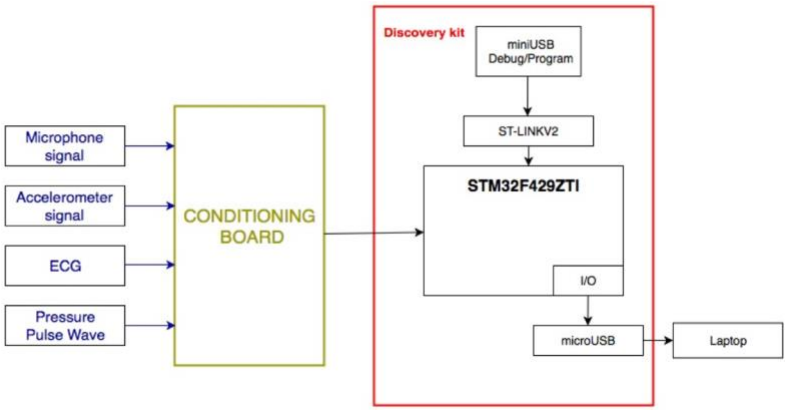

Figure 1.2 Block diagram of final configuration.

In detail, this thesis is organized as explained below:

- *Chapter 2:* ***Background***

  In the first part of the work, the state of the art concerning addressed topics, will be presented and described. In particular, human body characteristics, all the used electronic components, and the collected signals will be explained. ECG, phonocardiogram, Pressure Pulse wave and accelerometer signals are described and all the required mythologies for their acquisition are listed and analysed.

- *Chapter 3:* ***Signal Acquisition***

  This Chapter presents the implementation of the circuit that allows sensors signals acquisition: ECG electrode, MEMS microphones, MEMS accelerometer and Tonometer. In particular, the required sensors conditioning, must be made to extract only the useful signal frequency ranges and to perform a proper amplification; in this way, it is possible to take advantage of the ADC input dynamic range. In additions, this section describes the Firmware implementation and signals synchronization strategies.

- *Chapter 4:* ***Signal Analysis***

  In this chapter, all the signal analysis related to the features extraction will be explained. First of all, the addressed signals will be analysed: they will be firstly filtered and then, their characteristics will be extracted for PWV parameter detection purpose. In detail, all the algorithms implemented for the signal processing and feature extraction will be presented and described, several approaches will be compared and basing on the collected results the most reliable solution will be addressed.

- *Chapter 5 :* ***Final system prototype***

  In this section, the last developed prototype is presented. In particular, a lot of hardware adjustments will be applied and the conditioning circuit will be improved with the purpose to address the discovered problems and limitations. In additions, this system will be compared with the gold reference in terms of shape repeatability and characteristic stability. Finally, a quality check procedure will be developed to provide an indication between reliable and not reliable acquisition conditions.

- *Chapter 6:* ***Conclusion and future developments***

  In this last chapter will be illustrated all the deductions and possible future developments.

Chapter 2

Background

2.1 Anatomy and Physiology of Cardiovascular system

The Cardiovascular system is a set of organs and vessels, that transports blood through all the body, from the central organ (heart) to periphery (capillary), removing carbon dioxide and other wastes and bringing nutrients and oxygen. The main vessels types are arterial and venous and, with the heart, they compose the whole system; this consists of two circuits: the pulmonary loop and the systemic loop.

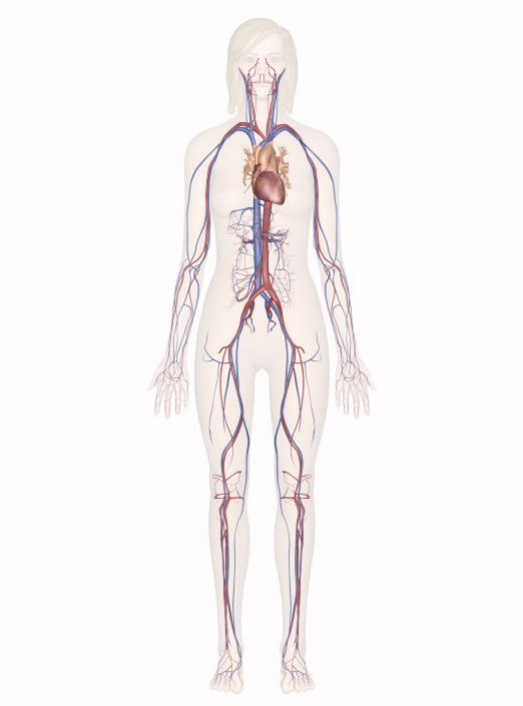

Figure 2.1 Circulatory circuits of human body composed by pulmonary and systemic loops *[3]*

The entire blood path starts in the arteries which receive the oxygenated blood at high velocity and pressure and transport it around the body. The blood passes through different sizes of arteries: from the aorta, the biggest one, to the arterioles and the capillaries, the final microscopic branches of arteries, where cellular nutrients are distributed and waste products are received. The deoxygenated blood, loaded with waste products, flows from capillaries to the venous systems. This capillaries-fusion forms venules and finally veins that converge into superior and inferior venae cavae. The two final main veins allow deoxygenated blood back to the heart [3].

The three primary functions of the human cardiovascular system are listed below.

- *Means of protection*: Circulatory System performs a protective action through white blood cells, which clean up cellular debris and delete pathogens that may have entered the body. In addition, red blood cells and platelets operate to protect wounds. Among other things, blood also transports antibodies, which provide selective protection from pathogens to which the body has already been exposed to;
- *Means of regulation*: the circulatory system helps to monitor body temperature and to keep it stable, by controlling the blood flow. Blood can help to regulate the body PH, that may be altered for the presence of sodium bicarbonate, which acts as a buffer solution;
- *Means of transport*: Circulatory System allows blood transport along the body and this permits to carry nutrients, oxygen and hormones.

Heart physiology

The *heart* is the most important organ of the cardiovascular system. It has an average size of about 13×9×6 centimetres and a weight of approximately 300 grams. With a cone shape and a wide base direct right and down, the heart has a peak that points to the left and towards the bottom. It is located in the chest cavity between the lungs, behind the breastbone and in front of the windpipe; in particular, the heart is situated above the diaphragm and more than half of it is located to the left of the centre line [4].

The human heart consists of two parts and each in turn is divided into a couple of chambers; there are two upper rooms, called *Atria,* and two lower rooms, called *Ventricles*. The first pair is separated by *Interatrial Septum,* while the second are divided by *Interventricular Septum*. In general, blood goes into Atria and then passes into Ventricles, which push it to the lungs, and finally to the rest of the body. The connection between chambers is regulated by four valves.

Two valves are called *atrioventricular (AV)* and allow blood to pass from atria to ventricles; at the same time, they prevent it from flowing backwards. The second two, called *semilunar (SM)*, permit blood to enter the pulmonary and systemic circuit; they as well avoid blood from reflux.

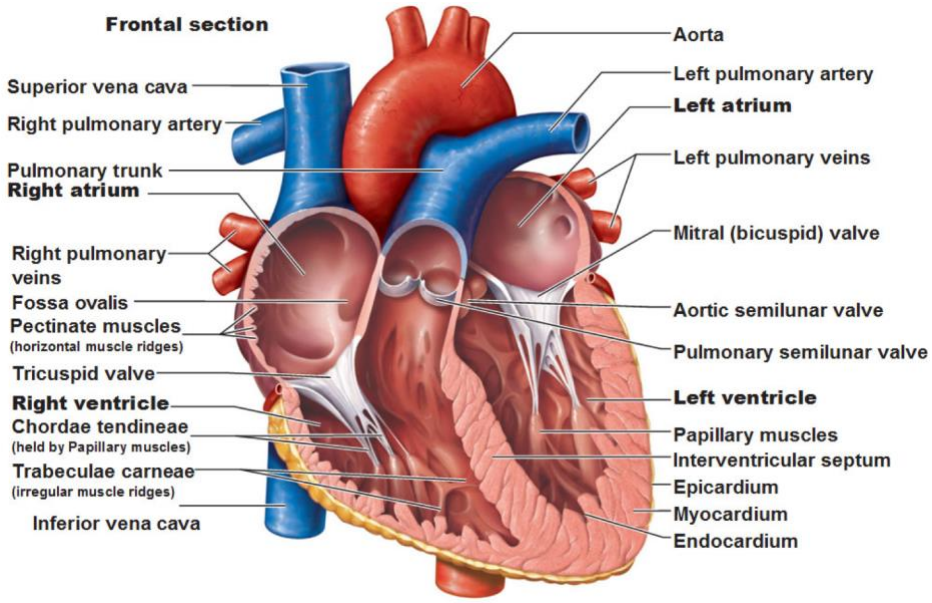

Figure 2.2 Cross-Section image of the heart anatomy (4)

The heart is contained in the *Pericardium*, a membrane that keeps this organ suspended inside the chest. *Fibrous pericardium* is the outer portion of the sac attached to the diaphragm at the bottom and sternum at the front. Between the lungs there is a space, called *Mediastinum*, surrounded by pericardium and *Mediastinal Pleura*; this is the same lining of the thoracic cage. Mediastinum contains the heart and operates as a thoracic cavity divisor. There are two layers of serous membrane that encase the heart: the first portion, known as *Parietal Pericardium,* covers the fibrous pericardium, while the second portion wraps the heart and is called *Visceral Pericardium* [4]. A fluid, called *Pericardial,* is produced by serous membranes to separate and lubricate the two membrane layers at every heartbeat. By so doing, it allows surfaces to flow smoothly one over the other

Cardiac Cycle

The cardiac cycle is defined as the time span between the ends of two successive heart contractions; it consists of an Atria contraction followed by a Ventricular relaxation. In particular, a chamber contraction is called **systole**; whereas a chamber relaxation is called **diastole**.

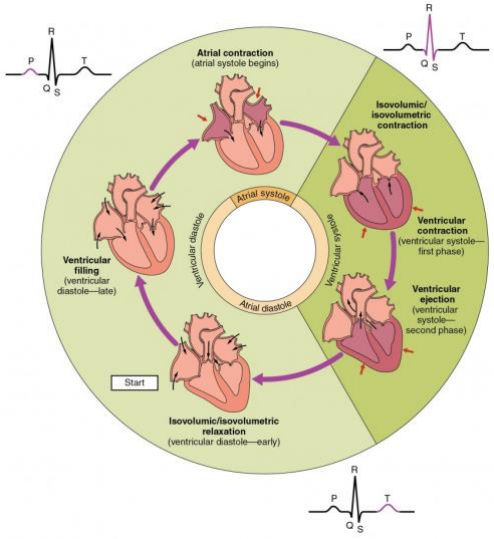

Figure 2.3 Cardiac Cycle [5]

As shown in *Figure* 2.3, for both right and left heart sections five different steps are individuated.

1- *Atrial Systole*

Along this period atria contracts and blood flows back to the ventricle across the AtrioVentricular Valves (AVV). The SemiLunar Valve (SLV) are instead closed [5].

2- *Isovolumetric Contraction*

The blood is collected by the ventricles and their pressure increase because internal volume remains the same. In this steps both AVV and SLV are closed.

3- *Ventricle Ejection*

Blood allows SemiLunar valve to open when the intra-ventricle pressure exceed the one outside. In this phase, semilunar and atrioventricular valves are respectively open and closed, so blood run into the artery and the vessels pressure increase.

4- *Isovolumetric relaxation*

At this point the “wash out” phenomena occur: blood goes to the artery except a little quantity that comes back to the ventricle. Consequently, SLV close and the ventricle pressure decrease.

5- *Ventricle filling*

AtrioVentricular valve open when the arterial pressure exceed the ventricle one. In this way blood easy flow to the ventricle without the need of contractions. In this step semilunar and atrioventricular valves are respectively closed and open.

During a single cycle, artery pressure is kept constant, but during the whole cardiac cycle it increases and decreases; in particular the diastolic pressure is between 60 to 80 millimetres of mercury, while normal systolic pressure ranges between 90 and 120 millimetres of mercury [5]. Finally, all the mentioned phases are regulated by pacemaker cells, which produce a series of specific electrical impulses.

Cardiac rhythmicity

The inherent rhythmicity of the cardiac muscle permits to get regular heartbeat by itself; indeed the outside regulatory mechanisms are not essential to excite the heart to contract.

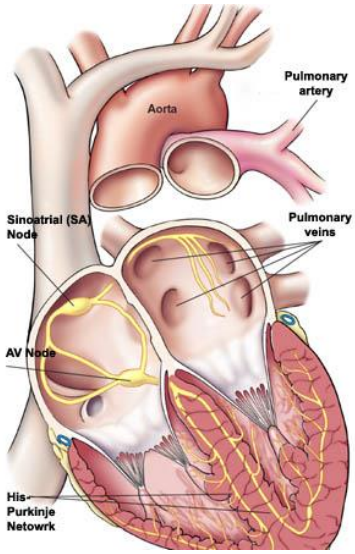

Figure 2.4 Heart's electrical system [6]

The heart actuates a periodical *Cardiac Action Potential* propagation: to have a correct behaviour, this important organ needs an autonomous coordination maintained by its internal conduction systems. This system is made up of tissue masses and nerve conductors; the former generate impulses, while the latter make it possible their transmission.

The initialization is implemented by the “pacemaker”, some specialized self-excited cells capable to have spontaneous depolarization: when a voltage threshold is outdated, action potential is generated. These cells are called Atrial node(SA), Artrio-Ventricular node(AV), Bundle of His and Purkinje Fibers. In particular, the Atrial node pacemaker is situated at the top of the right atrium and it is the initiator that allows contraction. The nerve conductors are composed of terminations that reach to ventricles and permit pulse to pass from the Atrial node into the Atrio-Ventricular node (5). This second pacemaker is situated at the bottom of the right atrium, in the lower area of interatrial septum. Once the AV node is overcome, the impulse spreads through *Bundle of His* into the *Purkinje Fibers*, situated all over the ventricles.

2.2 Electrocardiogram signal

The Electrocardiogram (ECG) signal is a graphical representation of the bio-potential variations over time and it produces a visual interpretation of transthoracic heart activity [7]. This type of analysis is the most ordinary clinical cardiac control; it is inexpensive, simple, risk-free and it is a useful detection tool for several cardiac abnormalities.

Every heart beat consists of a specific electric wave sequence. Thanks to this signal, ECG is able to provide the user with two types of information. The first, is the duration of the electric wave that passes through the heart, while the second is the amount of electrical activity that passes through it. As far as the former is concerned, information is obtained about the regularity of electrical activity, while the latter permits to evaluate the amount of charge within the heart.

ECG signal has a frequency range of about 0.05-100 Hz, while its dynamic range is 1–10 mV. Normally, the heart cycle frequency goes from 60 to 100 beats per minute (bpm); when bpm is low, there is bradycardia, otherwise when it is high, tachycardia occurs.

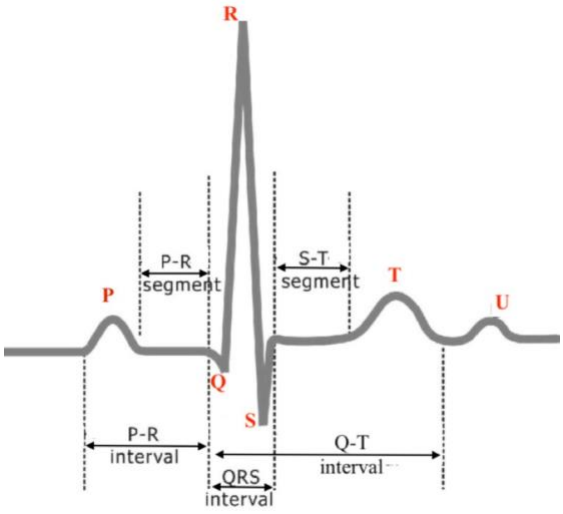

Figure 2.5 ECG signal and corresponding cardiac cycle phases [5]

Each ECG signal consists of 5 peaks identifiable with the letters P, Q, R, S, T, as shown in *Figure* 2.5; in some cases the U wave is also present [7]. The P wave, QRS complex and T-wave represent electrical depolarization and repolarization of the heart due to atria and ventricle contraction.

In particular, each peak has a specific meaning:

- P-wave represents the atrial depolarization, that allows their activation;
- QRS complex gives the final information about atrium repolarization and ventricle depolarization, which occur simultaneously. Its normal range is up to 120 ms;
- T-wave represents ventricular repolarization.

Between the described wave, their ranges are useful to identify a normal or an abnormal situation. The time interval PR is measured from the P wave to QRS complex and it is normally comprised between 120 and 200 ms. On the other hand, the QT interval, on the other hand, is evaluated from the beginning of QRS complex to the end of T-wave and its normal range can reach 440ms.

For cardiac disease detection, also the peak shape has to be analysed: in fact duration, amplitude and morphology give information about arrhythmias, conduction abnormalities and myocardial infections [8]. The *Table* 2.1 shows the abnormal characteristics of ECG signals and the corresponding diseases.

Table 2.1 Abnormalities on the ECG (7)

ABNORMALITY	CHARACTERISTICS
Bradycardia	peak-peak interval>1s
Tachycardia	peak-peak interval<0.6s
Hypercalcaemia	QRS interval<0.1s
Dextrocardia	Upset P-wave
Hyperkalemia	High T wave and no P wave
Sudden cardiac death	Irregular ECG
Sinoatrial block	Complete drop out of a cardiac cycle
Myocardial ischemia	Upset T-wave

2.2.1 ECG detection

Heart action potential registration must be carried out with at least two electrodes applied in non-equipotential places on the human body surface. The shape of the recorded signal depends on the electrodes location and, for this reason, it is important to standardize their position.

The first who took care of this location problem is *Wilhelm Einthoven* (Medicine Nobel prize in 1924), who schematized the human body as a conductor containing an electrical cardiac source. The electrical heart activity can be approximated as a dipole and, as such, it can be represented by a time-varying vector (H) that cyclically changes its intensity and direction. *Wilhelm Einthoven* placed electrodes at the top of an equilateral triangle that contains the heart; in this way, ECG detection depends only on physiological conditions. This electrode position provides the time trend of H-vector projection along the three frontal plane directions. Current doesn't flow along equipotential arms, so the potential at their ends (V_A, V_B and V_C) is the same in points A, B and C. Besides, electrodes constitute knit's knots and by applying the Kirchoff principle (in a closed mesh the sum of the potential differences must be zero), it is possible to deduce one derivation value knowing the others [9].

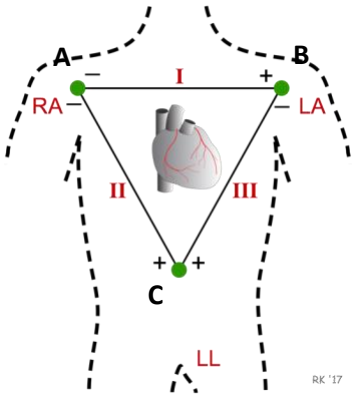

Figure 2.6 Einthoven trinagle

The triangle in *Figure* 2.6 is known as *Heinthoven triangle* and the points A,B and C are identified respectively as Right Arm (RA), Left Arm (LA) and Left Leg (LL). Finally, the connection between these points are identified by three versors: a_I, a_{II} and a_{III}.

The vector-H projection on the a_I, a_{II} and a_{III} direction, detects scalar quantities V_1, V_2 and V_3 according to the relation:

$$V_i = H \times a_i \qquad \text{with i=1,2,3}$$

In particular:

- V_1 represents the first derivation (I), ddp between RA and LA;
- V_2 represents the second derivation (II), ddp between RA and LL;
- V_3 represents the third derivation (III), ddp between LA and LL;

Electrocardiograph provides these scalar value, called *Standard Derivation*. H-vector decomposition has been hypothesized in the directions defined by the Einthoven triangle, and the registration of at least two of the three derivations allows the vector reconstruction [9].

G.A.Wilson has developed electrodes configuration using *Wilson's central terminal* (W) as reference point that is connected to each electrode with 3 equal resistors. W in this case, represent the three derivations potential mean.

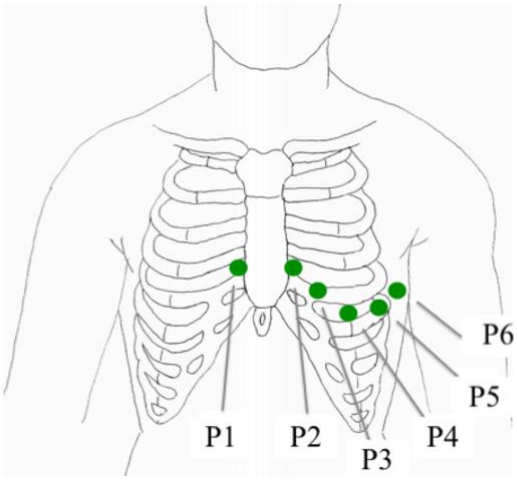

Figure 2.7 Position of precordial derivation

Using an *exploratory electrode*, potential differences with respect to W are evaluated in defined sites, called P_1, P_2, P_3, P_4, P_5,and P_6. As shown in *Figure* 2.7*,* they have specific anatomic position:

- P1: fourth intercostal space, to the right of the sternal margin;
- P2: fourth intercostal space, to the left of the sternal margin;
- P3: halfway between P1 and P2;
- P4: in the fifth intercostal space;
- P5: on the anterior axillary line aligned with p4;
- P6: externally aligned with P4 and P5.

These potential differences are called *Precordial Derivations* and are indicated with V_1, V_2, V_3, V_4, V_5, and V_6. These derivations reflect the whole heart activities and allow to obtain more information about H-vector position [9].

Another important diagnostic information is provided by the *Increased Derivations*, which use the same detection points of *Standard Derivation.* The derivation is carried out between reference potential V_W, obtained through two of the three electrodes, and the third electrode, as show in *Figure* 2.8.

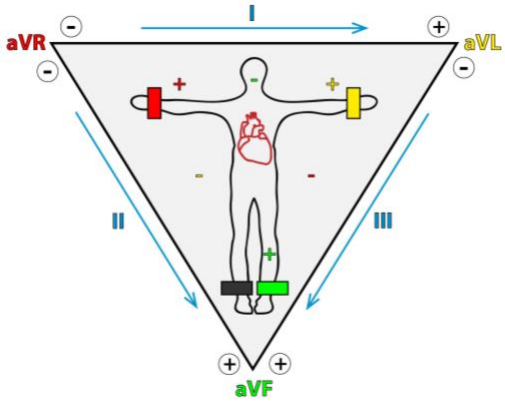

Figure 2.8 Increased Derivation

They are called *increased* because, in reference to the Wilson circuit, the ddp between W and its corresponding limb increases of about 50% due to the R elimination [9].

Thess derivation can be calculated according to the Standard derivations, with the equations below :

$$aV_R = -\frac{1}{2} \times (I + II)$$

$$aV_L = \frac{1}{2} \times (I - III)$$

$$aV_f = \frac{1}{2} \times (II + III)$$

2.3 Pressure Pulse Wave

The *Pressure Pulse Wave* is the result of the cardiac impulse which propagates through the cardiovascular system, causing an arterial wall expansion and narrowing. Normally, while heart pushes blood along the Aorta, a pressure changes is generated. This pressure wave is reflected and pushed back mainly by the arteriole, which provides the majority of peripheral vascular resistance [10].

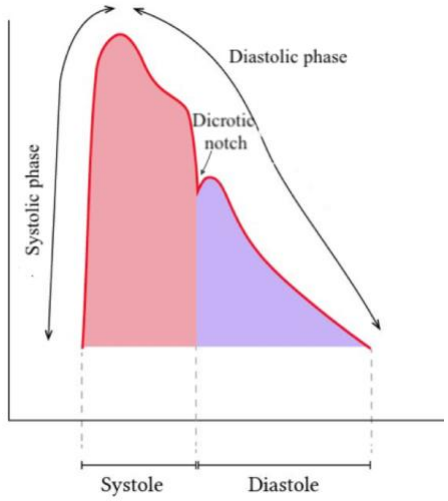

Figure 2.9 Arterial Pulse and its three phases

As show in *Figure* 2.9, it is possible to separate the arterial pulse waveform into three different components [11]:

- The *Systolic phase*, which begins with aortic valve opening and corresponds to left ventricular ejection, is characterised by rapid increase in pressure, followed by rapid decline;
- The *Dicrotic notch* indicates aortic valve closure;
- The *Diastolic phase* indicates blood runs off into peripheral circulation.

In *Figure* 2.10 the relationship between ECG and arterial pulse wave is shown [11].

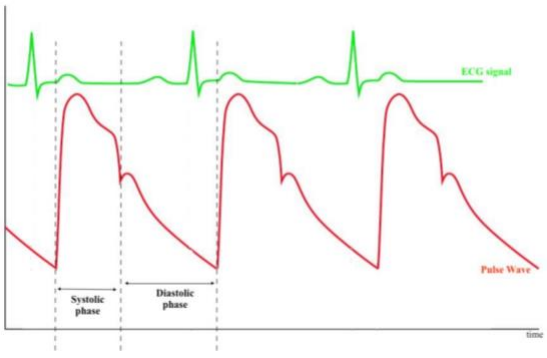

Figure 2.10 ECG and Arterial Pulse Wave compared at the same time [11]

Placing a pressure sensor on the skin, in correspondence with an arterial vessel, a displacement signal due to vessel wall tension alteration could be detected. This collected pressure variation is similar to the pressure impulse generated by the left Ventricular wall tension during contraction.

Laplace relationship, which governs wall tension, explains how this phenomenon could be detected. But, if the cover of the vessel has a thickness, as shown in *Figure* 2.11, the correct correlation is:

$$Tension = \frac{P(pressure) \times R(radius)}{2 \times h(height)}$$

The vessel tension is directly related to the pressure inside it and to the arterial radius, while it is inversely correlated to the height of the vessel wall [12].

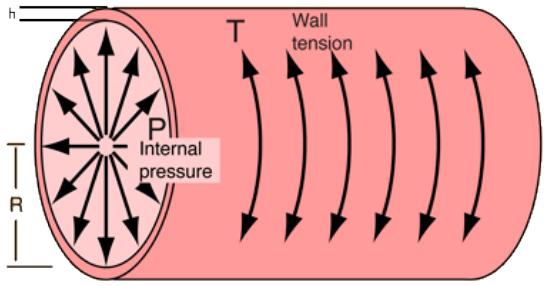

Figure 2.11 Vessel representation as a cylinder witht a wall that has a thickness

Thanks to this relationship it is possible to conclude that the tension change is due to various causes. As a matter of fact, the largest amount of expelled-blood volume occurs in *early and mid-systole* and for this reason, the result of changes in both volume and pressure causes major change in tension. However, the predominant effect during the *last part of the systole* and during the *diastole* is mainly due to pressure changes.

The *pulse rate* is influenced by a lot of common factors, such as age, emotional status, environment, exercise etc. In particular, the shape of the arterial pulse changes when it passes from central aorta to peripheral arteries. If the distance between heart and peripheral artery is large, distortion of peripheric arterial pulse will be notable. This impulse deformation is firstly due to the occurrence of different wave types in the same peripheric vessel (reflection) and, secondly, to the different elastic characteristics and the diameters of peripheral arteries [11].

2.3.1 Pulse detection and location

The cardiac impulse, which propagates through the cardiovascular system, is the results of the heart beating, causing an arterial wall expansion and narrowing. Normally, while heart pushes blood along the Aorta, a pressure changes is generated. This is due to the blood flow, which impacts on the vessel elastic walls; this pressure wave, continues along all the arteries. For this reasons, the pulse could be perceived in the other surface of the skin, for the arteries that are more exterior (i.e. in the neck the carotid pulse could be detected) [13].

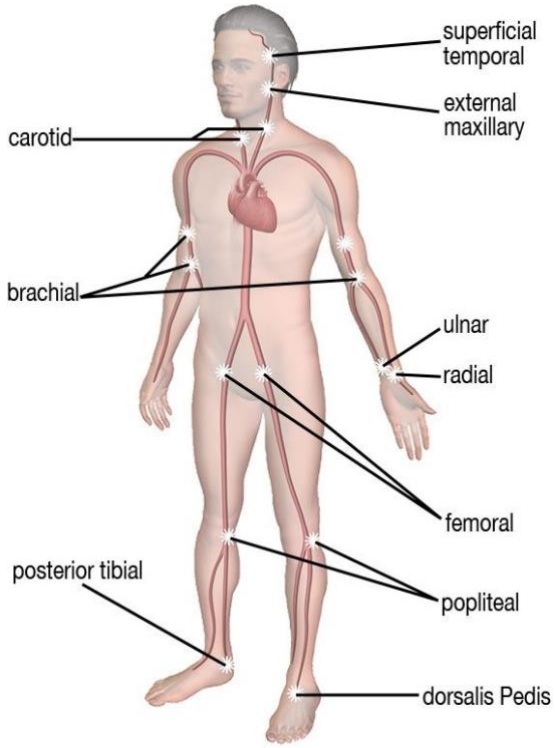

Figure 2.12-Pulse location

There are several points in the body skin where pulse can be more identifiable, as shown in *Figure* 2.12. These points of interest are: (i) at the side of artery close to surface; (ii) where the maxillary artery crosses the maxillary bone; (iii) at the point where the temporal artery passes close to surface; (iv) at the side of the neck; (v) on the brachial artery, which is situated in the inner part of the biceps; (vi) from the femoral artery; (vii) from the popliteal artery, which is situated behind the knee; (viii) from the dorsalis pedis artery located on the top of the foot.

2.4 Phonocardiogram signal

The Phonocardiogram (PCG) signal is a visual representation of sounds correlated with the heart pumping action [14]. These sounds are generated by vibrations set up in the blood inside the heart due to the abrupt closing of the valves, the motion of the heart wall and the turbulence and variation of the blood flow.

When the valves close normally, an ordinary heart sound is recorded, as shown in *Figure* 2.13*a*, whereas, when the blood flow becomes turbulent, as in the case of valve narrowing, a sound called *pathological murmurs* is detected (*Figure* 2.13*b*). This type of sound is the most common abnormal behaviour recorded in the heart. It is possible to distinguish this sound from the normal one because it has a longer duration and is much noisier. Turbulences could also be caused by other behaviours, such as local obstructions, diameter variations or valve insufficiency [15].

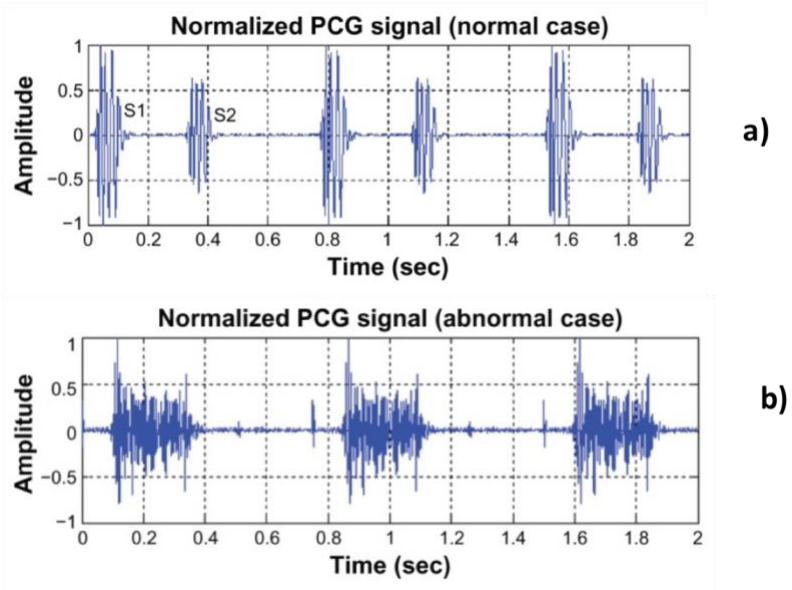

Figure 2.13 Normal(a) and abnormal(b) PCG signal [16]

It was discovered that this sound transcription could overcome some of traditional auscultation disadvantages. First of all, PCG is able to provide important information about the health state of the heart and its valves. Moreover, this signal allows to provide important information about valve disorders. In fact, cardiologists very well know the typical shape of PCG and any significant variation is considered symptom of pathology.

Despite obvious advantages, phonocardiogram signal for clinical diagnosis also has some negative aspects. For example, its interpretation is very difficult because many variables have an influence on the generation and transmission of heart sounds. Furthermore, during auscultation noise or artefacts could be present and these two phenomena can affect the normal sound shape [17].

2.4.1 Analysis of spectral characteristics

The basic cardiac sound signals are made up by four sounds; two of these are more recognizable and are called S1 and S2, while other two have lower amplitude and are called S3 and S4, as shown in *Figure* 2.14. These sounds has a short duration of about 0.8ms which include 0.4ms due to S1 and S2 and the last 0.4ms due to S3 and S4.

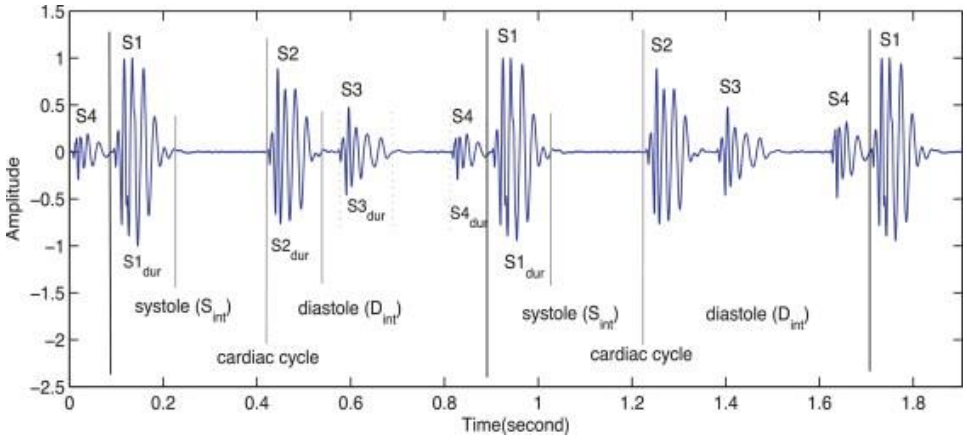

Figure 2.14- phonocardiogram signal

The sound S1 contains information about Mitral and Tricuspid valves closure. It is generated in the second part of Atrial contraction and in the first part of Ventricular contraction.

The sound S2 occurs in correspondence of semilunar valves closure: aortic valve and pulmonary valve.

The S3 and S4 correspond to the end of ventricle filling and at atrial contraction, respectively. They are characterized by very low frequencies and amplitudes.

These sounds cover a wide range of frequencies, from 15 to 700 Hz. It is possible to distinguish two different ranges of interest: normal heart sounds and heart murmurs. The first interval

ranges between 20 and 200 Hz, while the second from 30 to 700 Hz. Moreover, murmurs have some frequency components inside normal cardiac sounds [18].

Table 2.2- Frequency characteristics of some inter-cardiac sounds [19]

Cardiovascular events	Frequency range (Hz)
S3 and s4 sound	From 15 to 65
S1 and s2 sound	From 20 to 200
Mitral stenosis	From 40 to 80
Ejection murmurs	From 200 to 400
Regurgitation or insufficiency	From 250 to 700

There are a lot of frequency overlaps between pathological and normal sounds; for this reason it is very difficult to extract murmurs and classify them only by their own frequency information.

2.4.2 Review of feature extraction technique

The already existing post-processing methods to identify repeatable characteristics in the phonocardiogram wave are based on PCG extracted from the chest; for this reason signals present well distinguishable s1 and s2 waves. The most important techniques for S1 and S2 extraction will be explained below.

There are a lot of studies based on Gabor spectrum, Fourier transform (FT) or short-time Fourier transform (STFT), soft-computations and probabilistic methods.

As well as in many other recent article, in research made by Ari et al. [20], an energy-based technique was used with the purpose of PCG boundary determination and sound detection. Another example is the method developed by Cherif et al. [21] or by Choi et al. [22]. In these manuscripts the extraction of cardiac sounds information in time-frequency domain was used to recognize different heart sounds. Finally, the research made by Choi, Jian et all. [23] compares methods for sound shape extraction in order to make a cardiac sound signal segmentation. For the characteristics extraction, was used: the energy of Shannon after being normalized, the information given by the envelope of the Hilbert transform and, finally, the characteristic waveform of the cardiac sound. In particular, the analysed methods allow to extract envelope curves thanks to the time elapsed between the first and the second heart sound.

The abovementioned literature review proves that frequencies and amplitudes are two determinative features for cardiac sounds detection and identification. However, the most of cited manuscripts focus mainly separately on either amplitude or on frequency contents.

2.5 Pulse wave velocity

The *Pulse Wave Velocity* (PWV) allows to evaluate the pressure wave propagation velocity along the arterial tree; it is a cardiovascular parameter defined as a measure of arterial vessel stiffness [24]. As said before, a pressure wave is generated during systole, due to aortic wall contraction and dilatation, and then it moves along the whole arterial tree. The state of health is given by the speed of this movement.

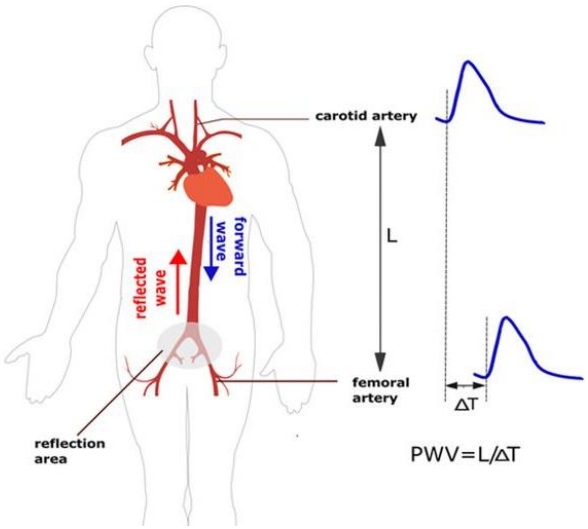

Figure 2.15 PWV detection scheme

Commonly, PWV is measured using two pressure sensors situated in a peripheral site (distal point) and near the heart (proximal point), and placed at pre-defined distance from one to another; this length is called *Pulse Wave Distance*. The time that the wave takes to transit from one sensor to the another, is called *Pulse Transit Time* (PTT).

Distance is divided by this calculated time and PWV is obtained:

$$PWT = \frac{Pulse\ Wave\ Distance}{PTT}$$

Several clinical devices usually uses different acquisition sites and different signals to calculate pulse wave speed. Traders and doctors have a conflictual opinions about which points have to be used. The former consider heart as proximal and fingers as distal points. By contrast, the latter consider carotid and femoral artery as proximal and distal points respectively (*Figure* 2.15).

Thanks to several studies carried out, this velocity value has been defined as a highly reliable parameter capable to predict cardiovascular mortality. It is effective on a large variety of populations, such as adult and children, and in a great quantity of diseases, such as renal disease and diabetes [25]. The PWV depends on the subject's age: the older the patient, the stiffer the vessels and the higher is the speed, at which the wave will propagate. The normal value of Carotid-Femoral PWV for each age group in a sample population, can be seen in the table below (*Table* 2.3).

Table 2.3- normal value of mean PWV for different age group [26]

Age group (years)	*n*	Mean PWV (m/s)	SD	95% CI Lower-upper limit	Range
10–19	156	5.04	0.72	4.92–5.15	3.12–7.33
20–29	110	5.86	0.92	5.68–6.03	3.92–8.14
30–39	109	6.32	0.82	6.16–6.47	4.08–8.26
40–49	108	6.85	0.91	6.68–7.03	5.0–9.84
50–59	164	8.15	1.17	7.97–8.33	5.46–12.5
60–69	103	8.47	1.09	8.25–8.68	6.46–11.2
>70	30	9.01	2.00	8.27–9.76	5.52–13.4
Total	780	6.84	1.65	6.73–6.96	3.12–13.4

2.5.1 Device for PWV measurement

Over the years, several techniques have been implemented to extract features from the cardiovascular system in a non-invasive way. Some devices, unlike magnetic resonance(MRI) and ultrasonic sensors, are very often used in a hospital environment although they are rarely employed by the population. The just mentioned techniques, are very expensive and difficult to use, and for this reason, new procedures have been adopted to detect the PWV. Pressure sensors, such as the tonometer, are considered the gold standard method; however, this technique is regarded as difficult to use because the operator's skills may influence the measurement. For this reason, pressure sensors are mainly employed in research [27].

In the early years of current century, different types of devices were designed for PWV non-invasively evaluation as can be seen in *Table* 2.4.

Table 2.4-Review of PWV measurements methods

Method	Devices	Path length
Applanation tonometry	*SphygmoCor* (AtCor Medical)	(Carotid-notch) – (femoral-notch)
	PulsePen (DiaTecne)	(Carotid-notch) – (femoral-notch)
Piezoelectric mechanotransducer	*Complior* (Alam Medical)	Direct distance from carotid to femoral site
Cuff-based Oscillometry	*SphygmoCor Xcel* (AtCor Medical)	(Thigh cuff-notch) – (notch-carotid) – (femoral-cuff)
	Arteriograph (TensioMed)	Direct distance from jugulum to symphysis
	Vicorder (Skidmore Medical)	Direct distance from sternal notch to thigh cuff
Photodiode sensor	*pOpmètre* (Axelife SAS)	$k \times$ subject's height
EcoDoppler	*Ultrasound*	Direct distance from the two Doppler recording points
MRI	*Magnetic resonance imaging*	MRI images
Invasive method	Vascular sheath with pressure sensors	Radiographic images

SphygmoCor® (AtCor Medical, Sydney, Australia), calculates PWV with carotid and femoral arteries pulses analysis. This instrument estimates the delay between tonometer signal and ECG waves. The SphygmoCor, shown in *Figure* 2.16, allows to perform PWV measurements with two phases. Initially the carotid wave and the ECG signal are recorded simultaneously and, in a second moment, the femoral and ECG waves have to be recorded. Thanks to ECG this instrument is able to synchronize different time of the two pressure waves [28]

SphygmoCor Xcel® device (Xcel, Atcor Medical, Australia) is a new SphygmoCor device that allows femoral and carotid signals to be acquired simultaneously. In this case, carotid pulse waves are measured by applanation tonometry, meanwhile a swollen cuff, positioned around the upper part of thigh, captures femoral pulse. The PWV is obtained with the measurement time between these two signals [29].

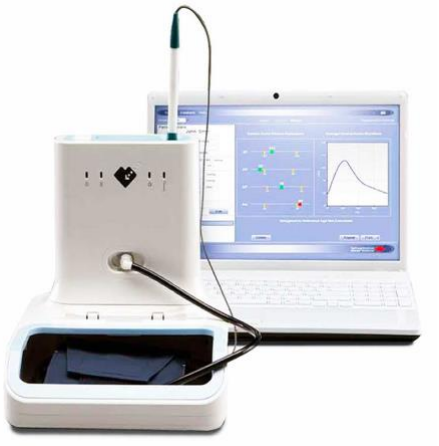

Figure 2.16-SphygmoCor

The *PulsePen*® (DiaTecne, Milan, Italy) consists of two parts: a tonometer and an integrated electrocardiogram (ECG). It allows to measure in a unobtrusive way the carotid and femoral pressure and the relative wave speed. It also provides other parameters such as blood pressure, pressure wave shape, pressure wave estimation and PWV [30, 18].

Figure 2.17-PulsePen

The *Complior*® (Colson, France), exploiting the piezoelectric affect, uses two mechanical pressure transducers. They are directly applied to the skin and allow instantaneous measurement of pressure impulses. This instrument uses two probes positioned on two different

arteries, commonly carotid and femoral, but it also allows to measure the PWV among different sites such as carotid–brachial and femoral–dorsalis pedis [28].

Figure 2.18- Complior

Arteriograph® (TensioMed, Budapest, Hungary) records oscillometric pressure curves by plethysmography to estimate PWV at an upper arm artery [28]. The artery pressure under cuff varies periodically, and oscillometric method records these oscillations. It provides an indirect measurement of the pressure wave period.

Figure 2.19-Arteriograph

The *Vicorder*® system (Skidmore Medical, UK) is an automatic device that uses cuffs places in a proximal and distal position of the interest area. To evaluate the carotid-femoral PWV, a cuff above the neck (at the right carotid height) and a larger cuff around the right upper part are used. As the cuff inflate to 65 mmHg, pulse wave is registered and transit time can be computed [31].

The *pOpmètre*® (Axelife SAS, France) is a tool that uses photodiodes as sensors. The device measures the time that impulsive waves spend to pass from finger until the tip. PTTs are continuously measured for 20 seconds and useful indices are extracted [32].

Despite the disadvantages mentioned above*, Image techniques* – ultrasound and magnetic resonance – are a good solution for the detection of cardiovascular signals, as described in the follow. They even work in problematic situations such as when it is necessary to acquire features on subjects with fat storage.

- *Ultrasound*

With US technique it is possible to detect PWV. This method uses the delay estimation between two Doppler waveforms that must be recorded at the same time and in two near points along the vessel. This method is effective thanks to high sampling frequency and to reliability of waveform foot. The distance between two points of the Doppler recording is measured over the body surface with a flexible measuring tape. [33].

- *Magnetic resonance*

With magnetic resonance it is possible to detect PWV, using blood flow velocity. This technique has high temporal and spatial resolution, is non-invasive and does not use geometric hypotheses. It also allows direct imaging of thoracic and abdominal aorta [34].

2.6 Employed Devices and Tools

In order to perform the PWV parameter extraction with a minimally invasive and inexpensive approach, some useful devices produced by STMicroelectronics have been used.

The adopted devices are listed below:

- The *HM301D* fully integrated, front-end chip for ECG application, allows ECG signal to be directly acquired by using a single derivation.
- The *STM32F429* based Discovery Kit permits to control: the ECG front-end configuration, the analog microphones MP33AB01H for PCG data acquisition, the ST tonometer LPS35HW for Pulse Wave data detection and the ST accelerometer MKI174V1 for the displacement signal acquisition.

- The *embedded USB* interface controller that allows PC data transfer.

In addition, two software are used for the algorithm implementation, debug and optimization: *Matlab™ R2018a* and *Keil-µVision5.* Another program is used to allows microcontroller to Interface data transfer: *VisualStudio*. All hardware and software tools are detailed in the following paragraphs.

2.6.1 Analog Front End HM301D

The STMicroelectronics HM301D is a highly integrated front-end chip for ECG applications. Thanks to the SPI interface, if a chain link exists, it is possible to exchange data between microcontroller and several HM301D devices.

This type of front-end is a bio-potential acquisition device that consists of 3 differential and one impedance channel. Adopting its master/slave configuration capabilities, it is possible to build a system featuring 16 simultaneous acquisition channels can support up to 16 input channels. The HM301D device has a completely integrated analog high-pass filter that deletes the DC component of the signal; simplifying in such way the further signal processing which can address inly the AC component. For each channel, the HM301D guarantees high resolution and low noise conversion for bio-potential signals up to 10 KHz. In addition, every channel grants a flexible cables and electrode configuration reducing the effort required for complex system implementation.

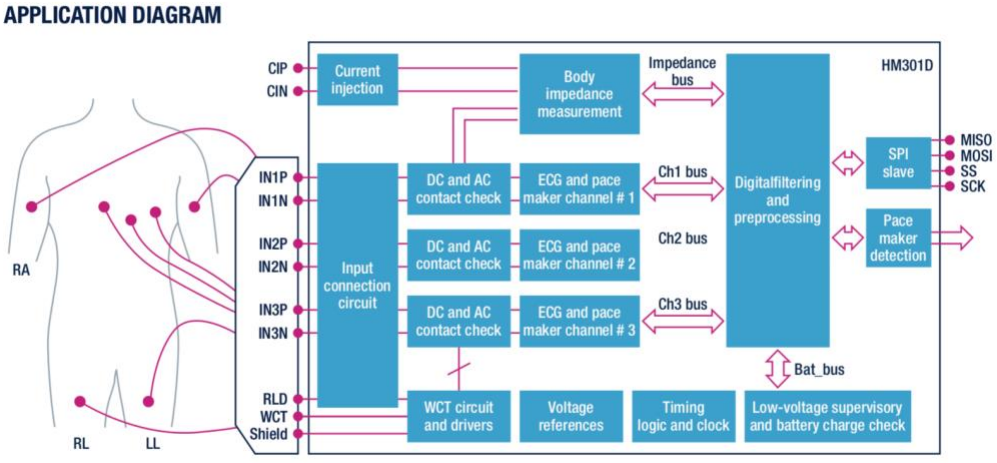

Figure 2.20 Application diagram of the Analog Front End HM301D

The quality of contact between electrodes and skin is controlled by injecting a small AC or DC current. Moreover, thanks to digital filtering and pre-processing block (DFP), HM301D enables the implementation of configurable bandpass filters and IQ impedance demodulation. Finally it permits the use of specific algorithms for lead-off control and pacemaker detection [35].

The ECG signal has significant range between 0.05 and 250 Hz. In order to ensure feature acquisition and to limit the presence of noise, Analog Front End must operate a signal amplification and the elimination of biological/non-biological interferences. The application scheme of HM301D is shown in *Figure* 2.20.

General section features:

- Three bio-potential acquisition channels that contain integrated analog high-pass filters;
- One bio-impedance measurement channel;
- Digital in-phase and quadrature (I/Q) demodulation;
- Extended supply ranges (AV_{DD}; IOV_{DD}; DV_{DD}): [1.6 - 3.6]V;
- Current consumption using 3 channel, without impedance channel off (I_{DD}): 1.3mA (typical value);
- Clock reconfigurability and external clock.

Bio-potential channel features:

- Differential input voltage (bandwidth 0.05 Hz - 10 kHz): ±0.8/ GAIN (typical value)
- Gain setting : 8,16,32,64
- ADC resolution: 16 bits
- Max Data Rate (ODR): 125 KSPS (typical value)
- Input referred noise (Gain 64): 0.6 µVrms (typical value)
- Common mode rejection ratio(CMRR): 100 dB
- Signal to noise ratio (SNR), with Gain=64 and Differential input signal frequency 10Hz: 72dB

Bio-potential Channel

This HM301D bio-potential channel is designed to collect any bio-potential signal such as the Electroencephalography (EEG) and the Electromyography (EMG), in addition to the ECG and the

pacemaker (PM). Its architecture consist of two sections, analogue and digital, which provide analogue and digital outputs respectively. The structure of the bio-potential channel is shown in *Figure* 2.21.

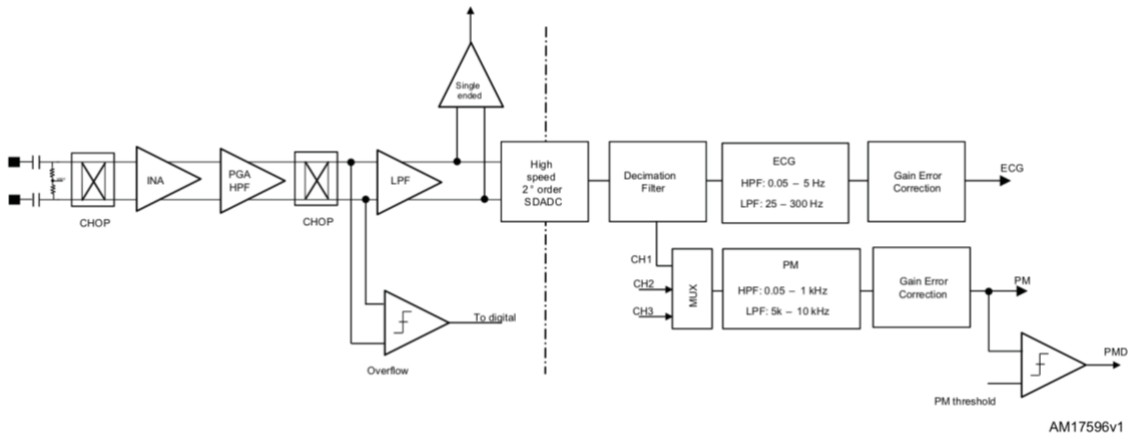

Figure 2.21 Architecture of bio-potential channel

Analog Section

The input signal passes through the analog high-pass filter and the DC component is then removed. When the start-up phase take place or after an overvoltage occurrence, in order to prevent a too low settling speed, a recovery mode is operated: the cut-off frequency starts from 5 Hz, moves to 0.7 Hz and, in the end, drops to 0.05 Hz. After the high-pass filter, the signal is fed to an antialiasing 110 kHz low-pass filter and finally it enters the amplification stage and is sent to the ADC [36].

Digital Section

The Channel converts two different signals – the "High Resolution Low Bandwidth" (HRLB) and the "Low Resolution High Bandwidth" (LRHB) – into the digital domain. The ECG trace, with a bandwidth of 0.05-300 Hz, is a typical example of HRLB signal. While the pacemaker, with its information content in the range of 0.05-10 kHz is a clear example of LRHB signal. All the HRLB signal paths are usable with the three bio-potential channels while only two LRHB signal paths can be connected to them. For both HRLB and LRHB signals, digitized data values are in binary one's complement format [36].

2.6.2 "STEVAL-IME002V1" Evaluation Board

The *STEVAL-IME002V1* evaluation board has been designed around the new HM301D Diagnostic Quality Analog Front End, with the purpose to demonstrate how to perform measurements with bio-electric and bio-impedance sensors. It contains a 32-bit microcontroller that is part of the STM32 family and its primary role is to supervise the SPI protocol of the analog front ends and to implement an USB connection with the PC.

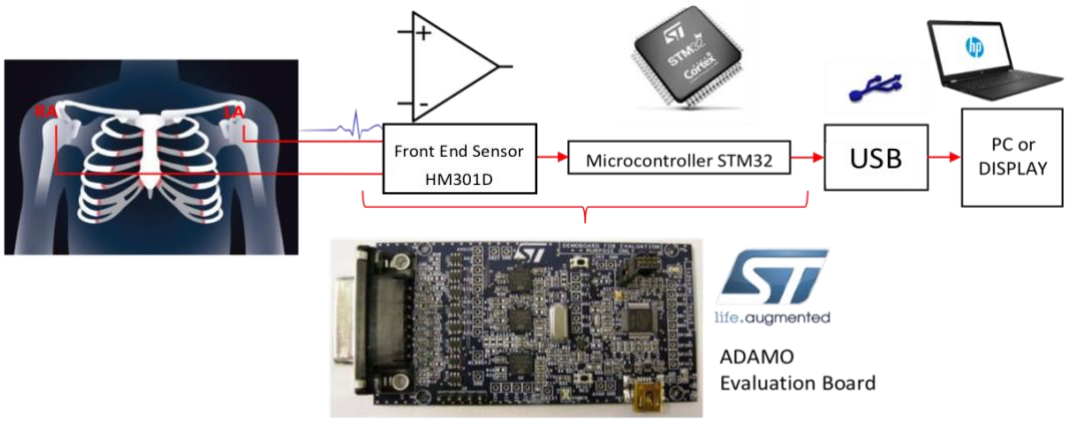

Figure 2.22 Board connection and its logic diagram.

This board has been designed to manage up to three HM301D devices in an SPI concatenation where the three sensors on the board switch thanks to a dedicated mux. The working daisy chain sequences are U1 (first HM301D on the board), U1 and U2 (second HM301D), U1 and U2 and U3 (third HM301D). Only one configuration is possible and the access order can't be modified. In *Figure* 2.22 the logical connections between input signal and PC graphical interface are shown.

By using this board it is possible to record the *Einthoven equilateral triangle* and all the lead connections: V1, V2 and V3, through U2, and V4, V5 and V6, through U3. Only two derivations have been used, as they are sufficient to acquire the requested features from the ECG signal.

2.6.3 Analog microphone MP33AB01H

The MP33AB01H is a low power compact microphone. The sensing element is an audio sensor capable of acoustic wave detection and produced using a specific silicon micromachining process [37]. This analogue microphone is guaranteed to operate within a large temperature range (from

-30°C to + 100°C). The MP33AB01H has an acoustic overload point of 125 dBSPL, with an SNR (Signal to Noise Ratio) of 66dB.

Table 2.5 shows the MP33AB01H microphone sound and electrical main specifications.

Table 2.5 Microphone sound and electrical specifications

Current consumption (I_{DD})	0.25Ma
Sensitivity at 1kKz (SO)	-38 Dbv (typical value)
Signal-to-noise ratio at 1kKz (SNR)	66 Db (typical value)
Distortion at 125 Dbspl (THD)	10 %

The microphone typical frequency response is reported in *Figure* 2.23.

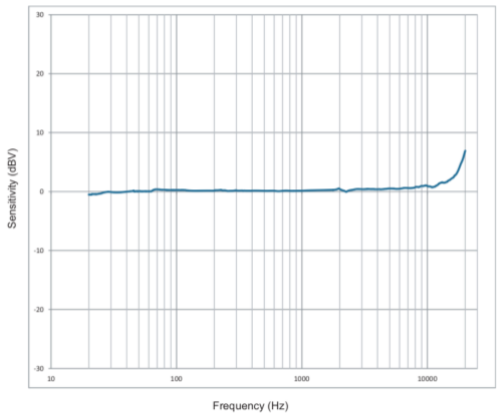

Figure 2.23 Normalized frequency response

Mechanical specifications and construction details

The microphone is a device that is composed by an integrated circuit and the sensor placed in the same package.

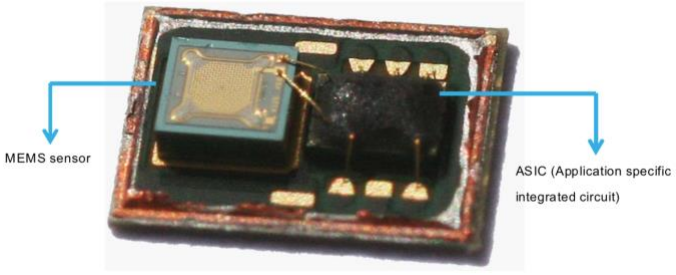

Figure 2.24 Microphone construction

The sensor, based on capacitive transduction, has been created using MEMS (Micro-Electrical-Mechanical Systems) technology. The capacitor consists of two silicon plates/surfaces one of which is fixed (red) and one movable (green); this configuration is displayed in *Figure* 2.25.

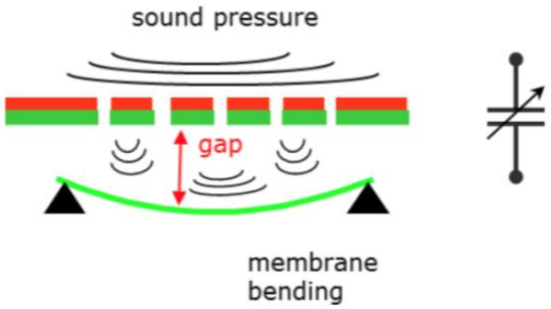

Figure 2.25 Principle capacitance

The sensor structure includes an electrode that covers the fixed surface to make it conductive, and some acoustic holes that allows sound to pass through, as shown in *Figure* 2.26. The movable plate is only fixed at one side of its structure. Hence it can move. The membrane moves back due to the ventilation hole that make it possible for the compressed air in the back chamber to flow out. This chamber permits the membrane to move inwards.

Therefore, the microphone MEMS sensor is a variable capacitor and its transduction principle is based on a change in the capacitance between a fixed plate and a membrane, where the movement of the latter is due to the incoming wave of the sound. The integrated circuit converts the variation of the polarized MEMS capacitance into an analogue output.

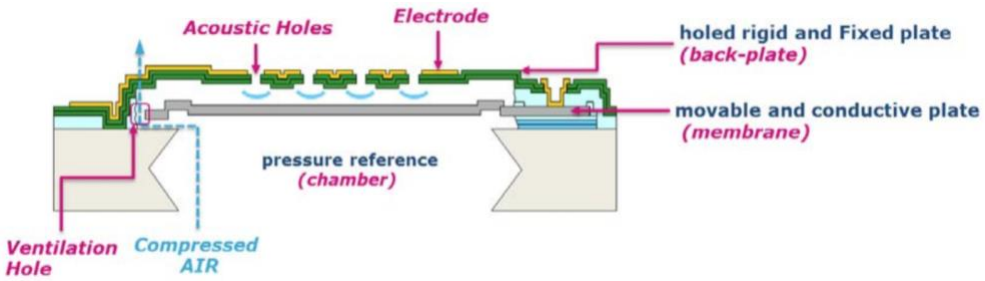

Figure 2.26 MEMS trasducer mechanical specifications

The packaging configuration places the ASIC (Application Specific Integrated Circuit) under the sound inlet and the MEMS sensor next to the integrated circuit. The pads of the device are located on the bottom of the substrate.

2.6.4 MEMS pressure sensor LPS35HW

The MEMS pressure sensor LPS35HW, illustrated in *Figure* 2.27, is used as a tonometer to extract the artery Pulse Wave from the skin surface.

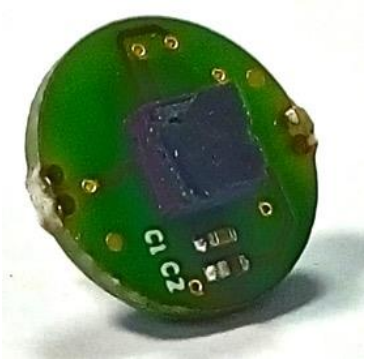

Figure 2.27 LPS35HW MEMS pressure sensor.

The LPS35HW works as a digital output barometer. This MEMS sensor is ultra-compact, comprises a sensing element and acts as a piezo-resistive pressure sensor. The device communicates from sensing element to the application through I2C or SPI.

ST has developed a dedicated process to improve the suspended membrane quality. This membrane constitutes the sensing element of the sensors and detects the absolute pressure. The LPS35HW is situated in a holed ceramic LGA package and the external pressure reaches the

sensitive element thanks to the presence of holes in the package. The sensor is guaranteed to operate in a temperature range between -40 °C and +85 °C. The main characteristics of this sensor can be seen in *Table* 2.6.

Table 2.6 Pressure sensor characteristics

Current consumption (I_{DD})	3 μA
Supply voltage (VDD)	1.7-3.6 V
Supply current in power-down mode (IddPdn)	1 μA
Frequency of work	180 Hz
Pressure data output	24-bit (typical value)

To improve the pressure sensor operability a 3D printed support was developed (*Figure* 2.28*)*.

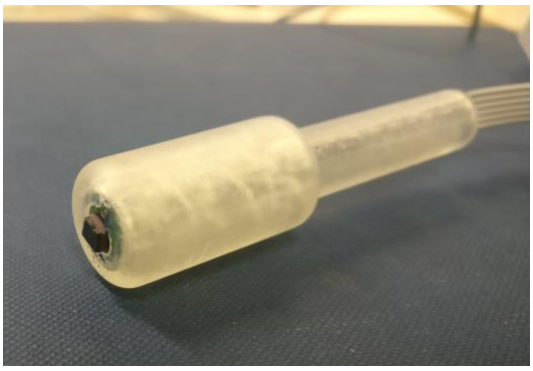

Figure 2.28- LPS35HW MEMS pressure sensor with 3D support

2.6.5 MEMS accelerometer LIS2DS12

The LIS2DS12 is a digital, low-power, high performance three-axis linear accelerometer that belongs to the "pico" family. The direction of the detectable accelerations in relation to the top view of the sensor is reported in *Figure* 2.29.

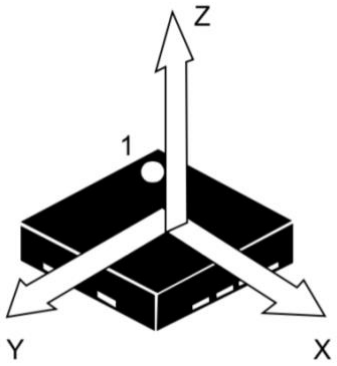

Figure 2.29 Direction of the detectable accelerations [38]

This sensor has user-selectable full scales of ±2*g*, ±4*g,* ±8*g or* ±16*g* and is able to detect acceleration providing output data comprised between 1Hz and 6400Hz. Moreover, it has an integrated 256-level first-in, first-out (FIFO) buffer permitting the user to garner data. The LIS2DS12 has a dedicated internal signal processing architecture designed to recognize movement and to detect acceleration. Finally, this sensor is provided in an LGA package and is guaranteed to work with temperatures ranging from -40 °C to +85 °C [38]. The main characteristic of the LIS2DS12 can be seen in *Table* 2.7.

Table 2.7 Accelerometer characteristics

Current consumption in high- resolution mode (I_{DD})	150 μA
Current consumption in high- resolution mode (I_{DD})	0.7 μA
Supply voltage (VDD)	1.62-1.8 V
Data output	16-bit (typical value)

STEVAL-MKI174V1

The STEVAL-MKI174V1 (*Figure* 2.30) is an adjustable board built to ease the assessment of the LIS2DS12 device product family. This board provides a good method for quick system prototyping and device analysis rating through the user application. The adaptor gives the complete LIS2DS12 pin-out and comes set-to-use with the needed decoupling capacitors on the VDD power supply line.

Figure 2.30 LIS2DS12 adapter board

The STEVAL-MKI109V3 motherboard supports the adapter and contains a high performance 32-bit microcontroller linking the sensor with the PC. Thanks to this connection, the dedicated software routines (Unico GUI) can be used for personalized applications.

2.6.6 Discovery Kit STM32F429 and STM32F429ZIT6 Micro

The STM32F429 (*Figure* 2.31) is a Discovery Kit board that provides 114 General-Purpose input/output pins (GPIO), each of which can be set by software. The STM32F429 contains various devices. One of them is the microcontroller unit STM32F429ZIT6, a 32-bit microcontroller characterized by a best performance and part of the STM32F4 family: it is created on the basis of the ARM Cortex-M4 core. The MCU contains three different 12-bit ADCs that share up to 16 external channels and allows both single-shot or scan conversions. Other devices available on the Discovery Kit are: “ST-LINK / V2”, a built-in debug circuit, a 2.4 TFT QVGA LCD, an external 64-Mbit SDRAM, a micro-AB USB OTG connector and, finally, LEDs and buttons that allow the user to interact with the board. The power supply of this board can be an external 5 V source or the host PC through a USB cable.

The STM32F429ZIT6 microcontroller unit is the main component of the Discovery Kit; it is able to operate at frequency up to 180 MHz, and comes with a single precision floating point unit (FPU). This device contains high-speed memories (2 Mbytes of Flash memory and 256 Kbytes of RAM) and large amount of peripherals connected to three different types of BUS: two APB buses (“Advanced Peripheral Bus”), two AHB buses (“Advanced High-performance Bus”) and a 32-bit “multi-AHB” bus array [39].

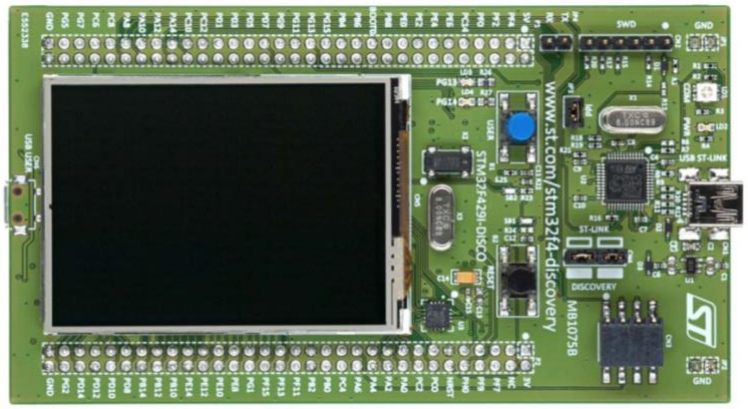

Figure 2.31- Discovery kit

In addition, STM32F429ZIT6 has 6 SPI interfaces ("Serial Peripheral Interface Bus") available and settable in slave or master mode, in full duplex or simplex transit mode. SPI1, SPI4, SPI5 and SPI6 can communicate up to 45 Mbit / s, while SPI2 and SPI3 up to 22.5 Mbit /s. Eight various master modes are supplied with the 3-bit prescaler [39].

2.6.7 Employed Software

The software employed to set, program and handle the MCU and its modules (i.e. interrupts, SPI, register setting, etc.) is Keil-µVision5, a development platform based on Windows operating system. It contains all the tools necessary to generate incorporated applications, including a macro assembler, a C/C++ compiler and an HEX file generator. µVision5 provides: tools for project creation, debugger, GDI interface, manual links and much more. Therefore, it make possible to direct interact with the STMF4 microcontroller family supporting all its specific characteristics.

The acquired signals are then analysed using *MatlabTMR2018a* software. With this tool the debug and the implementation of features extraction algorithm are made. Finally, the data collection from microcontroller to PC and its real time plotting are managed by a *VisualStudio* interface.

Chapter 3

Signal acquisition

The *Pulse Wave Velocity* is a parameter that could be measured using several different signals. Every kind of detected waves must be acquired from two different sites, one near the heart (*proximal point*) and another along the artery (*distal point*). By doing so, as illustrated in *paragraph 2.5* the Pulse Transit Time and the gap between them can be calculated.

The scope of this work is to develop a system that acquires and evaluates phonocardiogram waves for PWV extraction (Acoustic Pulse Wave). This is done by measuring the time difference that occurs between two characteristic points on the Carotid and Femoral phonocardiogram waves respectively.

To validate the PTT and PWV values computed by processing the PCG acquisitions, other signals have been considered and analysed for comparison purpose. In particular, two of them are used as reference and they are:

- *ECG signal* has been used in the first steps of this work where carotid-PTT and femoral-PTT are computed considering ECG R-Peak as proximal detection point.
- *The Pressure Pulse Wave* acquired by means of a tonometer sensors and used to extract the direct PTT between Carotid and Femoral sites.

Finally, the last acquired signal is the *Movement Pulse Wave* recorder by a MEMS accelerometer that is evaluated and then compared with the other considered signals to perform a *blood pulse* detection in arterial sites.

In the following paragraphs both hardware and software implementation and synchronization are explained. To perform a simultaneous detection, the HM301D sampling clock is used as global reference timing. In this way, ECG acquisition synchronizes the acquisition of all signals so that they can be directly compared each other.

3.1 ECG acquisition

The STM-STeval-IME002V1 evaluation board, as explained in *paragraph 2.6.2,* permits to perform ECG sampling with only one channel enabled (see *Figure* 2.22). First of all, signals must be simultaneously acquired and to make this possible the HM301D sampling clock is used as global reference timing. To do this, the STeval-IME002-V1 and the Discovery Kit are interconnected together, as show in *Figure* 3.1.

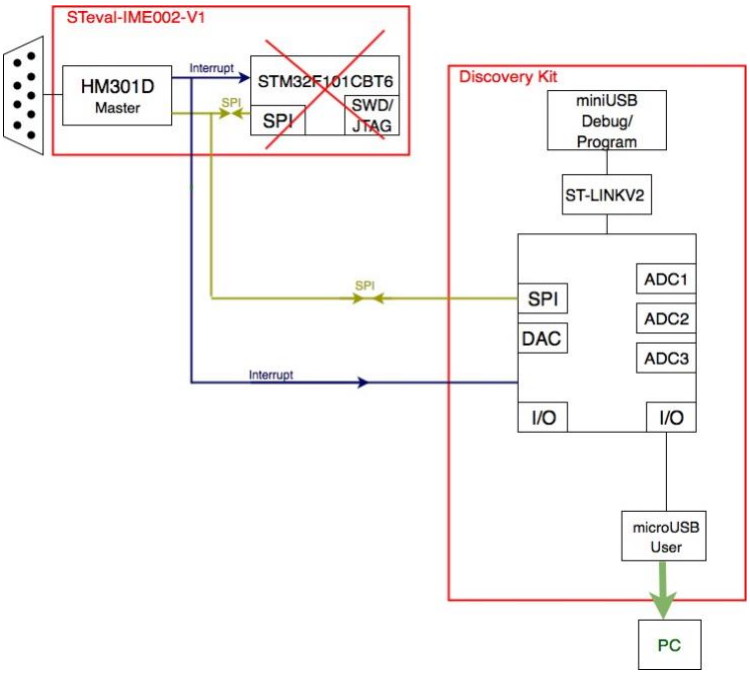

Figure 3.1 Board interfacing diagram

In order to perform an ECG signal acquisition at maximum sampling rate (1953Hz) the evaluation board has been improved and customized. In the following paragraphs all the introduced modification will be illustrated.

3.1.1 ECG Hardware implementation

The ECG can be acquired through the STeval-IME002V1 board in a default configuration using standard conditions. On the other hand, in this work some changes to the standard configuration need to be implemented and are explained in the following sections.

Power Supply Noise and Environmental Noise Filtering

During the early acquisitions a lot of noise problems were identified. In order to reduce them several hardware improvements are made.

The first adjustment concerns USB interconnection. The original too long cable produces a lot of interference; for this reason it has been replaced by a shorter one. Another problem concerns the power supply noise. To make the board immune to it two decoupling capacitors have been added on the analog (AVDD) and digital (3V3) supply rails; they constitute the most immediate and simplest noise reduction approach. So, in total the STeval-IME002V1 board has four additional capacities:

- 10 µF and 100 nF, capacitors placed between AVDD and GND pins;
- 10 µF and 100 nF, capacitors placed between 3V3 and GND pins.

The new configuration can be seen in *Figure* 3.2.

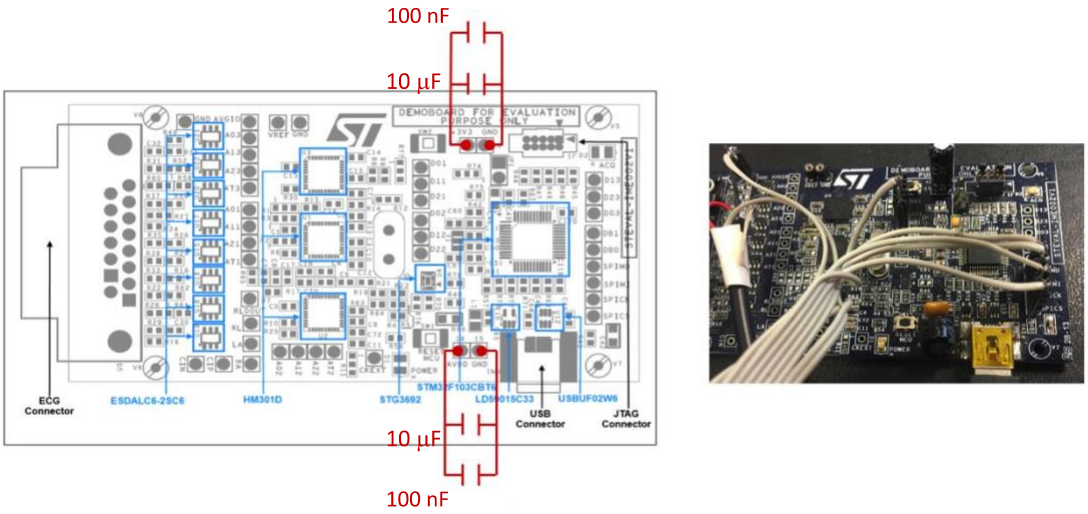

Figure 3.2 STeval-IME002V1modified board and schematic diagram

Electrodes configuration: Single lead

The STeval-IME002V1 board permits to record ECG signal using different types of setting. The original board setup was changed into a *single lead* configuration, so ECG signal acquisition was enabled with just two electrodes placed on the right and left arms.

Usually, in clinical environment, a specific configuration is employed to permit the 12-lead arrangement. This original board pattern has the Left Arm (LA) electrode signal as IN1P pin input of the HM301D and it is linked with Wilson Common Terminal (WCT) output pin. This setting is too complex and unnecessary for the final goal of this work, so a jumper was introduced to bypass the connection between pins IN1P and WCT (*Figure* 3.3). Finally, either the Right Arm (RA) or the Left Leg (LL) available electrode has to be enabled and configured by firmware: the single lead configuration was completed.

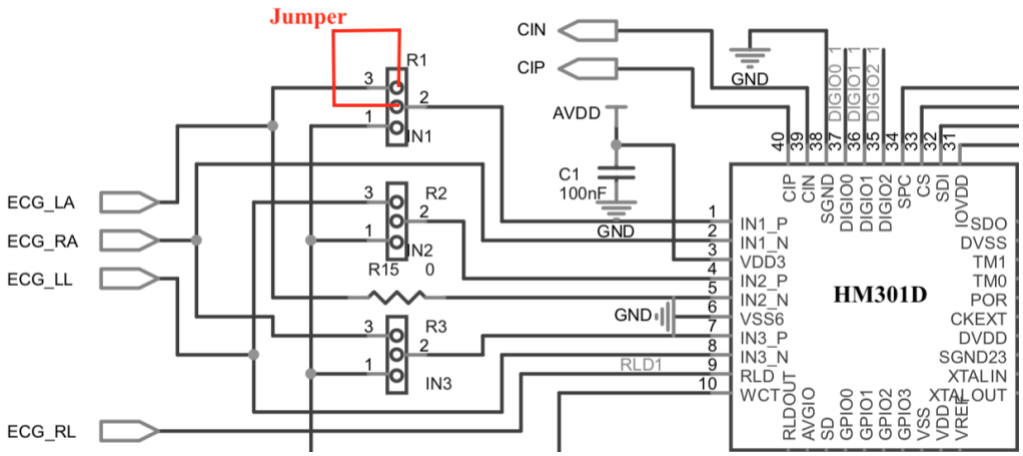

Figure 3.3 STeval-IME002VI schematic

Interface Implementation using Discovery Kit/Boards interface

In order to have a simultaneous acquisition of ECG and other signals such as Tonometer, Accelerometer and Microphone the STeval-IME002-v1 is not enough. In fact, it has a limited hardware configurability and resource availability. For this reason, the more powerful Discovery Kit MCU was adopted to supervise all the signals acquisitions process.

Therefore, an additional physical interface was arranged. It permits to redirect the HM301D SPI bus from the *STeval-IME002-V1* to the *Discovery Kit MCU*, as shown in *Figure* 3.1. Four SPI signals are employed for the purpose: *Master Output Slave Input* (*MOSI*), *Master Input Slave Output* (*MISO*), *Chip Select* (*CS*) and *Serial Clock* (*SCK*) , implementing the configuration shown in *Figure* 3.4.

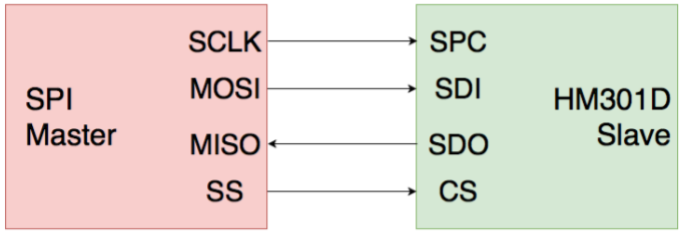

Figure 3.4 SPIs connection.

Lead of Detection

The developed system must be able to detect situations in which the ECG electrodes are disconnected or when poor contacts occur. In both cases the acquired data are inconsistent and feature extraction is not possible. For this reason, all HM301D bio-potential channels are able to notify in case of electrode placement issues: a contact check procedure, available on each HM301D bio-potential channel, gives an electrode contact resistance indication [40]. This electrode-to-skin verification is useful to guarantee a good signal detection during each ECG acquisition.

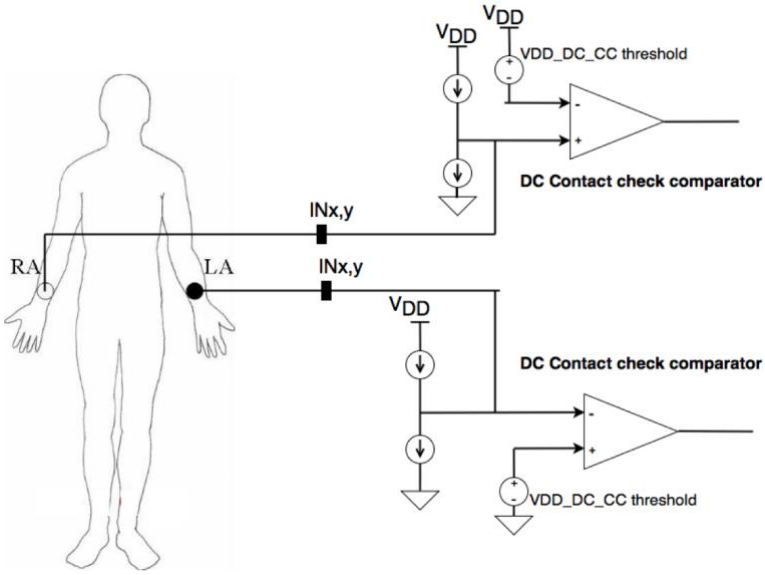

Figure 3.5 DC contact check architecture

As explained in *paragraph 2.6.1*, the quality of electrode to skin contacts is controlled by DC or AC current injection and the former is employed in this work. HM301D provides this contact check with a hardware implementation that consists of a current source and a current sink circuits linked to two

voltage comparators, as *Figure* 3.5 shows. Both are connected with each of the six bio-potential input channels $IN_{x,y}$ (x=1,2,3 and y=P,N), allowing to cover all the possible leads configurations.

In particular, current injected through the patient's body by one electrode goes back into the HM301D thanks to another electrode. The former acts as a current source while the latter brings the current sink to the same value as the associate current source. So, a voltage drop is generated and then detected by the two comparators with a programmable threshold. The DC-check process provides a flag available in a specific register that will be zero if the generated drop of voltage is acceptable or one if a bad contact occurs. This register will be read and a critical contact situation could be identified.

ECG data flow

Once acquired, Bio-potential signals are processed and evaluated along the data path from the electrodes to the microcontroller unit, as the block diagram in *Figure* 3.6 explains.

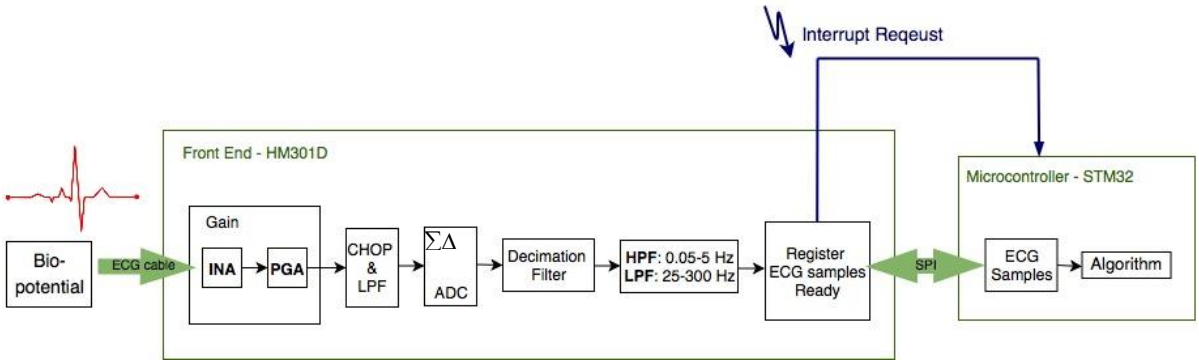

Figure 3.6 Bio-potential channel data flow

In the first stage, bio-potential signals are acquired using single lead configuration and then processed by the bio-potential analogue section. First of all, an *Instrumentation Amplifier* (INA) with a variable gain is used on the analogue signal, so that the amplified signal sustains a *Programmable Gain Amplifier* (PGA). Secondly, an analogue high pass filter with a cut-off frequency ranging from 5 Hz to 0.05 Hz processes the signal. At last, before digital conversion, there is a *chopper circuit* (CHOP) followed by a low pass filter with a 110KHz cut-off frequency. At this point, signal is converted into digital samples by using a 2^{nd} order 16-bit SigmaDelta ADC working at 2MHz. DC components are removed high pass filters stage, so only the necessary parts of the signal are converted.

Once processed, signal is divided by HM301D into two different sections, one for the *High Bandwidth Low Resolution* (HBLR) and another for the *Low Bandwidth High Resolution* (LBHR) the ECG belongs to.

At this point, the decimation filter occurs and the ECG sampling rate is reduced from 2MHz requested sampling frequency (f_s), a user selectable values defined in the proper configuration register. Along this ECG path, the signal is then processed by a low pass and a high pass filter; this process permits to decrease the ECG bandwidth according to the defined output data rate. Once a new ECG sample is available, the microcontroller directly reads the value from the sensor. At this stage, HM301D sensor activates an interrupt request and the associated routine allows the microcontroller to transfer the data. As previously explained, SPI carries out the data transfer and then a recognition algorithm permits to detect the R-peaks present in the ECG signal.

3.1.2 ECG Firmware implementation

After the previously explained hardware improvement, the new STeval-IME002V1 board configuration requires several software routine implementations.

Registers Setting

The ECG acquisition system can be configured by using the microcontroller firmware. So, writing all the HM301D registers, the appropriate bio-potential channels can be correctly set up.

The requested configurations are:

- *Channel Enable and Basic Function*

The health channels can be activated by SET0 register. This enables a lot of other HM301D sensor functions such as: *Shield Driver* (SD), *Wilson Common Terminal* (WCT), *Pace Maker* (PM) signal extraction and health channels digital filtering. In particular, this register will be configured to activate the SD, the digital filtering and the first health channel.

- *Contact Check*

As explained in the previous section (see *lead off detection*), DC-contact check permits to notify when the electrode contact becomes critic. To perform this control a lot of parameters need to be set: the input pins to be used as positive side (P-side) or negative side (N-side) and the value of threshold voltage and current injection. The SET9, SET10, SET11 and SET12 registers are defined and configured for this purpose. Finally, the IN1P (LA) and IN3N (RA) pins are chosen and used as positive and negative sides respectively. In both cases, the current injection is of 100nA, while the threshold used as comparison with the voltage drop is 102mV.

- *Gain*

The analogue section of HM301D consists of two main stages, the *Instrumentation Amplifier* (INA) and the *Programmable Gain Amplifier* (PGA). In order to optimize the ADC usable dynamic range, these components can be configured to provide the proper amplification. Moreover, by setting the SET13 register it is possible to select the INA and PGA gains, that are fixed at 16 and 4 respectively.

- *Filtering and Sampling Frequency*

Analogue and digital filters play an important role along the signal processing stages. HM301D permits to choose the most appropriate cut-off frequency value for analogue high pass filter and for both digital low pass and high pass filters. The ADC sampling rate is automatically set once the cut off frequency (fc) of digital low pass filter has been defined. In this case, the adopted sampling frequency is about 1953Hz, therefore fc is set to 600Hz through the SET15 register. The recovery mode, described in *paragraph 2.6.1*, is not enabled in this paper and the HM301D high pass filtering is required anyway. For this reason, the cut-off frequency for both analogue and digital filters is set to 0.05Hz.

Firmware implementation

First of all, the appropriate firmware procedure for reading and writing the sensor registers must be implemented. In this way, MCU can configure the HM301D sensor. Furthermore, the acquired data and the flag that detects when a poor electrode contact occurs, are read through the *SPI register reading function*.

The developed application has a "*cold start*", i.e. the first ten seconds of acquisition have not been considered and so the filter stabilization takes place. Then, the data are transferred with the USB-OTG to a PC, as *Figure* 3.7 shows. Finally, the stored data in .bit format file is processed and evaluated by Matlab algorithm in order to perform the PTT and PWV parameters extraction.

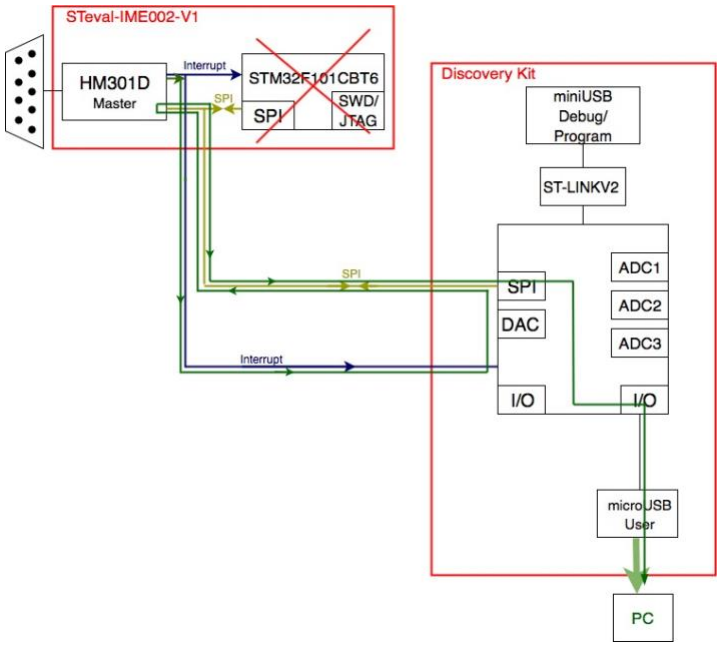

Figure 3.7 ECG data flow provided by the firmware

3.2 Pressure Pulse Wave acquisition

This system is able to acquire the *Pressure Artery Pulse*, a digital signal that comes from a ST prototypal pressure sensor. Due to the digital nature of the signal, processing is carried out at the software level. This signal was only used in the first step of this work; later it was no more considered and its acquisition channel have been used for accelerometer sensor data exchange.

3.2.1 Pressure Pulse Wave Hardware implementation

To manage the LPS35HW pressure sensor from to the Discovery Kit MCU, a physical interface was implemented. To carry out the communication, four SPI signals are needed: *Master Output Slave Input* (*MOSI*), *Master Input Slave Output* (*MISO*), *Chip Select* (*CS*) and *Serial Clock* (*SCK*). A couple of simultaneous pulses (Carotid and Femoral signals) are acquired thanks to two free SPIs on the Discovery Board. SPI3 and SPI6 have been adopted for this purpose.

3.2.2 Pressure Pulse Wave Firmware implementation

The employed sensor, Tonometer LPS35HW, can works in a continuous mode. In particular, this device acquires data according to the user-defined sample rate. In this case, the acquisition configuration is set to “one shot mode” and the sampling frequency is fixed at 170Hz.

3.3 Movement Pulse wave acquisition

Thanks to the use of a ST MEMS accelerometer (LIS2DS12) the implemented system is able to acquire the small movement related to the heart beat. Also in this case, due to the digital nature of the signal, processing is carried out at software level.

3.3.1 Movement Pulse Wave Hardware implementation

To manage the LIS2DS12 sensor from the Discovery Kit MCU, a physical interface was implemented. To carry out the communication, four SPI signals are needed: *Master Output Slave Input* (*MOSI*), *Mater Input Slave Output* (*MISO*), *Chip Select* (*CS*) and *Serial Clock* (*SCK*). To acquire the Movement Pulse Waves (Carotid or Femoral signals), an available SPI interface on the Discovery Board is needed. The employable SPIs are used by ECG and Pressure Pulse Wave signals acquisition so there are no others available interface. For this reason, SPI3 has been reused to address Movement Pulse Wave.

3.3.2 Movement Pulse Wave Firmware implementation

The employed sensor, Accelerometer LIS2DS12, can works in a continuous mode. In particular, this device acquires data according to an user-defined sample rate that is fixed at 200Hz. The device is able to detect acceleration along three axis (X, Y and Z), but for the scope of this work only Z direction has been considered.

3.4 Acoustic Pulse Wave acquisition

In this case, signal is analogue and the processing is carried out by both Hardware and Software implementation. The Hardware system is able to perform signal filtering and amplification while the digital conversion is carried out at the Software level.

3.4.1 Acoustic Pulse Wave Hardware implementation

First of all the choice of the microphone type has to be made. In general, phonocardiogram signal is very difficult to detect, so the ST sensor with the highest sensitivity and the highest signal-to-noise ratio (SNR) has been selected. Finally, is important for the sensor to have an analogue output. In this way, signal is filtered at the circuit level before being converted into the digital domain. The device MP33AB01H has been chosen because it features all the required characteristics, providing a -38dBV sensitivity and 64dB of SNR.

At the beginning, to perform pulse wave sound acquisition at Femoral and Carotid sites, several microphones were adopted and a chamber with a suitable shape was used. The usage of multiple sensors allowed to increase the signal-to-noise ratio: the SNR grows by three Decibels each time the number of microphones is doubled. The microphone signals are added coherently and for this reason the output amplitude increases by 6dB every time the number of microphones is doubled. On the other hand, the noise is added incoherently and its floor increases by 3dB [41]. Moreover, a mechanical shape is introduced to operates as a resonance chamber and gives advantages for signal acquisition: the sound amplitude increases and the environmental noise is reduced. In a first step, sixteen microphones are placed in two identical shapes made in a metal alloy (*Figure* 3.8).

Figure 3.8 Metal bell with eightteen microphones.

Despite of this implementation, microphone signals result strongly affected by support movements. This happens because the shape of used metal chamber is made by heavy material and causes a microphone to skin contacts. Consequently, another kind of acquisition system is introduced: a conical glass (*Figure* 3.9). This final configuration is lighter and easier to handle than the previous one.

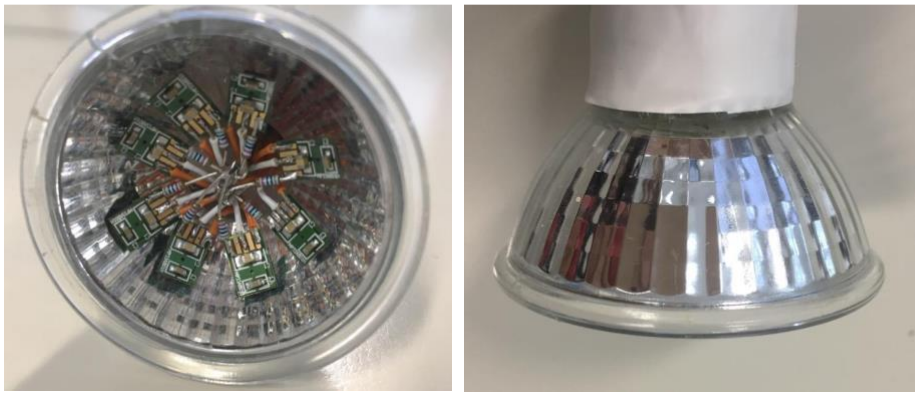

Figure 3.9 Conical glass with 8 microphones.

The conditioning circuit for this hardware implementation is made using the following components:

- *TLV2464 opAmp*

This component is a low power, four channels, operational amplifier with rail-to-rail input/output. The most important characteristics are listed in the *Table* 3.1 below.

Table 3.1 TLV2464 opAmp main characteristics.

Voltage supply (V_{DD})	up to 6V
Gain Bandwidth Product(G_{BW})	6.4MHz
Input voltage offset (V_{IO})	100µV
Output current (Io)	±40mA

- *OPA2244 opAmp*

Also this component is an operational amplifier providing two low-power channels. The primary characteristics are listed in the *Table* 3.2 below.

Table 3.2 OPA2244 opAmp main characteristics.

Voltage supply (V_{DD})	up to 36V
Gain Bandwidth Product(G_{BW})	430KHz
Input voltage offset (V_{IO})	700µV

- *LM317 Adjustable Regulator*

This component is needed to provide a voltage reference for the amplification and filtering stages. Along the amplification chain a reference of 1.5 V is chosen according with the ADC dynamic range that is 3.3 V. The device LM317 is an adjustable regulator with three pins that give a voltage value between 1.25V and 3.7V [42] as output. It is possible to set the output voltage thanks to a potentiometer situated between output, the adjust terminal and the ground. Also in this case, the decoupling capacitors are present in the circuit and the final configuration is shown in *Figure* 3.10.

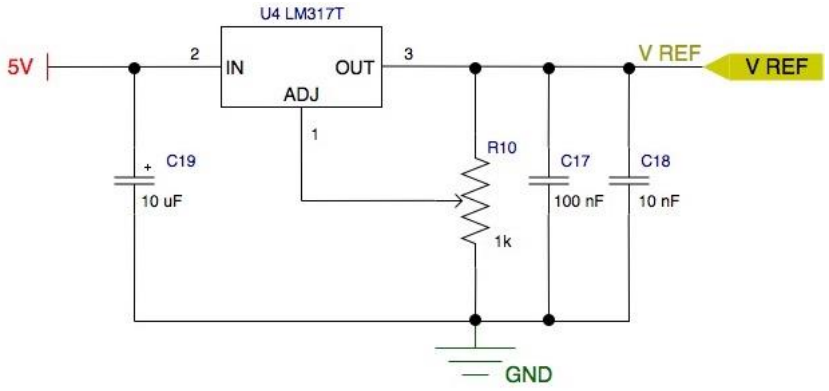

Figure 3.10 LM317T reference generator circuit

Analog Signal Conditioning [0.3-200] Hz

The conditioning circuit has been implemented according to the signal frequency characteristics, defining the bandwidth of interest between 0.3 and 200 Hz. In particular, the lower limit has been set at 0.3 Hz to avoid low frequencies signal distortion (between 2 Hz and 15 Hz). On the other hand, the upper limit has been defined at 200 Hz to keep all the signal information content. The final conditioning circuit is illustrated in *Figure* 3.11.

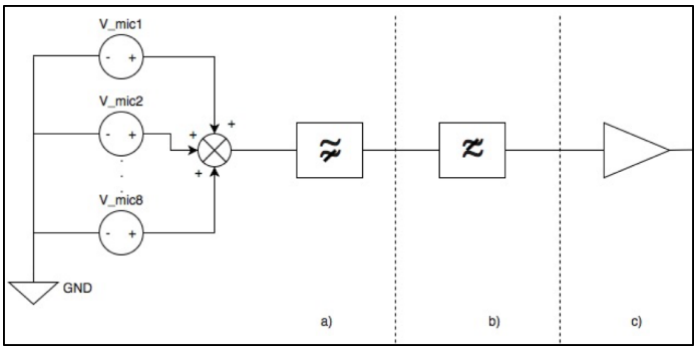

Figure 3.11 Microphone conditioning diagram

a) Mics summing and high pass filter

The first stage, thanks to the opAmp, performs a mic output summing and a offset elimination. It is used as a high pass filter with a cut-off frequency given by:

$$fc = \frac{1}{2 * \pi * C * R1} = \frac{1}{2 * \pi * 10\mu F * \left(47K\Omega + \frac{10\ K\Omega}{8}\right)} = 0{,}3Hz$$

The gain of this step is given by:

$$G = \frac{R2}{R1} = \frac{47K\Omega}{\left(47K\Omega + \frac{10\ K\Omega}{8}\right)} \cong 1$$

b) Low pass filter

The second stage consist of a unit gain with a second order low pass filter with a cut-off frequency of 200Hz.

c) Amplifier

The last conditioning stage introduce a pure amplification to take advantage of the ADC input dynamic range. The potentiometer presence allows the operator to set the gain, according to the required amplification level. In order to perform a “normal” signal detection (output of some mV) the gain is set to x100. Before the ADC input there is an additional first order high pass filter introduced to compensate the opAmp input offset error.

The illustrated conditioning circuit is the same for both Carotid and Femoral acquisition channels. All the cited components are showed in *Figure* 3.12*.*

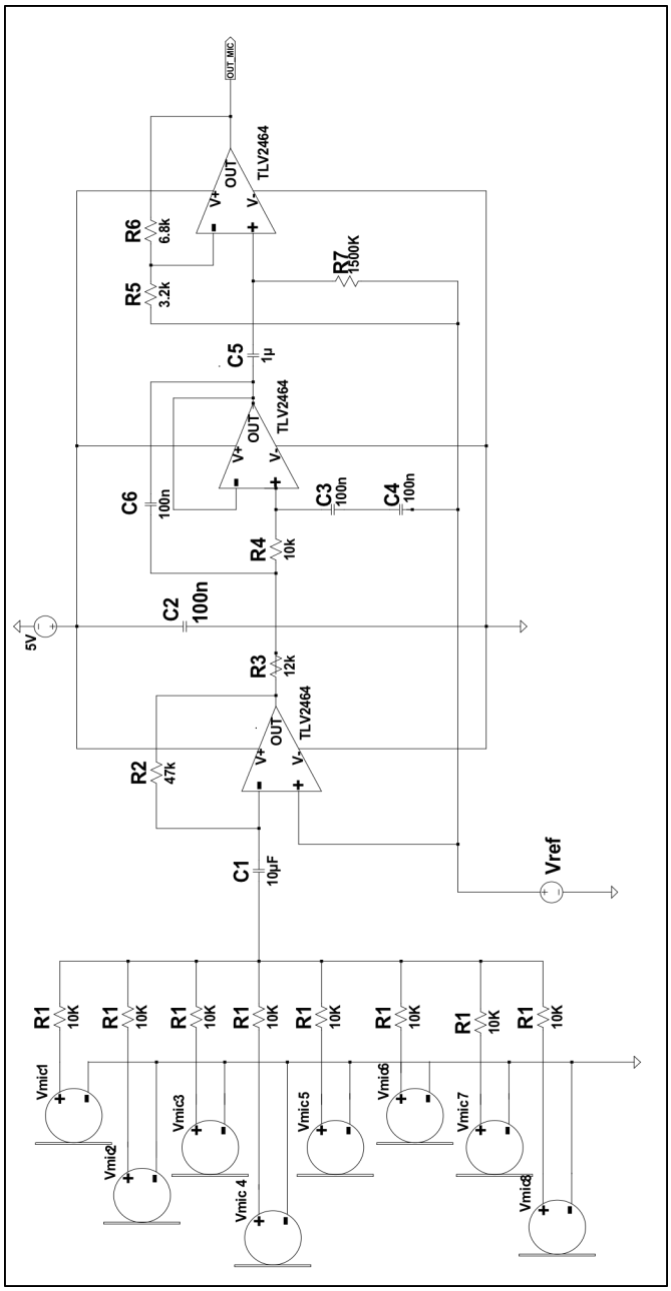

Figure 3.12 Conditioning circuit of both carotid and Femoral acquisition channels.

3.4.2 Acoustic Pulse Wave Firmware implementation

In this case several software procedures are needed to configure the ADCs and all the MCU peripherals used for acquisition and data transfer process.

Analog-to-Digital Converter (ADC)

In order to acquire the two microphone signals, only two available ADCs on the used MCU are needed. The configuration of adopted ADCs permits to obtain a 12-bit resolution; both scan and continuous conversion mode have been disabled addressing a single acquisition channel. To acquire the two microphone signals and to convert them into the digital domain are used the channel 13 of the ADC2, equivalent to PC3 pin on Discovery Kit, and the channel 5 of ADC1, equivalent to PA5.

3.5 Signal acquisition synchronization

The developed system is able to acquire three different signals family simultaneously: two directly connected to SPIs (ECG and Tonometer or Accelerometer) and one routed to the ADC (Microphone). First of all, a distinction between the simultaneous acquisition of Tonometer and Accelerometer signals must be made. In the former case there are two different sampling frequencies of 1953 Hz for ECG and 170Hz for the Tonometer, also in the latter case Accelerometer has a sampling frequency of 200 Hz.

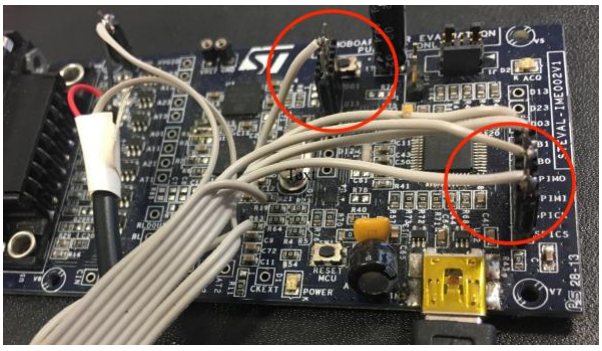

Figure 3.13 SPI and DGPIO connectors added on the board

For all acquired signals, in order to easily manage the acquisition clock domain, the same sampling frequency of 1953Hz is adopted. For this reason, on the *STeval-IME002-V1* is configured the *HM301D* General Purpose Digital I/O (DGIO1) to give as output the ECG-End-of-Conversion (EOC) flag. The used DGIO1 is connected to PC13 pin on the Discovery Kit. When an ECG sample is acquired and digitally

converter by the sensor, the DGO1 and the EOC flag are set to high logic value. This signal is routed to the MCU and configured as interrupt service request. It is possible to see in *Figure* 3.13 all the added connectors in order to allow the dialogue between the *STeval-IME002V1* and *Discovery Kit boards.*

A specific interrupt service routine is called every time a new ECG sample is present: all the signals are stored by the MCU from ECG's SPI and ADCs. Therefore, every interrupt, samples from ECG and Microphone are collected.

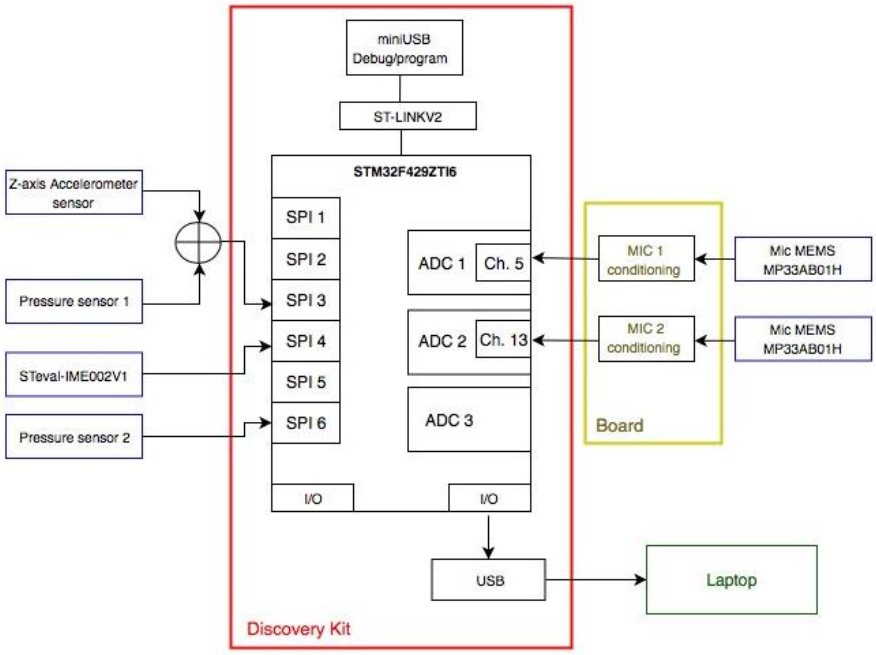

Figure 3.14 Developed system diagram

On the other hand, for Tonometer and Accelerometer synchronization a different approach is needed. In the first case, Tonometer working at a maximum frequency of 180 Hz, can be read every 11 ECG interrupts (obtaining a 177.5Hz sampling frequency). Later, at software level this signal will be conveniently resampled.

Instead, the accelerometer sensor is set to work at 200Hz and a sample from this sensor is acquired every interrupts. In this case, the same sample value is acquired several time by the acquisition system. Also in this case, at software level the signal will be processed and conveniently resampled.

The diagram in *Figure* 3.14 illustrates an overview of all acquired signals. The system permits to collect ECG, two Pulse Waves, one Acceleration wave and two Microphone Waves. As mentioned above, there

is a jumper that allows to collect five signals simultaneously swapping Tonometer and Accelerometer. The conditioning circuits implemented on the board is shown in *Figure* 3.15.

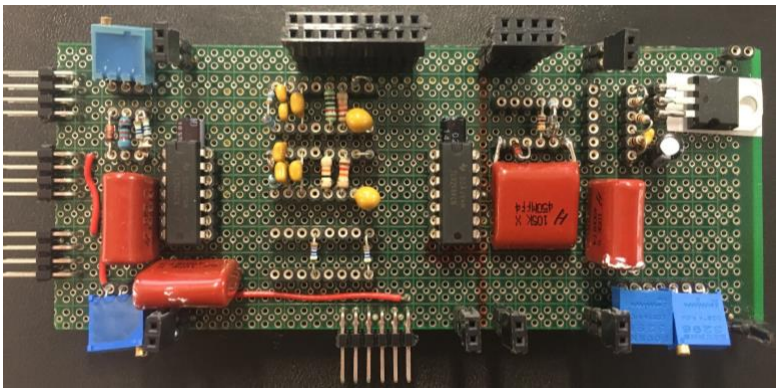

Figure 3.15 Conditioning circuits implemented on the board.

The final goal of this work is to evaluate the time interval between two simultaneous acquired signals, so it is of primary importance that conditioning circuit introduces a negligible time delay. This time transposition is usually due to the low pass filter (delaying signal) and high pass filter (introducing negative delay) processing.

In order to evaluate the amount of introduced time delay, every conditioning channel has been individually tested. A reference signal is generated and the time difference between the original one and the same after it passes through the conditioning chain is measured. The obtained values are:

- 1.5ms delay for ECG signal due to the STeval-IME002V1 Board;
- -2 ms delay for PCG signal due to the circuits.

By comparing this results with the time interval that have to be measured (PTT is in the order of magnitude of 100ms), the implemented conditioning circuit is a good compromise between reasonable cut-off frequency and the introduced time delay.

Chapter 4

Signal Analysis

In this chapter, the signal analysis related to the features extraction will be explained. To perform the comparison between the developed system and the existing solutions, the most used PWV measurement approach in clinical environment, the application tonometry, is reproduced. The addressed signal processing aims to extract the Carotid PTT and the Femoral PTT, that represent the time employed by arterial pulse to propagate from the heart to the Carotid Artery and from the heart to Femoral Artery respectively. In additions, the direct PTT evaluation between Carotid and Femoral sites is performed as well.

First of all, the signals acquired for the parameter extraction have to be firstly filtered and then, some specific characteristics have to be extracted. The ECG R-Peak is considered as the start point for the arterial pulse detection, while other three signals features have been selected to allow pulse detection in a peripheral site (carotid or femoral). In particular, as previously explained, ECG and Pressure Pulse Wave are used to validate the PTT and PWV computed by processing both Acoustic Pulse Wave and Movement Pulse Wave. For each type of signal a specific extraction algorithm was implemented and a specific feature was considered:

- *"R-peak"* for ECG that corresponds to the ventricular depolarization;
- *"Intersecting tangent point"* for Pressure Pulse Wave corresponding to the beginning of systolic phase of the arterial pulse;
- *"Ear-Intersecting tangent point"* for Acoustic Pulse Wave corresponding to S1 beginning.
- *"Intersecting tangent point"* for Movement Pulse Wave corresponding to the beginning of systolic phase of the arterial pulse.

In the following paragraph all the algorithms implemented for the signal processing and feature extraction will be presented and described in detail, several approaches will be compared and basing on the collected result the most reliable solution will be addressed. In particular to acquire the addressed signals, the hardware system illustrated in the previous chapter was employed. While, to address more realistic medical scenario a more usable and integrated system is needed, a description of this improved system will be provided in *Chapter 5.*

4.1 Reference signals filtering and algorithm implementation

In this paragraph, all the steps developed for Electrocardiogram and Pulse Wave signals processing will be explained: first the mean value has to be removed, then signal are normalized respect to their standard deviation and, lastly, the noise is removed by filtering. The first two operations are easily done, otherwise the last filtering operation is performed by using a Butterworth FIR filter of the 8th order designed by "*fdesign"* Matlab dedicated function. This function requires the filter type (band pass, low pass or high pass), the order and the desired corner frequency normalized to the Nyquist Frequency (fc/2).

Every filter function could be configured in a "*single mode"* using *filter* instruction or in a "*double pass mode"*, *filtfilt* instruction. The difference between the two implementations concerns the time delay introduction. In fact, *filtfilt* function performs a zero-phase filter, i.e. a signal processing in both the forward and reverse directions is carried out; instead, the *filter* function filtering only once the signal, so introduces a time delay. In this work, to avoid a time delay introduction *filtfilt* function has been employed for all signal processing.

4.1.1 ECG signal analysis

The final goal of this processing, is to locate R-peak in the ECG signal. In fact, the QRS complex must be individuated to detect every heart beats event and then to calculate the beginning of the corresponding pulse transit time. Both QRS-complex and R-peak individuation underpins the most of automated ECG analysis algorithm [43].

As explained in *paragraph 2.2,* R-wave individuates ventricles depolarization occurs in the heart. This event has the largest amplitude of the signal and the shortest lifespan (start from 60 to 100 ms) compared to the others. Every time a ventricle depolarization occurs, electrode system acquires the signal but this original data are very difficult to interpret. Indeed, each biological signal is affected by physiological randomness, variability and several kinds of noise (i.e. muscle noise). In particular ECG signal is influenced by a lot of artefacts due to power-line interference, electrode motion or baseline wander. Finally T-wave with high-frequency characteristics could be similar to QRS complex.

The ECG signal analysis consists of ECG filtering and algorithm implementation and in the following sections both this steps are explained.

ECG filtering

First of all, the frequency components of the signal that allow R-peak identification must be isolate and, for this, all the wave bandwidths have been analysed, as shown in *Figure* 4.1. It is possible to notice that for all the main components of the signal (the P-wave, QRS-complex and T-wave) all the signal frequency components are limited under 40Hz.

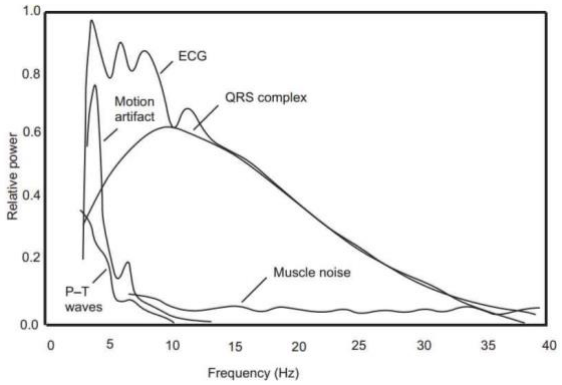

Figure 4.1 Relative power spectra of ECG signal [44]

For this reason, by using a Matlab tool, a 3^{th} order Butterworth low pass filter with a cut-off frequency of 40 Hz was implemented. By doing this, the only useful components of the signal are isolated, even if noise rejection at 50Hz is not enough. In this case, a notch filter, that let to remove a single particular frequency from the signal, was implemented through the *iirnotch* Matlab function. This is a second order and Infinite Impulse Response (IIR) digital filter that permits to cut the noise presence at 50Hz. In particular, this function requires as input two cut-off frequencies delimiting the one of interest; the two values used amount respectively at 49Hz and 51Hz, providing a cut-off frequency of 50Hz. This frequency choice has to be made because only an ideal filter arranges a mask deep-hole corresponding to the corner frequency.

As shown in *Figure* 4.2, in this way, the two frequencies chosen permit to get a good compromise in the amount and centre of the cut.

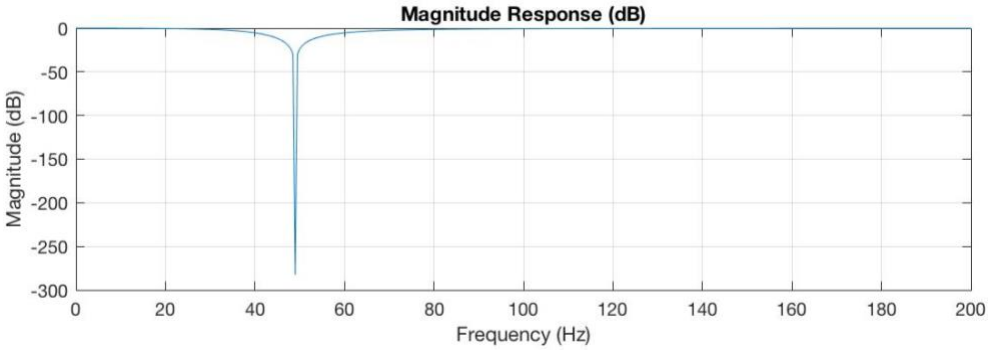

Figure 4.2 Iirnotch filter mask to remove a 50 Hz frequency components.

The obtained signal, compared to the original one, after these two filtering stages is depicted in *Figure* 4.3.

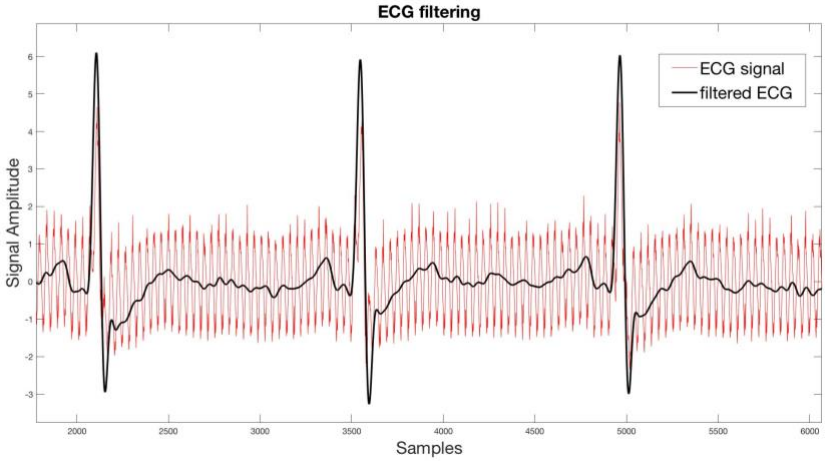

Figure 4.3 ECG signal filtering.

ECG algorithm implementation

Both signal pre-processing showed in the previous section and QRS-complex specificity explained above, permit to carry out a correct detection and localization of R-peak on ECG signal. In this point of view, in the last years a lot of literature has been developed and a lot of R-peak detection methods have been proposed. In order to implement the most reliable approach, the Pan-Tompkins QRS detection algorithm was chosen.

The Pan-Tompkins QRS detection algorithm

The real time QRS detection algorithm has been customized by Pan and Tompkins in 1985 and become one of the most popular in the Biomedicine signal processing environment. It is possible to found all reference to their work in the paper of J. Pan, W. J. Tompkins [45]. This R-peak identification algorithm was tested on the MIT public ECG signals database and results correctly detects on the 99.3% of the QRS complexes and only fails on the 0.67% of the events.

The developed algorithm permits to perform QRS-complex detections using specific characteristics of ECG signal such as slope, amplitude and width. By using a band-pass filter interferences decrease and a low amplitude thresholds can be used to perform a high detection sensitivity. Furthermore, a dual-thresholds technique is used and then a search back routine for missed beats is implemented with the aim of false negatives reductions. Algorithm provides an adaptive approach that automatically up-to-date all the thresholds and R-R intervals limit. In this way, accurate results are provided also in case of heart rate or ECG morphologies changes. Finally, this algorithm can operates in real-time and not requires excessive computing power since all the processing is done with integer arithmetic.

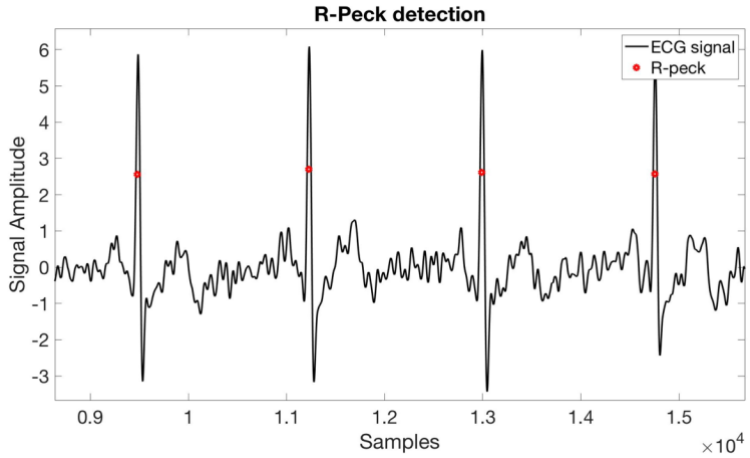

Figure 4.4 R-peak detection given by Pan & Tompkins algorithm.

In practise, firstly, the pre-processed electrocardiographic signal is limited by a band-pass filter at 50Hz. Then, the obtained signal is processed following a steps sequence composed by:

1. A derivate approximates by a filter;
2. an amplitude squaring process followed by a moving-window integrator that passes through the signal;
3. an adaptive threshold, applied for the QRS complex identification.

In this way, every R-peak can be individuated in the signal, as shown in *Figure* 4.4.

4.1.2 Pressure Pulse Wave signal analysis

Since the Pulse Wave signal, as said in *paragraph 3.2*, is acquired by a digital sensor, all the filtering steps are already performed on board the used tonometer. In fact, in this case, the usual corrupting sources do not influence the signal and it is result to be ready for the analysis. A typical carotid signal shape gives by pressure sensor (*Figure* 4.5) illustrates the absence of artefacts.

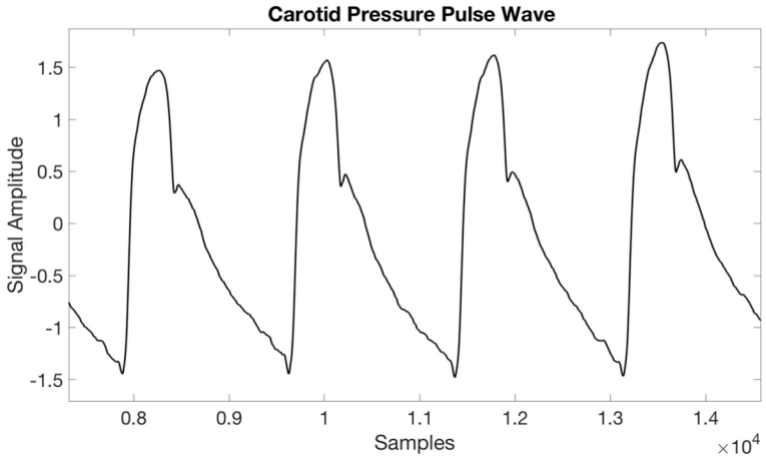

Figure 4.5 Carotid Pulse Wave acquisition

The Pressure Pulse Wave algorithm implementation for its features extraction is explained in the following section.

Pressure Pulse Wave algorithm implementation

In order to perform a feature extraction from Pressure Pulse Wave signal a specific algorithm is implemented. Usually, change in pressure shape along the propagation and not optimal viscoelastic characteristics of transmission don't make wave front detection easier. For these reasons, the most common point used for wave front individuation, *foot of the pressure wave,* was chosen as the most relatively free of reflections [46].

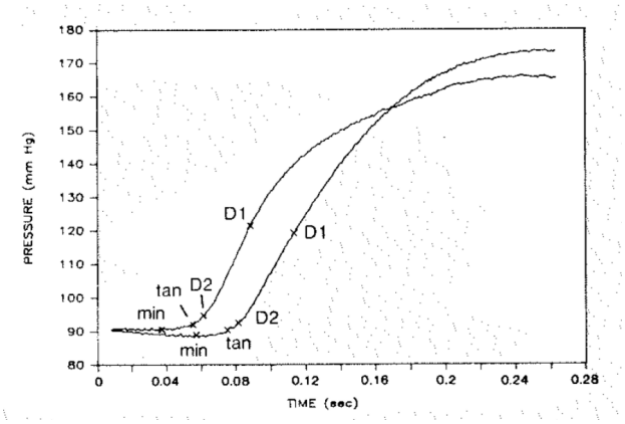

Figure 4.6 Position on the pressure wave of the four features [46].

Usually this characteristic points could be detected using four different methods shown in *Figure* 4.6 and listed below:

- The location of minimum diastolic pressure point (*min*);
- The location of first derivate pressure maximum point (*D1*);
- The location of second derivate pressure maximum point(*D2*):
- The location of the intersection between: the line tangent to the initial systolic upstroke, the pressure waveform and a horizontal line through the minimum point (*tan*).

The aim of this work is to employ the developed application in a clinical environment. For this reason, the characteristic most reliable and adopted for this purpose was chosen: the *intersecting tangent point* (tan). All the steps done for this detections are explained below.

1) High pass filter and minimums detection

A Butterworth Matlab 3^{th} order high pass filter at 0.5Hz is applied and all the relative minimums are counted. A threshold is defined as the 50% of the absolute minimum and this allows to individuate only the relative minimums at the lower part of the pressure wave (see *Figure* 4.7).

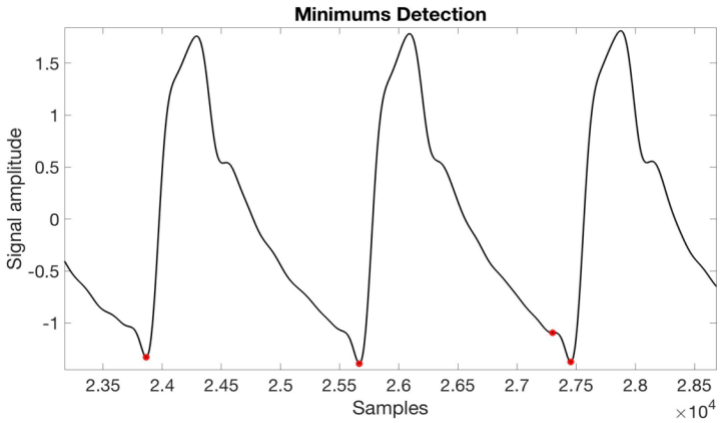

Figure 4.7 both relative and absolute minimums individuation.

2) First derivate evaluation and maximum extraction

The first derivate of Pulse Wave signal is calculated. This is then analysed starting from every signal minimum detected in the first step and moving for 700 samples. In this obtained window the first derivate maximum is taken, as *Figure* 4.8 shows.

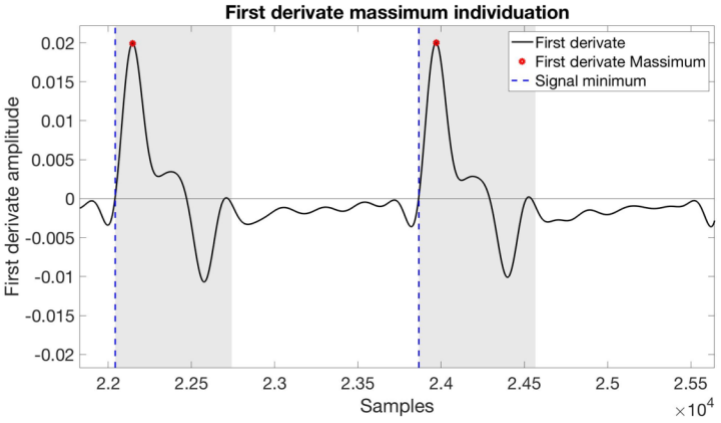

Figure 4.8 Range individuation in which the maximum is detected.

3) Tangent creation and check

In the original signal the points corresponding to the x-coordinate of the just extracted maximums derivate are individuated. In these, the tangents are created (*Figure* 4.9). Then, in order to verify that there are no more than one minimum for each tangent a check is accomplished. As could be seen in *Figure* 4.7, for example, the third and fourth minimums have a common maximum derivate point, and

so the same overlapped tangent location. By using the check, one of these common tangents is eliminated and just the minimum nearest to it is preserved. As shows in *Figure* 4.9 the third minimum is delated.

4) Point intersecting evaluation and signal projection

In the last step, through each minimum a horizontal line is traced and the intersection with the closer tangent is individuated. From this point, the corresponding abscissa is projected to the signal and so this individuates the "intersecting tangent point" (*Figure* 4.10), that is the final characteristic for pressure signal.

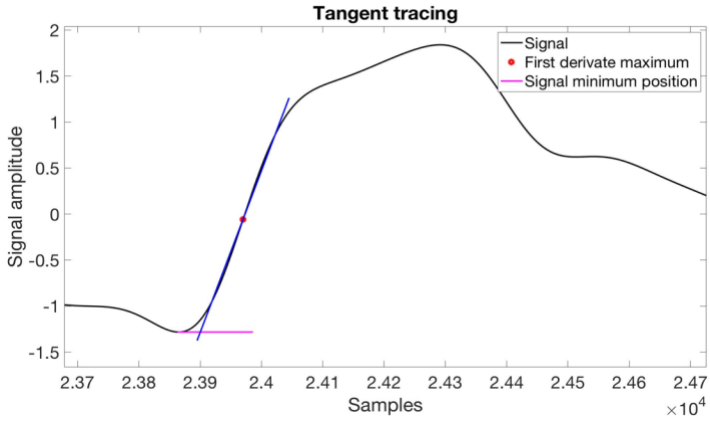

Figure 4.9 Intersection between tangent and y-axis of the minimum.

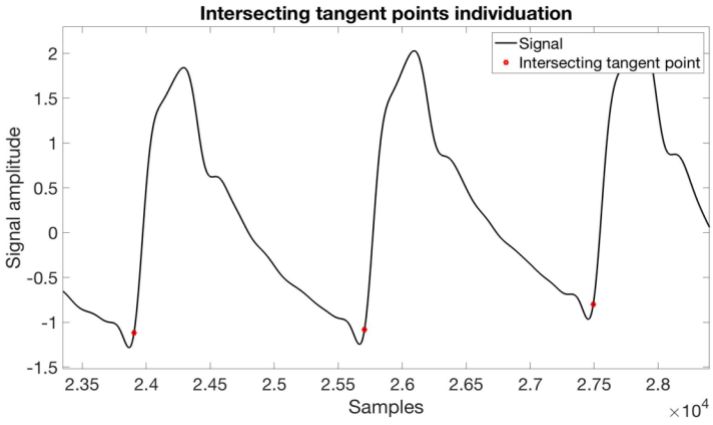

Figure 4.10 Final individuated characteristic points.

Results discussion

The Pressure Pulse Wave is the reference one for PWV calculation and the more cited by literature and developed device. This is processed following a previously explained algorithm steps, so intersecting tangent points are extracted and PTT are computed. Finally, by measuring the distance from femoral to carotid sites the PWV is estimated. This happens because, as shown in *Figure* 4.11, this signal has a quiet similar shape for both Carotid and Femoral arteries so the extracted intersecting tangent points can be related to each other.

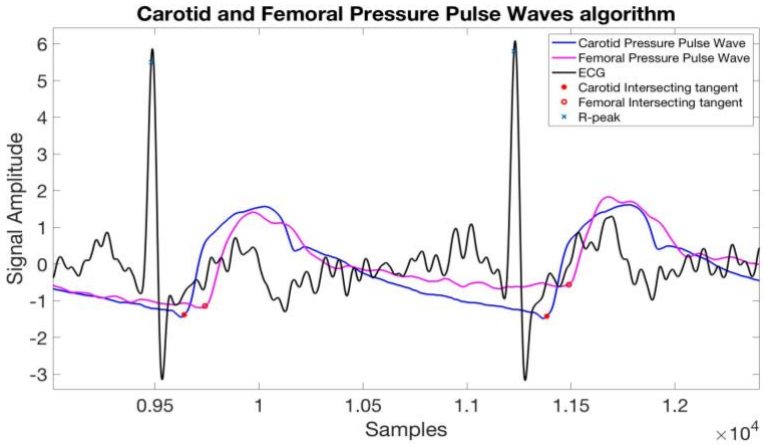

Figure 4.11 Comparision between Carot and Femoral PPG signals.

4.2 Phonocardiogram signal analysis

To capture the cardiac sound at Femoral and Carotid level, at first several microphones were adopted put in a container with a suitable shape (see *Figure* 3.9 in *paragraph 3.4.1*). The previewed configuration was used in the first stage of this work in order to analyse the available signal and to optimize the pass band of interest. However, for a medical applications the number of microphones, the ball shaped-capsule and its glasses material are not suitable. For this reason, a more usable system will be implemented in *Chapter 5.*

Spectral analysis and Signal filtering

The use of PCG signal for Pulse Wave Velocity calculations is totally a new experimental approach and there aren't in literature information about features extraction. Fort this reason, the first step of this

work is based on a frequency components analysis in order to just isolate the band of interest. As shown in *Figure* 4.12 and *Figure* 4.13, a Fast-Fourier Transform (FFT) was applied at both Carotid*(a)* and Femoral*(b)* signal.

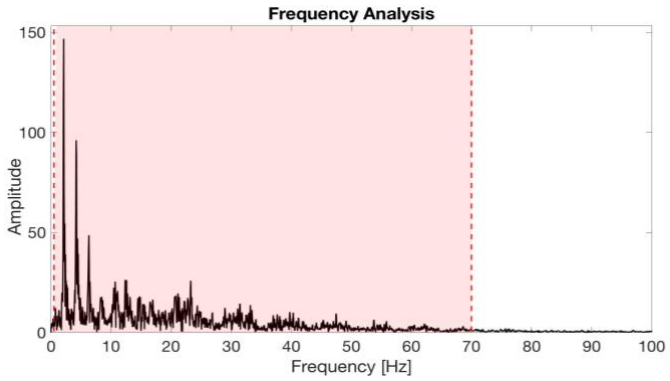

Figure 4.12 Carotid signals Spectral Analysis.

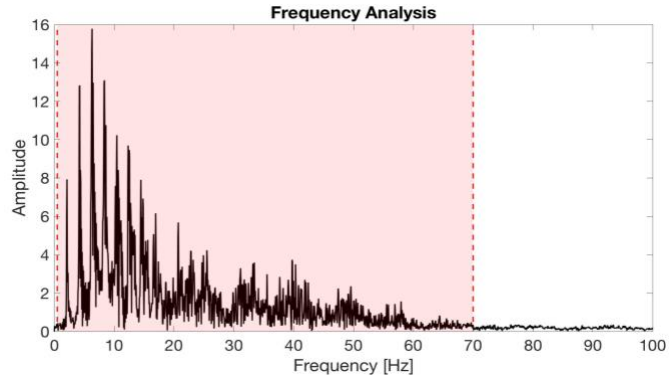

Figure 4.13 Femoral signals Spectral Analysis.

It is possible to notice that the most significant frequency components are limited under 70Hz. To eliminate the high frequency noise and the low frequency signal oscillation a filter between 2 and 70 Hz was implemented. The resulting signal is showed in *Figure* 4.14 and *Figure* 4.15.

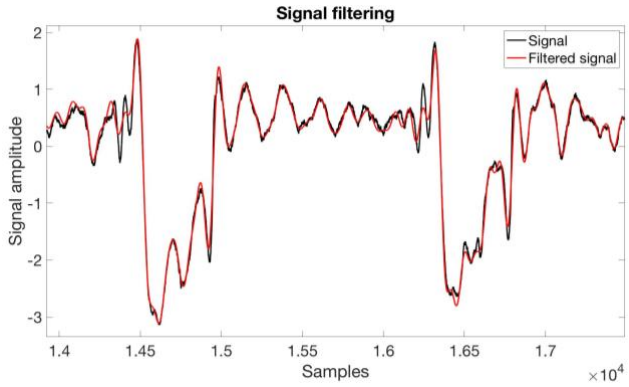

Figure 4.14 Phonocardiogram Carotid signal filtered between 2 and 60 Hz.

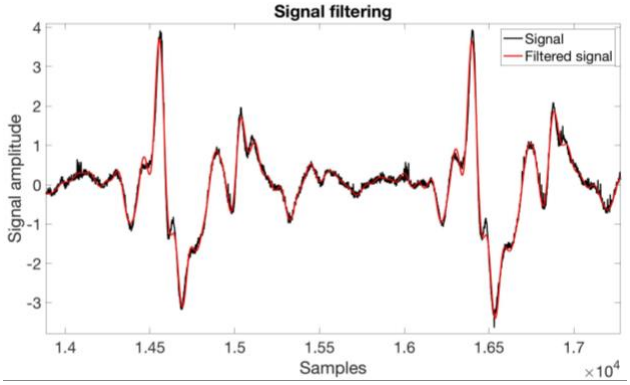

Figure 4.15 Phonocardiogram Femoral signal filtered between 2 and 60 Hz.

Algorithm implementation

As shown in *Figure* 4.14 and *Figure* 4.15*,* the shape of both the waves permits to uniquely identify a broad front so pulse detection can be easy performed. In particular, signal features individuation is made at the top of this signal rise, because it has been seen that is the part of the front less distorted by noises and so very repeatable.

Also in this case, a feature similar to the intersecting tangent point, called "*Ear*" *intersecting tangent point*, for the pulse wave was chosen and all the required steps for feature extraction algorithm implementation are explained below.

1) Low pass Filter at 1.5 Hz and Events identification

The first step permits to isolate each event, composed by S1 and S2. By a *Butterworth* Matlab 3th order filter at 1.5 Hz all the relative maximums are counted, as shown in *Figure* 4.16*(a).* then, in order to perform a S1-S2 interval (d) isolation, events periodicity (*T*) is calculated and according with the length of pulse phenomena (*L*), *d* can be defined. So, knowing that *L*=*T*/2 *(see paragraph 2.4.1*, the final S1-S2 interval value is given by the following equation:

$$d = L = \frac{T}{2}$$

The signal obtained putting together all the S1-S2 events and eliminating the rest is shown in *Figure* 4.16*(b)*.

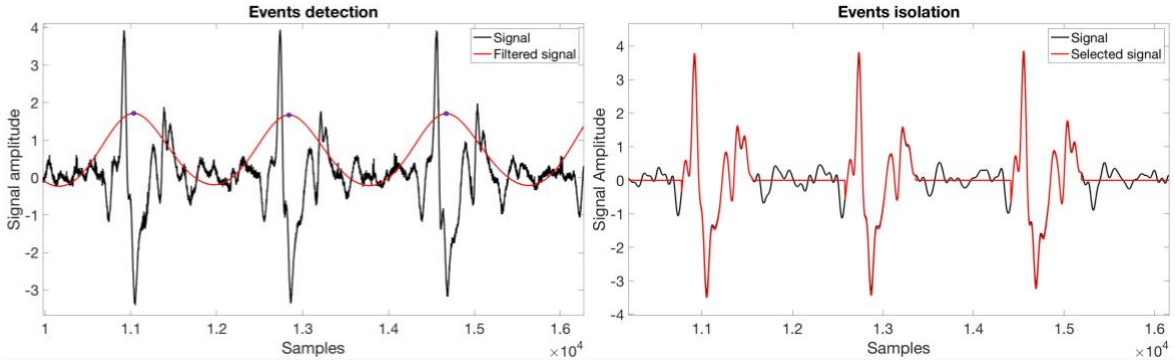

(a) *(b)*

Figure 4.16 First step of algorithm implementati on composed by Events detection (a) and Events isolation (b).

2) Front identification

For every S1-S2 sound, by using a threshold, defined as 50% of total signal amplitude, all the minimums under is can be individuated. Since the minimums founded are usually more than one each front, a criterion to identify the right one has to be performed. According to the front shape, for each minimum the corresponding maximum, that comes first, is detected; then, the difference in amplitude between every minimum and relative maximum are calculated and the ones not corresponding to the biggest front are eliminated. For example, in *Figure* 4.17 the third absolute minimum is delated and the good front is taken.

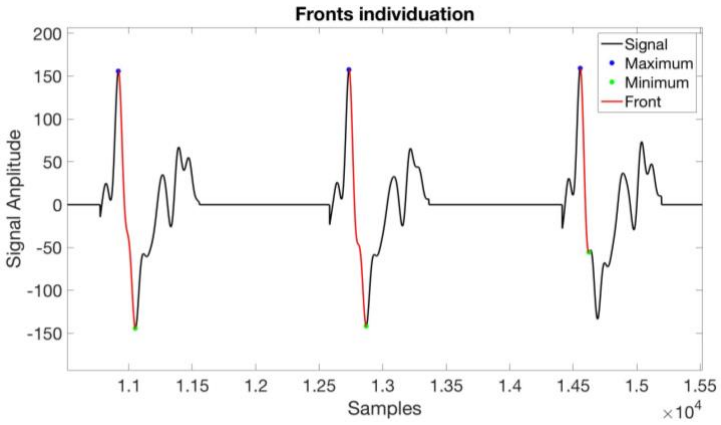

Figure 4.17 Second step of algorithm implementation: Front identification.

3) First derivate calculation

Then, each front first derivate of the Acoustic Pulse Wave is calculated. Starting from every signal maximum detected and proceeding to each corresponding signal minimum individuated, the first derivate minimum is taken (*Figure* 4.18).

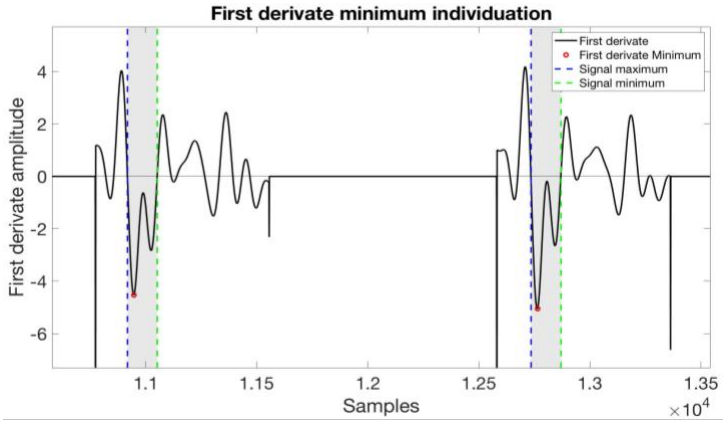

Figure 4.18 First derivate minimum identification.

4) Tangent creation

The corresponding first-derivate minimum points are individuated in the original signal and their tangents are created (*Figure* 4.19).

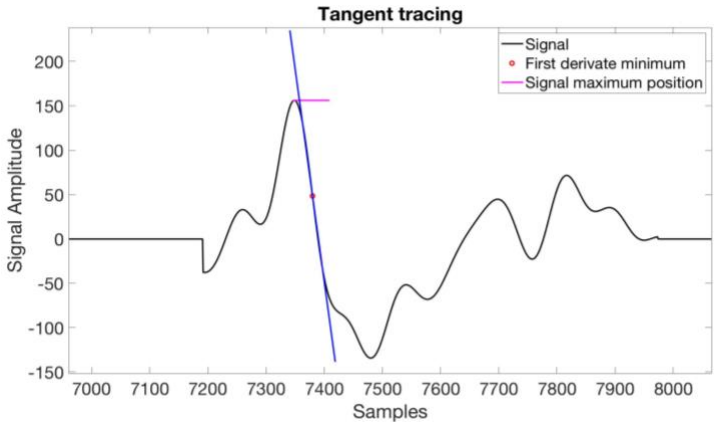

Figure 4.19 Tangent to the minimum derivate points and axis through maximum intersection.

5) Point intersection evaluation and signal projection

Through each maximum a horizontal line is traced and the intersection with the closer tangent is individuated. From this point, the corresponding abscissa is projected to the signal and this individuates the "*Ear*" *intersecting tangent point* (*Figure* 4.20). This is the final feature used to determinate the pulse passage in both Carotid and Femoral sites.

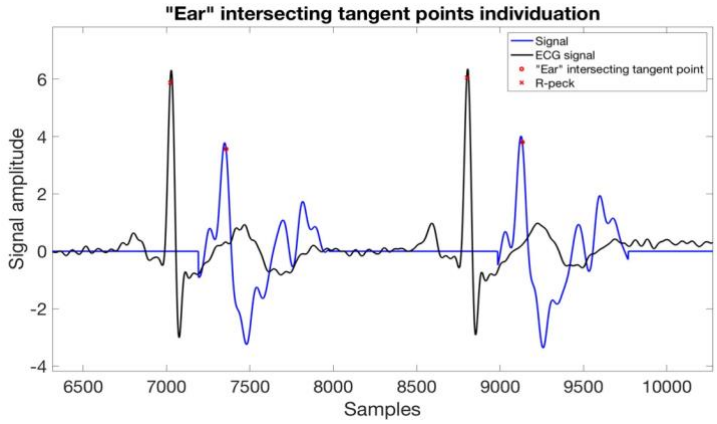

Figure 4.20 Final characteristics individuation.

Results discussion

As previously explained, the developed system is able to simultaneously acquires ECG and PPG or PCG signals. Therefore, a one by one acquisition of Microphone and Tonometer in two different subjects have been made. In this way, for both PCG (*Figure* 4.21) and PPG (see *Figure* 4.11 in *paragraph*

4.1.2) signals the shapes of Carotid and Femoral waves are compared with each other. In particular, also in this case it is possible to notice PCG signal has a similar shape for both two acquisition sites, so it is a good solution for the aim of this work.

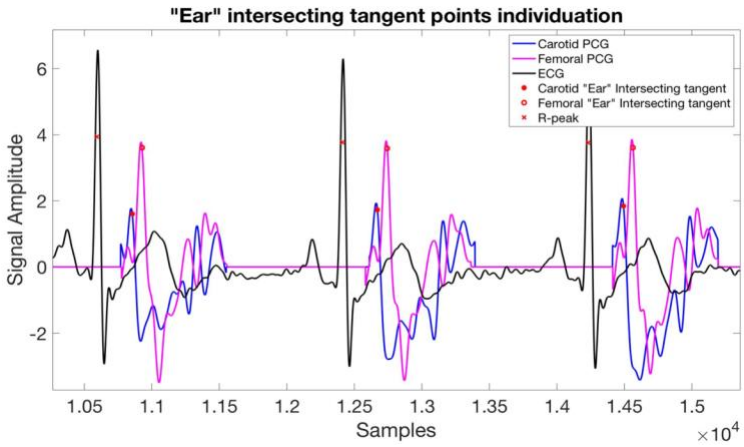

Figure 4.21 Comparision between Carotid and Femoral PCG signals.

In this tests, features extraction for each type of signal (Pressure Pulse Wave or Acoustic Pulse Wave) let to compare the PTT obtained with the new acoustic signal and the one extracted with the standard pressure wave. This, as shown in *Table* 4.1, was done both referring to the ECG and in the direct way.

Table 4.1 Algorithm results from subject 1(a) and subject 2(b)

Acquisition number	Parameters	Acoustic Pulse wave			Pressure Pulse Wave		
		Direct PTT (ms)	Referred to ECG R-peak		Direct PTT (ms)	Referred to ECG R-peak	
			Carotid or proximal (ms)	Femoral or distal (ms)		Carotid or proximal (ms)	Femoral or distal (ms)
1	**Features**	**40,15**	176,17	216,18	**49,72**	92,88	142,6
	Dev. std.	*1,2*	*2,68*	*1,94*	*2,1*	*3,35*	*2,39*
2	**Features**	**39,88**	173,29	213,52	**49,46**	94,55	143,91
	Dev. std.	*1,39*	*2,68*	*2,65*	*2,26*	*4,02*	*3,84*
3	**Features**	**40,1**	171,31	211,31	**46,89**	97,82	145,92
	Dev. std.	*1,28*	*3,2*	*2,98*	*2,04*	*3,81*	*3,49*

a)Subject 1

Acquisition number	Parameters	Acoustic Pulse wave			Pressure Pulse Wave		
		Direct PTT (ms)	Referred to R-peak		Direct PTT (ms)	Referred to R-peak	
			Carotid or proximal (ms)	Femoral or distal (ms)		Carotid or proximal (ms)	Femoral or distal (ms)
1	**Features**	**61,96**	129,12	192,63	**56,6**	125,35	182,86
	Dev. std.	*2,38*	*3,09*	*3,58*	*1,29*	*2,81*	*2,93*
2	**Features**	**62,3**	130,77	192,13	**55,75**	120,46	176,21
	Dev. std.	*2,22*	*3,49*	*4,42*	*2,36*	*3,86*	*4,42*
3	**Features**	**63,7**	133,06	197,34	**55,51**	121,38	176,9
	Dev. std.	*2,77*	*3,11*	*3,4*	*2,26*	*4,26*	*3,87*

b)Subject 2

As it is possible to see, for the data obtained through the new adopted acoustic signals there is a low variability into the same acquisition (standard deviation starts from 1.5 to 3 ms) and a quiet good repeatability (PTT value ranges from 40.15 to 39.87 ms for the first subject and from 61.96 to 63.7 ms for the second). On the other hand, there is a quiet big difference between the PTT values given by Acoustic Pulse Wave and the reference one.

In order to analysed this discrepancy, a lot of other acquisitions were made by changing the boundary conditions; in detail, the instrument position and pressure application or the subject condition (apnoea or not) have been varied and then analysed. But also changing all this parameters the obtained PTT values don't correspond yet to the reference ones.

4.3 Signal components analysis

As explained in *paragraph 2.6.3,* the MEMS microphone sensor is practically a variable capacitor; in detail, its transduction principle is based on a change in the capacitance between a fixed plate and a membrane, so it transforms a perturbation of the atmospheric pressure (i.e. sound) into an electrical quantity. In this thesis work, a capacitive MEMS microphone is adopted and the pressure variation, due to mechanical mass vibration, is transformed into a capacitance variation [47]; the final goal is to place this sensor in contact with the skin. In this way, the capacitance variation is generated by atmospheric pressure and skin translation, both resulting from the artery physical movement caused by the pulsatile blood flows in it. Also when microphones are placed into a glass capsule (see *Figure* 3.9), both contributions are still presents, since sensors-to-skin contact occurs through the conical chamber.

For both Carotid and Femoral sites, Movement and Acoustic Pulse waves have been recorded by respectively by using accelerometer and a high sensibility microphone. In particular, since accelerometer sensor is located in contact with the skin, it lets to acquires displacement signal; the high

sensibility microphone, unlike the accelerometer, is placed close to the skin but without contact, so it can record only sound. By doing so, each signal components can be analysed separately. The following paragraphs will describe in details this approach.

4.3.1 Accelerometer signal

In order to isolate all signal components generated by skin movements, MEMS accelerometer LIS2DS12, described in *paragraph 2.6.5,* is adopted by replacing the MEMS microphones in the glass chamber reported in *Figure* 3.9. As already discussed, the device allows acceleration detection along three axis (X, Y and Z), but for the scope of this work only Z direction has been considered. Indeed, the Z axis is always perpendicular to the skin, so contains the main contribution on the movement information.

Spectral analysis

As explained in *paragraph 3.3.2,* accelerometer sensor is set to work at 200Hz so it must be conveniently decimated and filtered so int can be synchronized with ECG acquisition. The signal decimation is carried out by low pass filter with 100Hz cut-off frequency, equal to half the sampling frequency. Subsequently, signal is resampled at the chosen 200Hz sampling frequency. The obtained signal is shown in *Figure* 4.22.

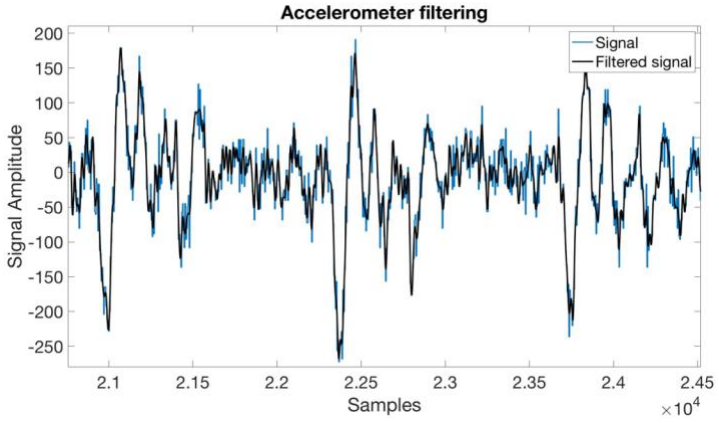

Figure 4.22 Accelerometer signal.

Also in this case, a frequency components analysis allow the identification and isolation of the frequency of interest. As shown in *Figure* 4.23*,* a FFT (Fast-Fourier Transform) was applied to the Carotid signal and it is possible to notice that the main information content is limited under 20Hz.

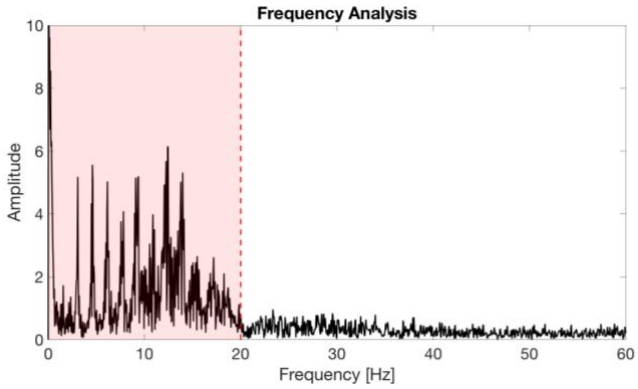

Figure 4.23 Spectral Analysis of accelerometric signal

4.3.2 Brüel & Kjær 4943 microphone signal

In order to isolate all signal components generated without skin contact, a collaboration with "*Istituto Nazionale di Ricerca Metrologica*" (INRiM) acoustic laboratory has been carried out. This is a national public structure performing scientific research on the field of materials science, metrology science and new technologies application.

The test has been made by using Brüel & Kjær 4943 (with a serial number of 2645657), acquired in an anechoic chamber. The employed sensor is a high sensibility microphone usually adopted as calibration reference, thanks to its optimal specification and performances [48]. The room called "anechoic chamber" is not influenced by external noises and allows the completely absorption of sound waves reflections. For these reasons, it can simulates a quiet open-space of infinite size and is a suitable solution to avoid the external noise can affect the results.

The just mentioned room is a "full anechoic chamber" and permits all directions energy absorption. In this test, instead, a "hemi-anechoic chamber" was employed (*Figure* 4.24); it is made by a solid floor used as support surface for cars or industrial machinery that should generally be tested. This floor is still isolated from external vibration thanks to damper and absorbent buffers presence.

Figure 4.24 Hemi-anechoic chamber.

Acquisition system configuration

In order to perform microphone signals acquisition, three components are needed:

- the Brüel microphone, calibrated with Brüel calibrator and supplied with 200V;
- the Spectrum analyser (*Sinus)*, that allow microphones electrical outputs receptions;
- the Laptop with *Samuray* software useful for data analysis.

The acquisition system is shown in *Figure* 4.25.

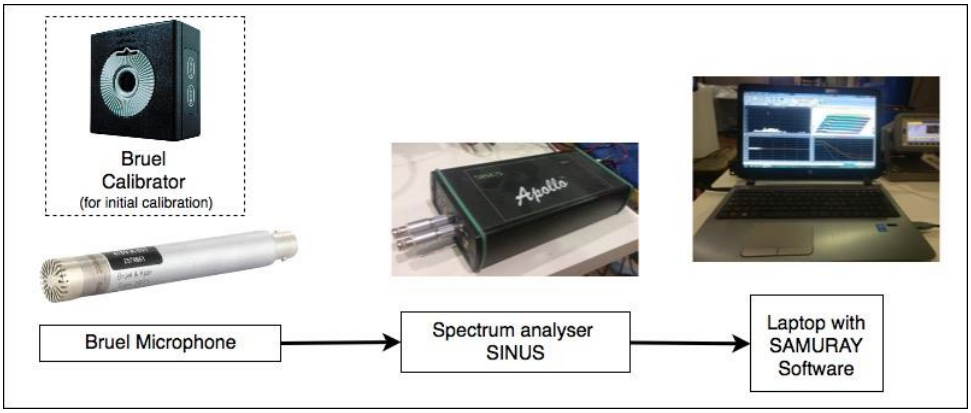

Figure 4.25 Developed acquisition system diagram.

The acquisition has been made by placing two microphones, the first near the Carotid artery, but without direct contact. While the second placed in direct contact with the skin, as shown in *Figure* 4.26. In particular, the former signal allows acquisition of sound generated by carotid artery movement, while the latter, collects a reference wave for pulses identification.

Figure 4.26 Two microphones position.

Spectral analysis

As explained in *paragraph 2.4.1*, for standard heart auscultation, sound signal is considered in the range of frequencies from 15 to 700 Hz. But, in this specific application scenario Acoustic Pulse Wave acquisition cannot be considered a heart auscultation (peripheral sites are investigated) and it is made by using different kind of microphones. For this reason and to better the effective bands of interest, before filtering, signal has been analysed in the frequency domain performing the FFT. The obtained spectrogram is shown in *Figure* 4.27.

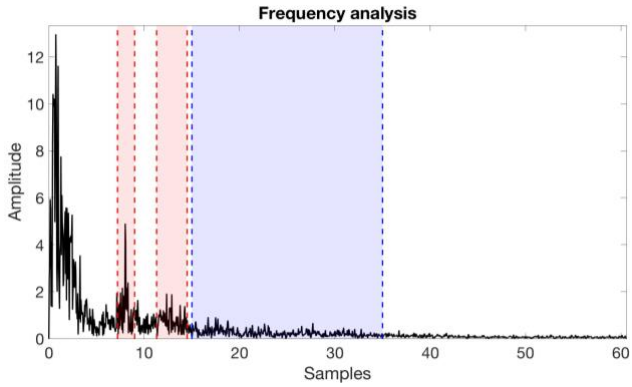

Figure 4.27 Microphone signal frequency analysis.

As it is possible to see, the main information content is limited under 35Hz, but the signal has two frequency components also around 8Hz and 12Hz. It is possible to see how the low frequency contribution (8 and 12Hz) are present on both the Accelerometer and Brüel&Kjær4943 acquisitions.

So, either the phenomena is considered from the pure sound point of view or it is considered from the pure movement point of view, the conclusion is that 8-12Hz contributions are still present and cannot be explicitly associated to the sound or the movement component. This is an important indication for the signal processing approach that have to be adopted on the MEMS microphone configuration. In fact, the better results are expected to be achievable using the movement component of the signal, thus in order to avoid any sound related contribution, the 8-12Hz bands should be removed from the MEMS microphone acquisition.

4.3.3 Obtained signals

Thanks to described analysis, MEMS Microphone signal can be divided in two different frequency ranges mainly containing displacement contribution rather than sound contribution. These intervals are respectively set between 0.5-20 Hz, without 8 and 12 Hz components (*Figure* 4.28), and 15-35Hz (*Figure* 4.29). For the shake of simplicity, signals are renamed as Displacement and Sound respectively, even if it is not full formal and accurate classification.

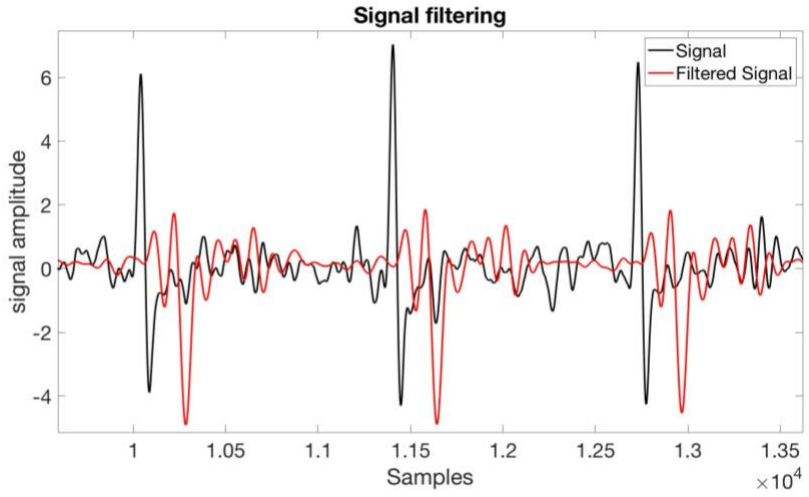

Figure 4.28 Microphone signal filtered between 0.5 and 20 Hz (Displacement component).

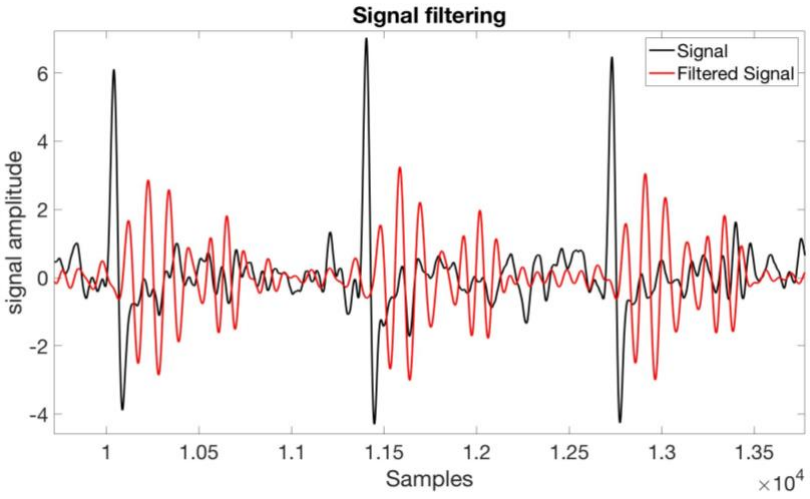

Figure 4.29 Microphone signal filtered between 15 and 30 Hz (Sound component).

4.4 Signal choices

The aim of this step is to identify the most repeatable signal characteristic. In particular, the Displacement and Sound signals defined in *paragraph 4.3.3*. and the Movement Pulse Wave, are considered. Accelerometer signal has been chosen to be processed and analysed since it has a similar shape when compared with the other (see *Figure* 4.22). The choice of the most reliable signal will be made using two different approaches:

- analysis of shape repeatability;
- assessment of characteristics stability.

Both methods will be explained in the following paragraphs.

4.4.1 Shape repeatability

The first information about shape repeatability can be obtained visually. First of all, for each signals, as explained in paragraph 4.2, all events (heart beat) have been isolated. Since the acquisitions have been made simultaneously with ECG, events can be easily overlapped and aligned considering as reference the corresponding R-peak on ECG signal.

In the *Figure* 4.30 and *Figure* 4.31 signals acquired at Carotid and Femoral artery respectively, are represented. In these pictures there are (a)Movement Pulse Wave, (b)Displacement Pulse Wave and (c)Sound Pulse Wave.

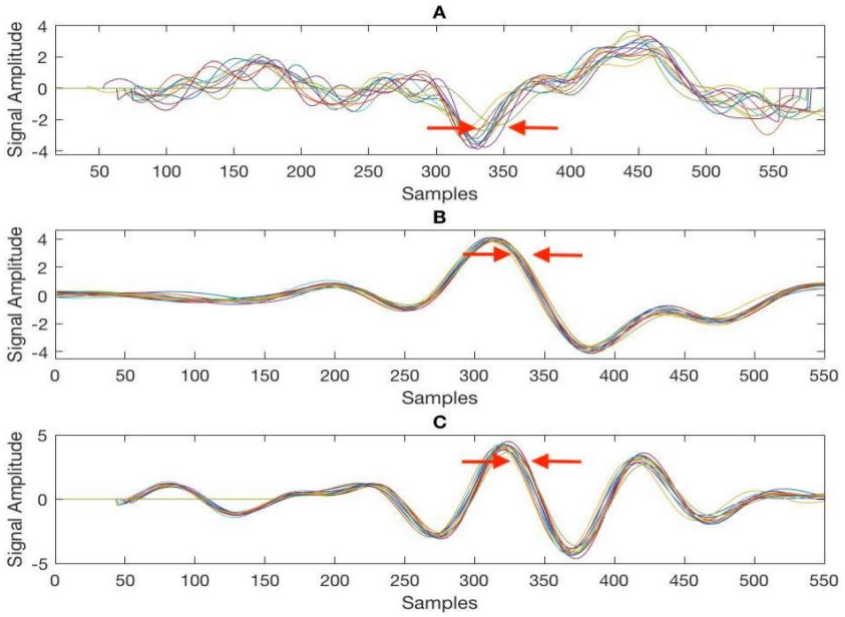

Figure 4.30 Frequency analysis of Carotid signal.

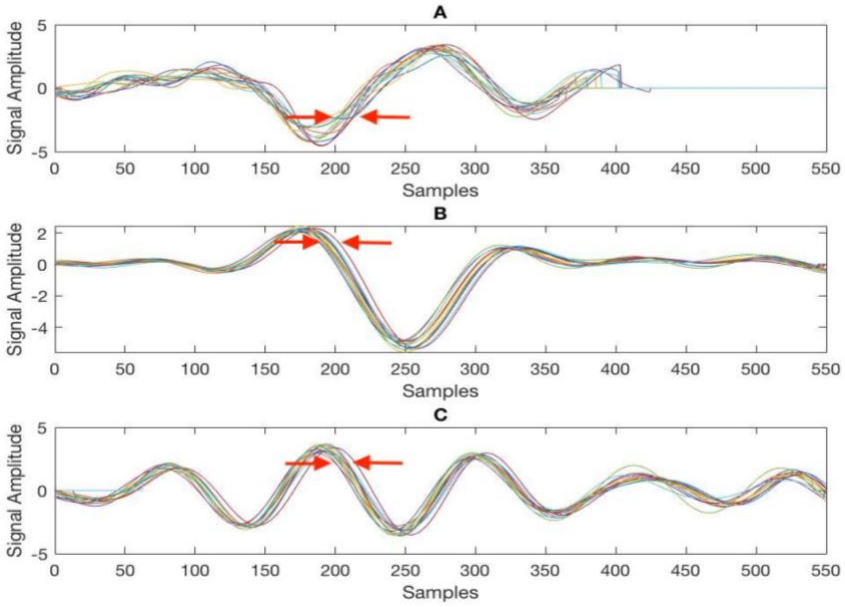

Figure 4.31 Frequency analysis of Femoral signal.

4.4.2 Characteristic stability

Finally, in order to identified the most repeatable signal that allows feature extraction, both Movement and Acoustic signals have to be acquired simultaneously. From these signals, Movement Pulse Wave, Displacement Pulse Wave and Sound Pulse Wave can be isolated and analysed. All the obtained characteristics have been compared with each other to identify which of them has the smallest variability and the greater repeatability.

For both Movement and Displacement Pulse waves, as shown in *paragraph 4.2*, once the signal has been filtered, each event is isolated and its minimum point is identified. Then, according to the largest front isolation the corresponding maximum is detected and the intersecting tangent point is taken. The difference concerns characteristic location. In particular, the former (*Figure* 4.30 *and Figure* 4.31*, A*) takes the "foot" of the right front, so it use the same algorithm implementation used for Pressure Pulse wave signal; on the contrary, the latter (*Figure* 4.30 *and Figure* 4.31*, B*) uses the "ear" *intersecting tangent point* and its algorithm implementation is explained in *paragraph 4.2.* The two obtained characteristics are displayed respectively in *Figure* 4.32 and *Figure* 4.33.

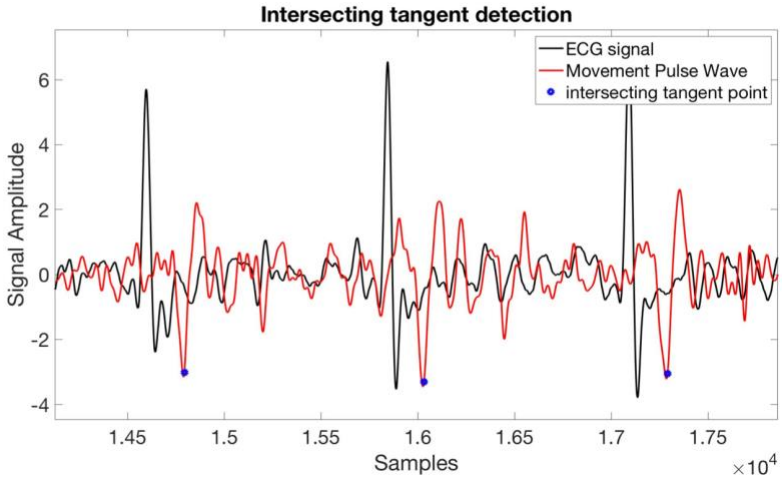

Figure 4.32 Movement Pulse Wave intersecting tangent points extraction.

Unlike the previous ones, Sound signal requires a specific algorithm implementation because, as it is possible to see in *Figure* 4.29, it has a different shape from the other two. Also in this case, the use of Sound signal for PWV calculations is a totally new experimental approach and in literature are not available information about features extraction. For this reason, several attempts have been made to identify the best characteristic to be used to identify the pulse passage in both Carotid and Femoral sites. Finally, since looking at the signal it is possible to easily distinguish S1 from S2, the intersecting tangent point located in the wider front of S1 has been chosen.

The signal is processed following almost the same steps sequence explained in *paragraph 4.2* for "ear" *intersecting tangent* extraction. In particular, once the signal has been filtered, each S1 event has to be isolated knowing that its length is about T/4 (see stage *a* in the section *algorithm implementation* of *paragraph 4.2*). For every S1 sound, minimums points can be identified and, according to the left largest front isolation, the corresponding maximums, that come first, are detected.

Like the movement signal, also in this case the intersecting tangent point called "Ear" is taken (*Figure* 4.34) and renamed as "Sound-Ear".

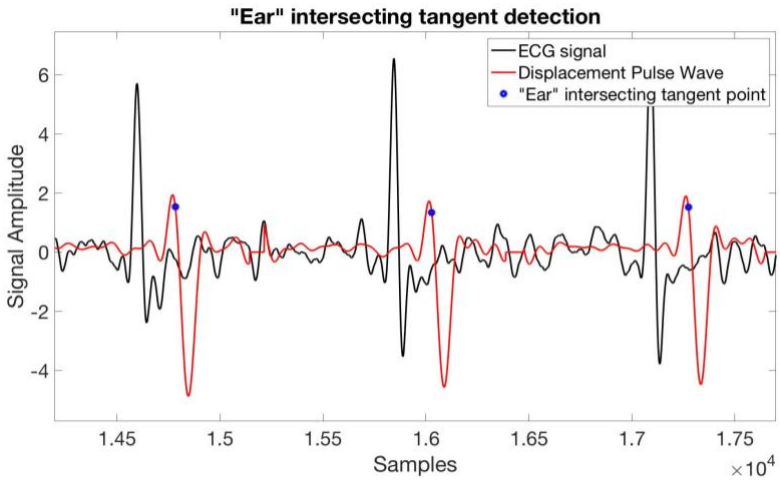

Figure 4.33 Displacement Pulse Wave filtered between 0.5 and 20 Hz and "Ear" intersecting tangent points extraction.

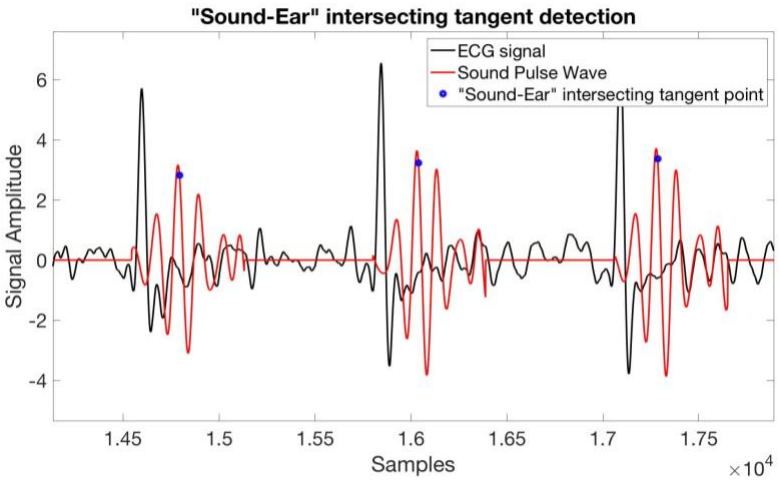

Figure 4.34 Sound Pulse Wave filtered between 15 and 30 Hz "Sound-Ear" intersecting tangent points extraction.

4.4.3 Results discussion

First of all, shape analysis highlight that all signals have a similar shapes for both two acquisition sites, so they are a good solution for the aim of this work. Moreover, as it possible to see, the same analysis show a great repeatability for both Acoustic signals filtered between 0.5-20 Hz and 15-30Hz (sections B and C of *Figure* 4.30 and *Figure* 4.31). In particular, considering the portion of wave where features have to be detected (highlighted by two red arrows), the shapes are quite similar pulse over pulse. On the contrary, in this specific section, accelerometer signal (section A of *Figure* 4.30 and *Figure* 4.31) has a higher variability, especially in Femoral acquisition site.

Finally, features extracted for each type of signal, i.e. Movement Pulse Wave, Displacement Pulse Wave and Sound Pulse Wave, have been compared to each other. This, has been done only in the direct way and the results are reported in *Table* 4.2.

Table 4.2 intersecting tangent characteristics extracted from the three signals.

Acquisition sites	Acquisition	Movement signal		considerer	discarded	Displacement signal		considerer	discarded	Sound Signal		considerer	discarded
		PTT (ms)	Dev. Std. (ms)			PTT (ms)	Dev. Std. (ms)			PTT (ms)	Dev.Std. (ms)		
CAROTID site	1	**91,73**	*2,73*	7	12	**91,39**	*1,48*	19	0	**103,30**	*1,72*	19	0
		90,42	*3,14*	14	6	**90,43**	*1,77*	20	0	**102,29**	*2,09*	15	5
		90,17	*3,09*	12	8	**91,68**	*2,19*	20	0	**100,56**	*2,04*	19	1
	2	**108,44**	*2,41*	7	14	**101,23**	*2,56*	19	2	**113,49**	*2,59*	20	1
		107,28	*3,40*	11	9	**102,81**	*1,97*	19	1	**112,99**	*2,39*	19	1
		107,64	*2,89*	11	4	**102,01**	*1,93*	15	0	**113,37**	*2,59*	15	0
	3	**98,69**	*2,33*	15	4	**103,61**	*2,63*	18	1	**59,50**	*2,83*	10	9
		100,44	*3,44*	14	6	**105,91**	*2,02*	20	0	**117,56**	*2,12*	17	3
		99,37	*2,91*	15	7	**106,15**	*2,57*	22	0	**118,15**	*2,88*	21	1
FEMORAL site	1	**163,88**	*2,64*	5	13	**162,60**	*1,02*	18	0	**167,35**	*1,18*	18	0
		159,89	*3,81*	8	8	**163,09**	*1,38*	16	0	**167,16**	*1,77*	16	0
		159,25	*3,24*	6	10	**163,29**	*1,19*	16	0	**168,40**	*1,03*	15	1
	2	**145,24**	*10,62*	5	12	**158,02**	*2,15*	17	0	**163,47**	*2,53*	17	0
		150,02	*2,93*	14	4	**157,68**	*2,27*	26	0	**163,45**	*2,38*	26	0
		147,74	*4,21*	20	8	**158,45**	*2,50*	28	0	**164,44**	*2,41*	28	0
	3	**160,89**	*4,01*	10	6	**163,09**	*1,18*	16	0	**168,40**	*1,03*	16	0
		157,43	*3,92*	9	6	**163,35**	*1,08*	15	0	**168,16**	*1,25*	15	0
		161,23	*2,95*	5	11	**162,45**	*1,78*	16	0	**167,38**	*1,76*	16	0

As it is possible to see, for the data obtained through both acoustic signals filtering approaches, there is a low variability (standard deviation starts from 1 to 3 ms) but also a quite low repeatability. In particular, PTT value has a gap of 15ms for Carotid and of 5ms for Femoral acquisition sites. In order to justify these behaviours, several attempts were done: probably, there could be noises sources or uncontrolled acquisition conditions, that influences signal. For these reasons in the following chapter an improved acquisition system is implemented.

Unlike the acoustic signals, for both carotid and femoral sites, Movement signal features have a greater variability. In particular, values listed in *Table* 4.2, have been obtained by using a check: the ones with a standard deviation higher than 4 have been eliminated. In fact, Movement signal is characterized by a biggest amount of discarded events with respect to the acoustic signals.

Finally, thanks to both shape repeatability and characteristic stability analysis, it is possible to conclude that Movement signal can't be considered enough reliable for the PWV parameter extraction.

Chapter 5

Final system prototype

In this section, the last developed prototype is presented. As explained in the previous chapters, the final goal of this work is to developed a handy and easy to use system for PWV parameter extraction. In those terms the hardware implemented so far (*Figure* 3.9) is not suitable for the final application purpose; furthermore, results highlight some residual noises or other artefacts presence, which can impact the PWV parameter extraction. For these reasons, some improvements on the acquisition systems will be addressed.

Thanks to the previous analysis, a lot of hardware adjustments have been applied and the conditioning circuit has been modified with the purpose to address the discovered problems. In additions, this system has been compared with the gold reference in terms of shape repeatability and characteristic stability. Finally, a quality check procedure was developed to provide an indication between reliable and not reliable signals.

5.1 Hardware implementation

First of all, it has decided to address a single microphone sensor. The main drawback of this approach is a reduced SNR, so the acquisition must be made in a controlled environment. Furthermore, the chamber is eliminated and only an adjustable neck-band or groin-band is needs as microphone support. In this way, it is possible to address a low cost system less influenced by operator skills.

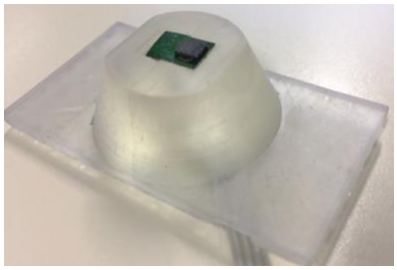

Figure 5.1 3D printed support to improve the operability.

On the other hand, an higher amplification gain is needed. Finally, to improve the sensor operability a 3D printed support was developed for both carotid and femoral acquisition sites (*Figure* 5.1). The final customized systems is shown in *Figure* 5.2.

Figure 5.2 Final acquisition system made by 3D printed support put in an adjustable neck-band.

The conditioning circuit for this new implementation is made by using the same components of the previous one (see *paragraph 3.4.1*). Also in this case, circuit has been implemented according to the signal frequency constraints, defining the bandwidth of interest between 0.3 and 200 Hz. This conditioning circuit, has a lower high-pass cut-off frequency and an additional stage used to improve signal amplification. The final configuration is illustrated in *Figure* 5.3.

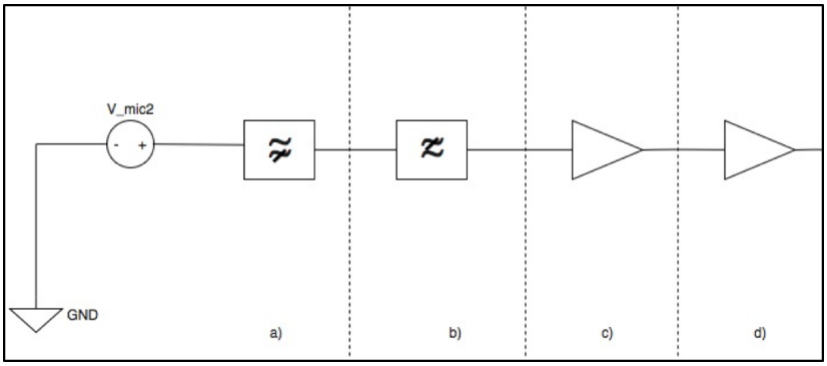

Figure 5.3 Microphone final analog signal processing diagram.

The second and third stages has the same behaviour of the previous implementation, while the first and the last stage have been modified. In particular the stage a) perform a only offset elimination and is used as a high pass filter with a cut-off frequency given by:

$$fc = \frac{1}{2 * \pi * C * R1} = \frac{1}{2 * \pi * 10\mu F * (47K\Omega + 10K\Omega)} = 0{,}27Hz$$

The gain of this step is given by:

$$G = \frac{R2}{R1} = \frac{47K\Omega}{(47K\Omega + 10\ K\Omega)} \cong 0.8$$

Moreover, in order to obtain a greater signal amplitude an to manage the gain limits of the single op-amp, the amplification stage is distributed on two devices. In order to perform a "normal" signal detection (output of some mV), the gain of the second stage is set to x100. Before the ADC input there is an additional first order high pass filter introduced to compensate the opAmp input offset error. The proposed conditioning circuit is the same for both Carotid and Femoral acquisition channels. All the cited components are showed in *Figure* 5.4.

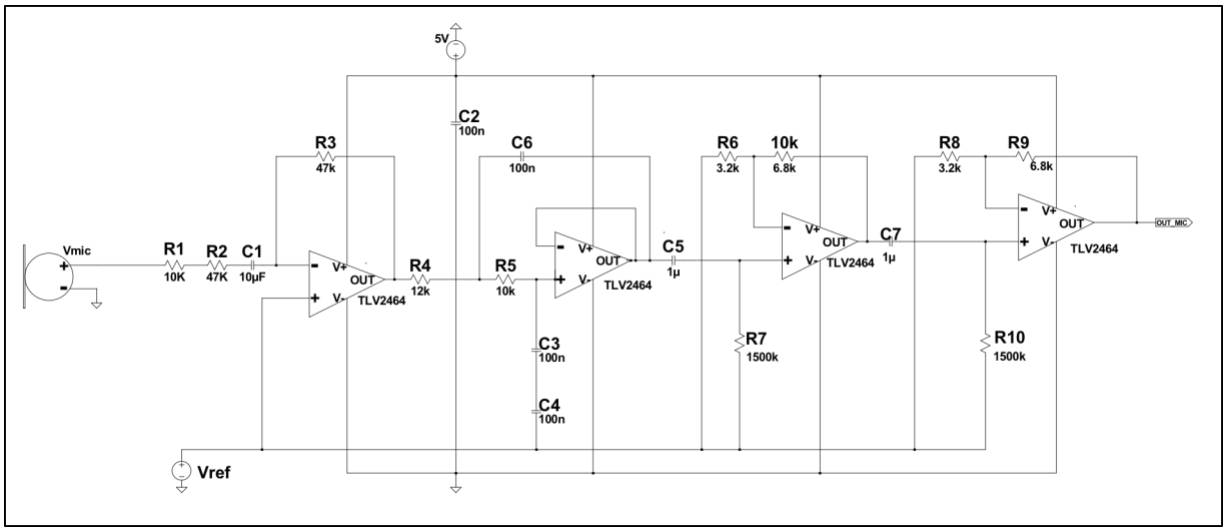

Figure 5.4 Conditioning circuit of both carotid and Femoral acquisition channels.

5.2 Signal analysis and feature extraction

Also with this improved acquisition system, signal is filtered and then evaluated by using the previous developed algorithm (see *paragraph 4.2*). The obtained Displacement and Sound Waves are illustrated in *Figure* 5.5 and *Figure* 5.6 respectively.

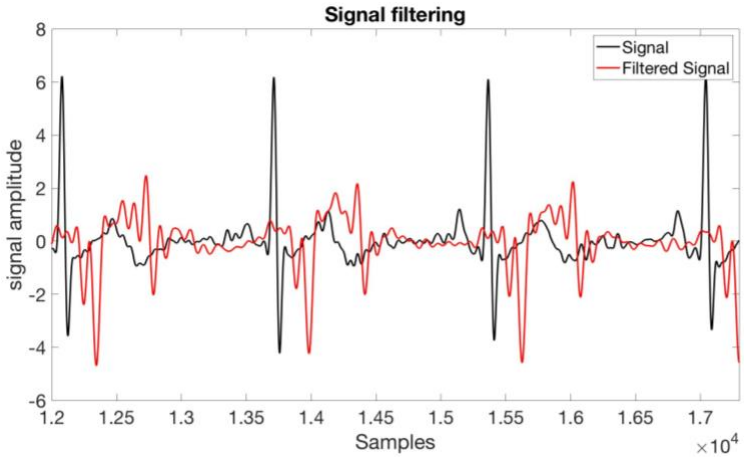

Figure 5.5 signal filtered between 0.5 and 20Hz.

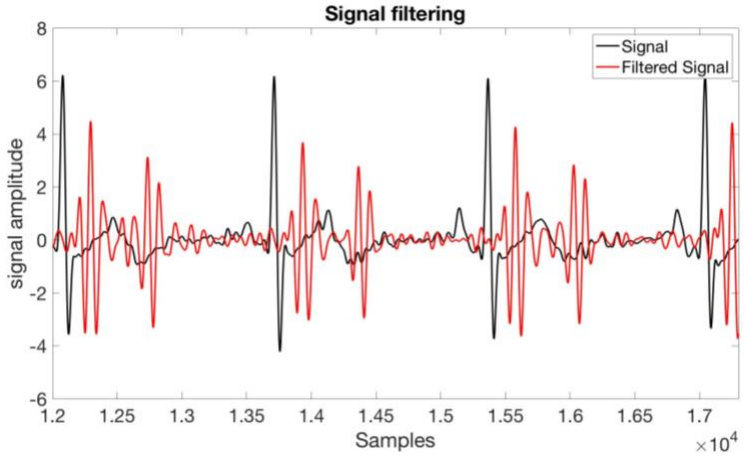

Figure 5.6 Signal filtered between 15 and 30Hz.

Shape repeatability

First of all, signal shape repeatability is evaluated by using the previously explained method (see *paragraph 4.4.1*). In particular, where features have to be detected (highlighted by two red circles in *Figure* 5.7 and *Figure* 5.8), signals must be as much as possible similar cycle over cycle.

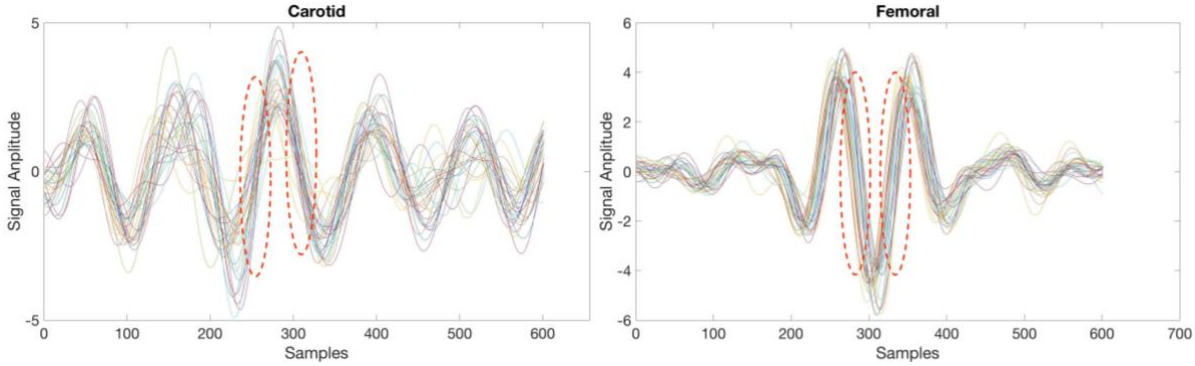

Figure 5.7 Shape repeatability analysis of signals filtered between 15 and 30 Hz.

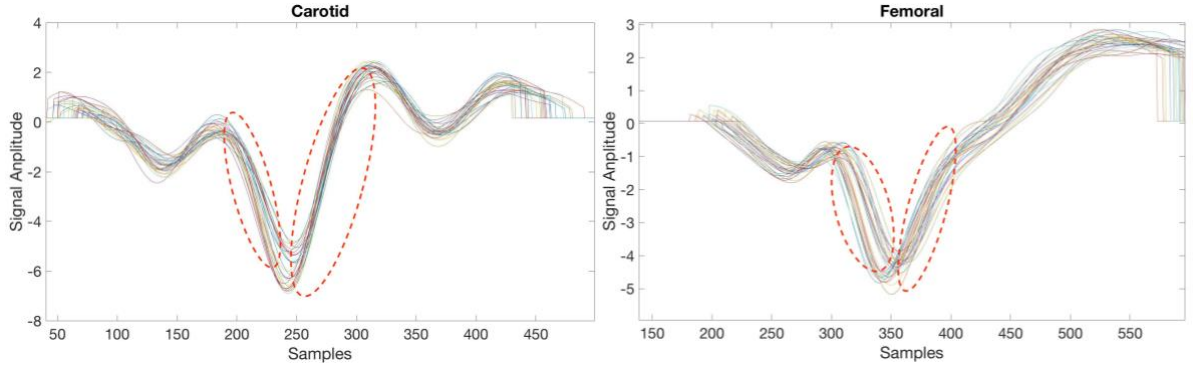

Figure 5.8 Shape repeatability analysis of signals filtered between 0.5 and 20 Hz.

As it is possible to see, in the highlighted points, the Displacement signal (*Figure* 5.8) is almost equal over the time. On the contrary, the Sound signal (*Figure* 5.7) has a larger variability and the position of Carotid greater fronts are not the same to Femoral ones: probably, there could be noises sources or uncontrolled acquisition conditions in Carotid site unlike the Femoral one, that influences signal. For these reasons, this signal cannot be considered reliable for PWV parameter extraction.

Features stability

As it is possible to see, Displacement signals have a different shape than the same ones obtained with the old acquisition system configuration. So, a new feature is needed and several attempts have been made to isolate the most repeatable characteristic marked by low variability. For this extractions purpose, four features similar to the intersecting tangent point are calculated:

- The *ear-right intersecting tangent point*, located at the top of the right greatest front respect to the absolute minimum;
- the *foot-right intersecting tangent point,* located in the lower part of the right greatest front respect to the absolute minimum;
- the *ear-left intersecting tangent point*, located at the top of the left greatest front respect to the absolute minimum;
- the *foot-left intersecting tangent point*, located in the lower part of the left greatest front respect to the absolute minimum.

To perform all this features extractions, proper algorithms based on the previous one, explained in *paragraph 4.2,* are needed. In particular, fronts identification and first derivate minimum or maximum calculation are not the same. In case of left "ear" and left "foot" features, the first derivate minimum is taken, while for the right "ear" and right "foot" features, the first derivate maximum is selected. All the detected features are illustrated in *Figure* 5.9.

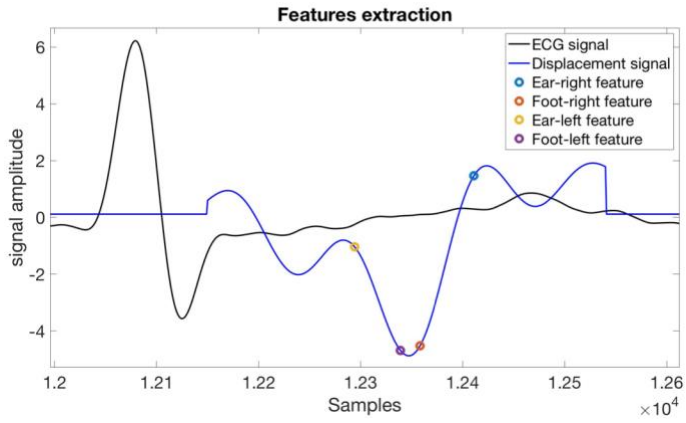

Figure 5.9 Features location.

All the extracted characteristics, let to evaluate the PTT obtained with the new Displacement signal in term of variability and repeatability. This, as shown in *Table* 5.1, was done referring to the ECG.

Table 5.1 Displacement signal features extracted and analysed.

CAROTID site					FEMORAL site				
FEATURES	Parameters	1	2	3	**FEATURES**	Parameters	1	2	3
"Ear-right"	PTT	**161.15**	**160.07**	**166.30**	"Ear-right"	PTT	**222.97**	**221.41**	**231.84**
	std.dev.	*3.20*	*4.31*	*3.25*		std.dev.	*2.74*	*2.68*	*4.37*
"Foot-right"	PTT	**135.25**	**133.87**	**132.70**	**"Foot-right"**	PTT	**183.65**	**181.07**	**183.05**
	std.dev.	*2.70*	*2.19*	*2.18*		std.dev.	*2.16*	*2.01*	*2.21*
"Ear-left"	PTT	**116.23**	**115.06**	**121.11**	"Ear-left"	PTT	**156.68**	**154.53**	**161.19**
	std.dev.	*3.98*	*3.74*	*3.53*		std.dev.	*3.08*	*3.04*	*2.81*
"Foot-left"	PTT	**133.74**	**132.71**	**138.71**	**"Foot-left"**	PTT	**175.72**	**173.90**	**181.97**
	std.dev.	*2.80*	*2.29*	*2.97*		std.dev.	*2.23*	*2.99*	*2.51*

As it is possible to see, for the data obtained through both right and left "foots", there is a low variability into the same acquisition (standard deviation starts from 2 to 3 ms) and a quiet good repeatability (PTT value ranges from 132.70 to 135.25 ms for Carotid site and from 181.07 to 183.65 ms for femoral site). For this reason signal features individuation is made around the minimum, because it has been seen that is the part of the front less distorted by noises and so very repeatable. The "Foot-right" was chosen thanks to its more high Shape repeatability, as *Figure* 5.8 shows.

5.2.1 Comparison with golden reference

In this test, features extraction for Pressure and Displacement Pulse Waves let to compare the PTT obtained with the new acoustic signal with the one extracted with the golden standard approach. This was done both referring to the ECG and to the Pressure Wave.

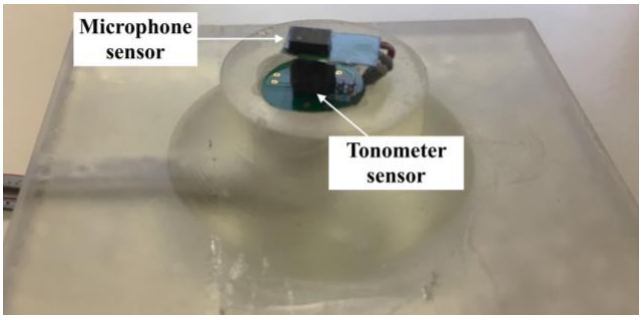

Figure 5.10 3D-printed support for Tonometer and microphone location

In order to perform, on the same site, a simultaneously Pressure and Displacement Pulse Waves acquisition, the acquisition support (*Figure* 3.9) is improved by overlapping Tonometer sensor LPS35HW to the microphone sensor, as *Figure* 5.10 shown. .

Also in this case, an adjustable neck-band and groin-band are adopted for the microphone and tonometer mechanical support, as shown in *Figure* 5.11.

Figure 5.11 Final acquisition support with overlapped Tonometer and Microphone.

Features extraction algorithm allow a coherent evaluation between the two acquired signal types. This check is done by comparing the Displacement Pulse Wave intersecting tangent point, defined as the “foot” of the greater front, with the “foot” of the reference pressure wave(*Figure* 5.12and *Figure* 5.13).

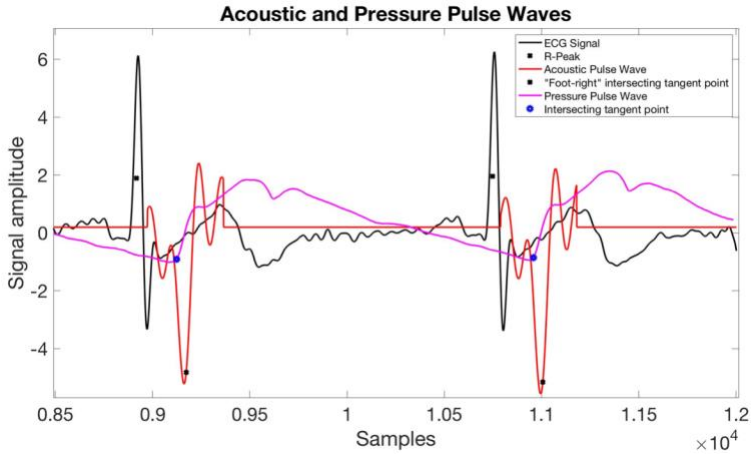

Figure 5.12Acoustic Pulse wave and Pressure Pulse Wave simultaneously aquired in Carotid site.

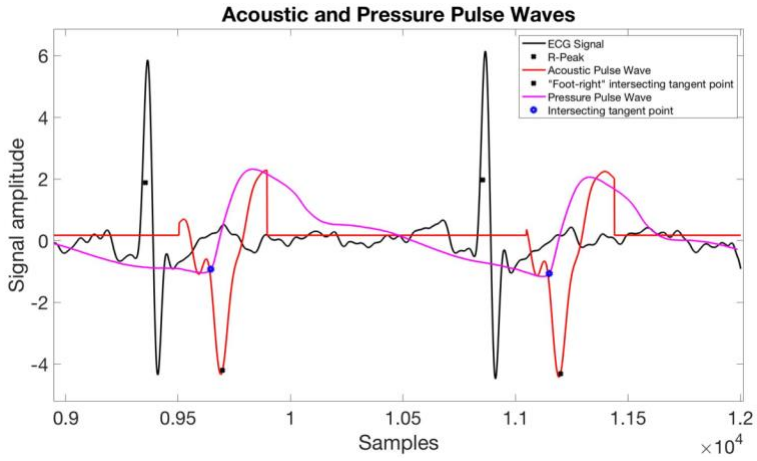

Figure 5.13 Acoustic Pulse wave and Pressure Pulse Wave simultaneously aquired in Femoral Site.

The time difference between pulse passage individuated on the new acoustic signal and the one extracted on the reference wave, for both Carotid and Femoral sites, is expected to be the same. If it is true the new selected feature is coherent with the one detected by using tonometric approach.

This comparison is done by Acoustic and Pressure Pulse Waves acquisition on the same subject in both Carotid and Femoral sites one by one, as reported in *Table* 5.2.

Table 5.2 comparision between Pressure and Acoustic Pulse waves.

Subject	Parameter	CAROTID site		FEMORAL site	
		Acoustic "foot" respect to Pressure "foot"	Acoustic "foot" respect to ECG "R-peck"	Acoustic "foot" respect to Pressure "foot"	Acoustic "foot" respect to ECG "R-peck"
1	PTT (ms)	**27.50**	135.08	**26.15**	181.46
	std.dev. (ms)	*1.11*	*2.44*	*1.09*	*1.92*
2	PTT (ms)	**28.92**	136.79	**26.11**	182.75
	std.dev. (ms)	*0.94*	*2.54*	*0.76*	*1.54*
3	PTT (ms)	**28.35**	135.49	**27.04**	177.54
	std.dev. (ms)	*1.03*	*2.46*	*0.84*	*2.25*
4	PTT (ms)	***27.35***	*134.01*	***27.63***	*181.06*
	std.dev. (ms)	1.4	2.41	1.49	2.81

5.3 Final Check

In conclusion, the intersecting tangent point evaluated on the greater front of the Displacement Pulse Wave, seems to be a good way for PWV parameter estimations. But, in some cases, the detected value is not fully in line with the reference one, obtained by using Tonometer signal. Several analysis were made in order to justify this behaviour, when the frequency bands of the signal are well separated, the computed PTT is good and an example of this situation is reported in *Figure* 5.14. While, when the level of noise is such that low frequency band are not well distinguishable (*Figure* 5.15) then the extracted PTT values differ from the expected.

For this reason, a sort of SNR parameter, based on Fast Fourier Transform (FFT) analysis, has been introduced to discriminate between those situations. In particular the signal power computed in the 0.5 to 20Hz range is divided by the signal power computed on frequency higher than 40 Hz. The computed SNR value, updated every 3 seconds, is displayed on the graphical user interface running on the control laptop. It is expected that acquired samples will provide reliable results when SNR value is greater than 30.

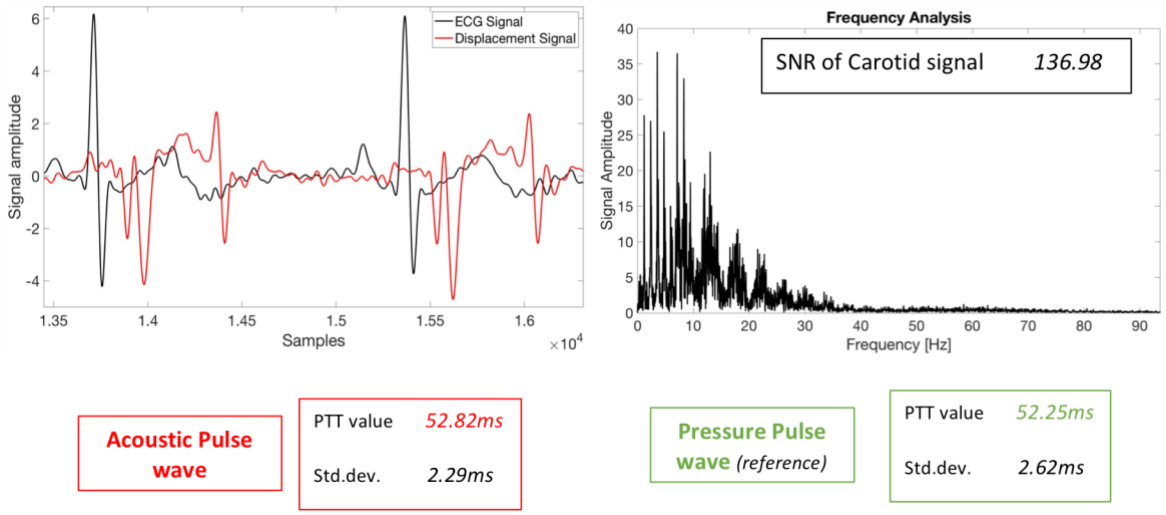

Figure 5.14 Good Displacement signal and its FFT are reported on top; the corresponding PTT value and SNR are illustrated on the bottom.

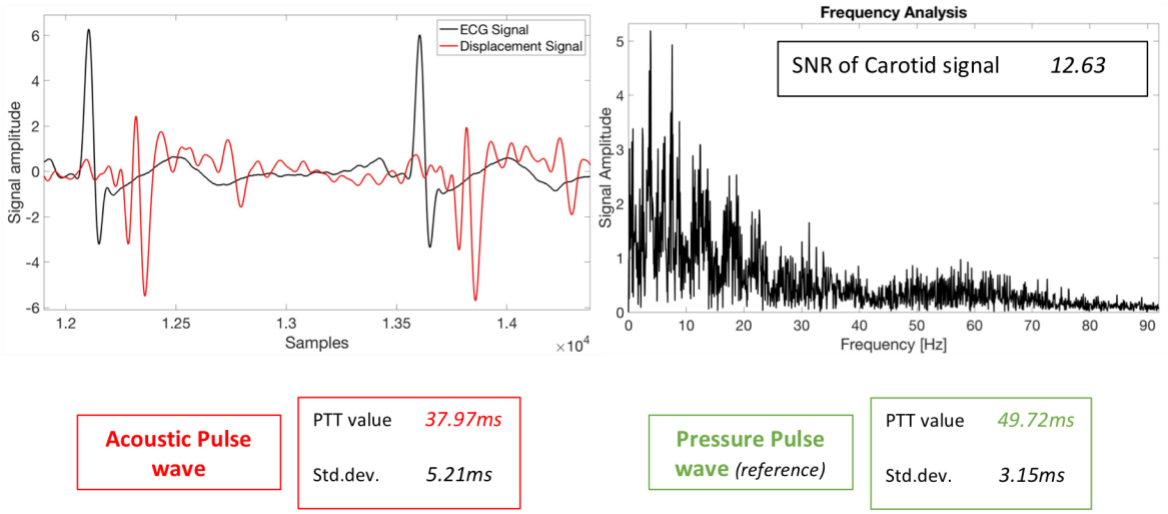

Figure 5.15 Batter Displacement signal and its FFT are reported on the top; the corresponding PTT value and SNR are illustrated on the bottm.

Together with the SNR value, on the graphical interface it is possible to display also the signal FFT analysis (updated every 3 sec.) as reported in *Figure* 5.16.

Figure 5.16 Signal, FFT and SNR plotted by VisualStudio tool.

Both carotid and femoral Microphone signals are acquired in these controlled conditions and, then, compared to the subsequently recorded by the reference one, as shown in *Table* 5.3.

Table 5.3 PTT calculation by Microphone and Tonometer.

acquisition	parameters	Respect to R-peck		Microphone	Tonometer
		CAROTID	FEMORAL		
1	PTT (ms)	139.16	189.70	**51.06**	**51.02**
	std.dev. (ms)	*2.80*	*2.66*	*2.57*	*3.3*
	SNR	53.67	433.24		
2	PTT (ms)	138.90	194.36	**54.10**	**54.33**
	std.dev. (ms)	*2.99*	*2.76*	*1.65*	*2.9*
	SNR	70.3	350.95		
3	PTT (ms)	137	190	**53.34**	**50.07**
	std.dev. (ms)	*2.86*	*3.08*	*1.58*	*2.69*
	SNR	49.88	423.56		
4	PTT (ms)	142.86	195.45	**52.82**	**52.25**
	std.dev. (ms)	*3.47*	*3.57*	*2.29*	*2.62*
	SNR	60.45	545.22		

As it is possible to see, data obtained with the controlled acoustic signal have a lower variability, both referring to the ECG and also in the direct carotid-femoral measurement (standard deviation in the order of 2-3 ms). But the main achievement, is a sensibly reduced discrepancy between PTT values given by Acoustic Pulse Wave and the Pressure Pulse Wave. For these reasons, it is possible to conclude that Microphone signal, properly filtered, can be considered a reliable approach for PWV parameter extraction.

Chapter 6
Conclusion and feature development

In conclusion, all the described analysis has to be made to customize a low-cost and operator-free systems for PWV parameter estimation. MEMS Microphone sensors, because of their low-cost and good performances, represents a good choice for PWV evaluation purposes.

Four different signals have been acquired, filtered and evaluated by ad-hoc algorithms. These processes were done by the realization of dedicated conditioning circuits and by implementing appropriate algorithms, both the development activities have been extensively explained in the previous chapters.

Acoustic Pulse Wave, Movement Pulse Wave, Pressure Pulse Wave and ECG have been recorder and compared; in particular, they have been processed for Pulse Wave Velocity extraction and the obtained results have been discussed. Several problems have been discovered which can be linked to acquisition system limitations and physiological signals artefact. In detail, the first developed system, composed by eight microphones located in a conical glass chamber, was strongly affected by noises and the given PTT values often differed when compared with the reference one. In additions, for a practical medical applications purpose, the number of microphones, the ball shaped-capsule and its glasses material are not representing a good choice.

For these reasons, to address more realistic application scenario, a more usable system based on a single microphone sensor, supported by an adjustable neck-band or groin-band, has been implemented. This system is low-cost, easy to use and is minimally influenced by operator skill.

According to the aim of this thesis work, the so called Displacement Pulse Wave signal, resulted as the best approach and several comparisons made with respect to the gold references allowed to deeply characterize the customized device. In particular, it was demonstrated that the selected feature, “foot-right” intersecting tangent point, is coherent with the foot of the sphygmic wave adopted in the tonometric approach. Finally, a quality check procedure was developed to provide an indication between reliable and not reliable signals for PWV detection purpose.

The final system prototype could be further enhanced to improve the reliability and the ease of use. In particular, adjustments that can be addressed in future developments are:

1- The creation of a more stable support system for the microphone location, in order better remove the noise sources related to the uncontrolled acquisition conditions.
2- Better investigate the usage of the Sound Pulse Wave signal for PWV parameter estimation. In fact, MEMS microphone sensor used for sound detection, can be located with less precision on acquisition sites and should be still able to proper detect an usable signal. In additions, it will be possible to take advantages from beamforming techniques to improve directionality and environmental noise rejection.
3- Data obtained with the Displacement Acoustic signal, have a low variability and a high repeatability, but so far, are acquired from only one subject. To achieve a more detailed and reliable characterization, more subjects have to be considered in future trials.
4- Finally, microphone sensor can be overlapped to other sensors, such as tonometer and simultaneously acquired and sensor fusion algorithms can be developed to improve system performances and usability.

Bibliography

[1] S. a. S. Atal, "One Size Does Not Fit All: Developing Emerging market Strategies by Country Not Region", AlixPartners publication, 2012.

[2] http://www.innerbody.com/image/cardov.html.

[3] B. D. Hoit, R. A.Walsh, Normal Physiology of the Cardiovascular System, chapter 5.

[4] M. L. Entman, M. F. Oliver, S.W. Jacob," Human cardiovascular system",2012.

[5] O. services, Cardiac Cycle, "Anatomy and Physiology 2", OpenStax CNX.

[6] https://my.clevelandclinic.org/health/articles/17064-heart-beat.

[7] I. Kaur, "Electrocardiogram Signal Analysis - An Overvie, International Journal of Computer Applications (0975 – 8887)", 2013.

[8] R. R.Ponceb, "Feature Extraction of Electrocardiogram Signals by Applying Adaptive Threshold and Principal Component Analysis", Journal of Applied Research and Technology, 2015.

[9] F. P. Branca," Fondamenti di ingegneria clinica vol.1", Springer Verlag, 2000.

[10] D. I. Moxham, "Understanding Arterial Pressure Waveforms", Southern African Journal of Anaesthesia and Analgesia, 2014.

[11] A. Yartsev, "Deranged Physiology- Normal Arterial Line Waveforms", 2018.

[12] Ranganathan and V. S. F. S. N.," The art and Science of Cardiac Physical Examination with Heart Sounds and Pulse Wave Forms", Humana Press, 2007.

[13] S. W. Jacob, M. L. Entman et all., "Human cardiovascular system", Encyclopædia Britannica, November 07, 2017.

[14] D. Gill, N. Gavriely et all., "A Probabilistic Model for Phonocardiograms Segmentation Based on Homomorphic Filtering (Biosignal)", Thailand: IJBET, SWU, 2006.

[15] S. E. Babatunde, "A review of signal processing techniques for heart sound analysis in clinical diagnosis", Journal of Medical Engineering & Technology, 2012.

[16] W. Phanphaisarn, A. Roeksabutr, P. Wardkein et all., "Heart detection and diagnosis based on ECG and EPCG relationships", Medical Devices: Evidence and Research, August 2011.

[17] B. S. Emmanuel, "A review of signal processing techniques for heart sound analysis in clinical diagnosis", Journal of Medical Engineering & Technology, 2012.

[18] Z. Jiang and S. C., "Cardiac sound murmurs classification with autoregressive spectral analysis and multi-support vector machine technique", Computers in Biology and Medicine 40, 2010.

[19] H. N. and M. R. Homaeinezhad," Detection and Boundary Identification of Phonocardiogram Sounds Using an Expert Frequency-Energy Based Metric", Annals of Biomedical Engineering, 2012.

[20] S. Ari, K.A. Shiva Kuman, G. Saha, "On an algorithm forboundary estimation of commonly occurring heart valvediseases in time domain", INDICON, 2006.

[21] L. H. Cherif, "Choice of the wavelet analyzing in the phonocardiogramsignal analysis using the discrete and the packet waveletransform", Expert Syst., 2010.

[22] a S. M.Debb and F. B., "Ime-frequency analysis of the first and the second heartbeat sounds", Appl.Math. Comput., 2008.

[23] J. Choi, S. and Z., "Comparison of envelope extractionalgorithms for cardiac sound signal segmentation", ExpertSyst, 2008.

[24] https://www.datasci.com/solutions/cardiovascular/pulse-wave-velocity-(pwv)

[25] P. Palatini, E. Casiglia, J. Gasowski et all., "Arterial stiffness, central hemodynamics, and cardiovascular risk in hypertension", Vasc Health Risk Manag, 2011.

[26] A. Díaz, C. Galli, M. Tringler et all., "Reference Values of Pulse Wave Velocity in Healthy People from an Urban and Rural Argentinean Population", Hindawi Publishing Corporation, 2014.

[27] T. Pereira and C. C., "Novel Methods for Pulse Wave Velocity Measurement", 2015.

[28] M.W. Rajzer, W. Wojeciechowska, M. Klocek et all., "Comparison of aortic pulse wave velocity measured by three techniques: Complior, SphygmoCor and Arteriograph", Journal of Hypertension, 2008.

[29] A. Q. Mark Butlin," Large Artery Stiffness Assessment Using SphygmoCor", Technology Pulse, 2016, pp. 4:180-192 .

[30] P. Salvi, G. Lio, C. Labat at all., "Validation of a new non-invasive portable tonometer for determining arterial pressure wave and pulse wave velocity: The PulsePen device", Journal of Hypertension, 2004.

[31] S.S. Hickson, M. Butlin, J. Broad, A.P. Avolio et all., "Validity and repeatability of the Vicorder apparatus: a comparison with the SphygmoCor device", Hypertens Res , 2009.

[32] M. Alivon, T. Vo-Duc Phuong, V. Vignon et all.," A novel device for measuring arterial stiffness using finger–toe pulse wave velocity: validation study of the pOpmètre", 2015, p. 108:227–234 .

[33] J. Calabia, P. Torguet, M. Garcia, I. Garcia et all., "Doppler ultrasound in the measurement of pulse wave velocity: Agreement with the Complior method". Cardiovascular Ultrasound, 2011.

[34] L. Joly, C. Perret-Guillaume, A. Kearney-Schwartz et all., "Pulse wave velocity assessment by external noninvasive devices and phase-contrast magnetic resonance imaging in the obese", Hypertension, 2009.

[35] STMicroelectronics, "HM301D ECG analog front-end", May 2014.

[36] F. Librizzi and A. B., "ST's Wellness solution :reliable Heart Monitoring", STMicroelectronics.

[37] STMicroelectronics, "MEMS audio surface-mount bottom-port silicon microphone with analog output", 2013.

[38] STMicroelectronics, "MEMS digital output motion sensor: ultra-low-power, high-performance 3-axis "pico" accelerometer", Datasheet - production data, 2017.

[39] STMicroelectronics, Discovery kit with STM32F429ZI MCU, 2016.

[40] STMicroelectronics, "HM301D Diagnostic quality acquisition system for bio-electric sensors and bio- impedance measurements", Datasheet, 2015.

[41] P.O. Box, "Application Note, High Performance, Low Noise Studio Microphone with MEMS Microphones, Analog Beamforming, and Power Management, Analog Devices".

[42] T. Instruments, "LM317 3-Terminal Adjustable Regulator", Texas Instruments Incorporated , 2016.

[43] L.A.Geddesetal, "Pulse transit time as an indicator of arterial blood pressure", vol. 18, Psychophysiology, 1981, pp. 71-74.

[44] R. Pratap, M. Choudhary, "Suppression of noise in the ECG signal using digital IIR filter", January 2008.

[45] T. Jiapu Pan and W. J., "A Real-Time QRS Detection Algorithm", Vols. BME-32, IEEE TRANSACTIONS ON BIOMEDICAL ENGINEERING, 1985.

[46] Y.C. Chiu, M. P. A. et all., "Determination of Pulse wave velocities with computerized algorithms", vol. 121/5, American Heart Journal, 1991, pp. 460-1469.

[47] P. Malcovati and A. Braschietto, "The Evolution of Integrated Interfaces for MEMS Microphones", micromachines, 26 June 2018.

[48] https://www.bksv.com/en/products/transducers/acoustic/microphones/microphone-preamplifier-combinations/4189-A-021

[49] https://www.alldatasheet.com/view.jsp?Searchword=SFH7050

[50] http://www.pathwaymedicine.org/cardiac-action-potential-cellular-basis

[51] R. Gordan, J. Gwathmey, "Autonomic and endocrine control of cardiovascular function", 2015 .

[52] https://www.healthline.com/health/how-to-check-heart-rate

[53] https://patient.info/doctor/pulse-examination

[54] R. Singh et all., "Computer aided analysis of phonocardiogram", Journal of Medical Engineering and Technology,, 2007.

[55] S. Choi et all., "Detection of valvular heart disorders usingwavelet packet decomposition and support vector machine", Expert Syst., 2008.

[56] M. F O'Rourke, A. P. and X.-J. J., "Pulse wave analysis", Br J Clin Pharmacol, 2001.

[57] R. Inderbir Kaur, "Electrocardiogram Signal Analysis - An Overview", vol. Volume 84 , nternational Journal of Computer Applications (0975 – 8887), December 2013.

[58] Andrew, L. Wentland, T. M. and G. O.,"Review of MRI-based measurements of pulse wave velocity: a biomarker of arterial stiffness", Cardiovascular Diagnosis e Therapy, 2014.

[59] T. Pereira, C. C. and J. C., "Novel Methods for Pulse Wave Velocity Measurement", J Med Biol Eng., 2015.

[60] N. Gupta, R. P., S. S. and S. M., "Neural network classification of homomorphic segmented heart sounds", Appl. Soft Comput. J., 2007.

[61] S. Gabarda, G. Cristobal, J. M.-A. and R. Ruiz-Merino, "Detection of anomalous events in biomedical signals by Wigner analysis and instant-wise Renyi entropy", EURASIP, 2006.

[62] B. Fethi and D. A., "Features for Heartbeat Sound Signal Normal and Pathological, London, UK: Bentham Science", 2008.

[63] S. Ari, K. Hembram and G. Saha, "Detection of cardiacabnormality from PCG signal using LMS based leastsquare SVM classifier", Expert Syst, 2010.

[64] D. Nedumaran and D. B., "Efficient computation of phonocardiographic signal analysis in digital signal processor based system", International Journal of Computer Theory and Engineering, 2010.

[65] Z. Dokur and T. O., "Feature determination for heartsounds based on divergence analysis", Digit. Signal Process.Rev, 2009.

[66] T. O¨lmez and Z. D., "Heart sound classification usingwavelet transform and incremental self-organizing map", Digit. Signal Process, 2008.

[67] https://www.webmd.com/hypertension-high-blood-pressure/hypertension-working-heart#1

[68] D.Kumar, P. Carvalho, M. Antunes et all. "Third heart sounddetection using wavelet transform-simplicity filter", 2007.

[69] F. J. Moran, "Clinical Methods: The History, Physical, and Laboratory Examinations. 3rd edition., Boston: Butterworths", 1990.

[70] Z. Yan, Z. Jiang A. Wei, "The momentsegmentation analysis of heart sound pattern", Comput.Methods, 2010.